Elucidation of the central regulation of the hypophysiotropic corticotropin-releasing hormone- and thyrotropin-releasing hormone-synthesizing neurons in the rat

Ph.D. Thesis

Tamás Füzesi

Department of Endocrine Neurobiology
Institute of Experimental Medicine
Hungarian Academy of Sciences

Semmelweis University
János Szentágothai Ph.D. School of Neuroscience

Tutor: Csaba Fekete M.D., Ph.D., D.Sc.

Opponents: József Kiss M.D., Ph.D., D.Sc.
Dóra Reglődi M.D., Ph.D.

Chairman of committee: Katalin Köves, M.D., Ph.D., D.Sc.
Members of committee: Krisztina Kovács, Ph.D., D.Sc.
Zita Halász, M.D., Ph.D.

Budapest
2010

TABLE OF CONTENTS

1. List of abbrevations

3V	- 3rd ventricle
α-MSH	- Alpha-melanocyte-stimulating hormone
ABC	- Avidin-biotin complex
ac	- Anterior commissure
Aca	- Anterior commissure anterior part
Acb	- Accumbens nucleus
ACo	- Anterior cortical amygdaloid nucleus
acp	- Anterior commissure posterior part
ACTH	- Arenocorticotropic hormone
ADP	- Anterodorsal preoptic nucleus
AGRP	- Agouti-related protein
AHi	- Amygdalohippocampal area
AHiAL	- Amygdalohippocampal area anterolateral part
AHiPM	- Amygdalohippocampal area posteromedial part
alv	- Alveus of the hippocampus
AMCA	- 7-amino-4-methyl-coumarin-3-acetic acid
aPVN	- Anterior parvocellular subdivision of the PVN
Arc	- Arcuate nucleus
ArcL	- Arcuate nucleus lateral part
ArcM	- Arcuate nucleus medial part
AVPe	- Anteroventral periventricular nucleus
BAT	- Brown adipose tissue
BMA	- Basomedial amygdaloid nucleus anterior part
BNST	- Bed nucleus of stria terminalis
BNSTad	- Bed nucleus of the stria terminalis anterodorsal area
BNSTal	- Bed nucleus of the stria terminalis anterolateral area
BNSTav	- Bed nucleus of the stria terminalis anteroventral area
BNSTif	- Bed nucleus of the stria terminalis interfascicular nucleus
BNSTpr	- Bed nucleus of the stria terminalis principal nucleus
BNSTtr	- Bed nucleus of the stria terminalis transverse nucleus

BNSTia	- Bed nucleus of the stria terminalis intraamygdaloid division
CA1	- Field CA1 of hippocampus
CA3	- Field CA3 of hippocampus
CART	- Cocaine-and amphetamine-regulated transcript
cc	- Corpus callosum
CCK	- Cholecystokinin
CeA	- Central amygdaloid nucleus
CNS	- Central nervous system
CPu	- Caudate putamen (striatum)
cst	- Commissural stria terminalis
CRE	- cAMP-response-element
CREB	- cAMP-response-element binding protein
CRH	- Corticotropin-releasing hormone
CTB	- Cholera toxin β subunit
D3V	- Dorsal 3rd ventricle
DBH	- Dopamine-β-hidroxilase
DG	- Dentate gyrus
DPAG	- Dorsal periaqueductal gray
f	- Fornix
fi	- Fimbria of the hippocampus
DMN	- Hypothalamic dorsomedial nucleus
FITC	- Fluorescein isothiocyanate
GLP-1	- Glucagon-like peptide 1
HDB	- Nucleus of the horizontal limb of the diagonal band
HPA axis	- Hypothalamic-pituitary-adrenocortical axis
HPT axis	- Hypothalamic-pituitary-thyroid axis
I	- Intercalated nuclei of the amygdala
ic	- Internal capsule
ICjM	- Islands of Calleja major island
icv.	- Intracerebroventricular
IL	- Interleukin
IM	- Intercalated amygdaloid nucleus main part

IR	- Immunoreactive
LA	- Lateroanterior hypothalamic nucleus
LEnt	- Lateral entorhinal cortex
LH	- Lateral hypothalamic area
LHb	- Lateral habenular nucleus
LGP	- Lateral globus pallidus
LPO	- Lateral preoptic area
LS	- Lateral septal nucleus
LSD	- Lateral septal nucleus dorsal part
LSI	- Lateral septal nucleus intermediate part
LSV	- Lateral septal nucleus ventral part
LV	- Lateral ventricle
MC3R, MC4R	- Melanocortin 3 and 4 receptors
ME	- Median eminence
MeAD	- Medial amygdaloid nucleus anterodorsal part
MEnt	- Medial entorhinal cortex
MePD	- Medial amygdaloid nucleus posterodorsal part
MePV	- Medial amygdaloid nucleus posteroventral part
MHb	- Medial habenular nucleus
MN	- Mammillary nuclei
MPA	- Medial preoptic area
MPO	- Medial preoptic nucleus
MPOC	- Medial preoptic nucleus central part
MRe	- Mammillary recess of the 3rd ventricle
MS	- Medial septal nucleus
MSG	- Monosodium glutamate
mt	- Mammillothalamic tract
MTu	- Medial tuberal nucleus
opt	- Optic tract
ox	- Optic chiasm
NPY	- Neuropeptide Y
NTS	- Nucleus tractus solitarii

PACAP	- Pituitary adenylate cyclase activating polypeptide
PB	- Phosphate buffer
PBS	- Phosphate buffered saline
pcf	- Precommissural fornix
Pe	- Periventricular hypothalamic nucleus
PFA	- Paraformaldehyde
PHAL	- Phaseolus vulgaris-leucoagglutinin
PLCo	- Posterolateral cortical amygdaloid nucleus
PMCo	- Posteromedial cortical amygdaloid nucleus
PMV	- Ventral premammillary nucleus
PI3K	- Phosphoinositide 3-kinase
PNMT	- Phenylethanolamine-N-methyltransferase
POMC	- Proopiomelanocortin
pPVN	- Periventricular parvocellular subdivision of the PVN
PV	- Paraventricular thalamic nucleus
PVA	- Paraventricular thalamic nucleus anterior part
PVN	- Hypothalamic paraventricular nucleus
py	- Pyramidal tract
PYY	- Peptide YY
RCh	- Retrochiasmatic area
Re	- Reuniens thalamic nucleus
S	- Subiculum
SCh	- Suprachiasmatic nucleus
SFO	- Subfornical organ
SI	- Substantia innominata
sm	- Stria medullaris of the thalamus
SO	- Supraoptic nucleus
sox	- Supraoptic decussation
SPa	- Subparaventricular zone of the hypothalamus
st	- Stria terminalis
T3	- 3,5,3'-triiodothyronine
TRH	- Thyrotropin-releasing hormone

UCN3	- Urocortin 3
UCP	- Uncoupling protein
VDB	- Nucleus of the vertical limb of the diagonal band
VMN	- Hypothalamic ventromedial nucleus
VP	- Ventral pallidum

2. Introduction

The maintenance of energy homeostasis is based on the balance of food intake and energy expenditure. Although both the quantity of consumed food and the rate of energy expenditure depend considerably on external circumstances, the central nervous system (CNS) strictly controls the balance of these two processes. For this central regulatory mechanism, the brain has to sense the actual conditions of the peripheral energy stores. The periphery sends metabolic signals to the CNS via two main pathways: by production of hormones and metabolits and through the vagus nerve.

These peripheral signals precisely inform the brain about the actual status of the gastrointestinal tract and the condition of the energy stores.

2.1. Energy homeostasis-related hormones

2.1.1. Insulin

Insulin that is synthesized in the B-cells of the pancreatic islands was the first humoral signal to be implicated in the control of body weight. Insulin is most well known about its function in the regulation of blood glucose levels and storage of lipids, however, insulin also acts as an important peripheral satiety signal. The concentration of circulating insulin is elevated in response to carbohydrate intake, but also proportional to the amount of body fat. Both basal and feeding-related release of insulin is increased in obese animals. Central administration of insulin not only reduces food intake in rodents (1), but also potentiates the secretion of other satiety factors, such as cholecystokinin (CCK) (2). Thus, increase of circulating insulin levels maintains the normal glucose levels in the blood but also influences the brain to limit further food intake and weight gain.

In addition to insulin, other anorectic hormones such as glucagon and amylin are also released from the pancreatic islets.

2.1.2. Leptin

Among the peripheral feeding-related hormones, leptin has the most profound and most widespread effects on the energy homeostasis. The largest source of circulating

leptin is the white adipose tissue (3). The importance of leptin is underlined by the observation that the leptin deficient (ob/ob) mice, in which the gene encoding leptin has an autosomal recessive mutation, develop robust hyperphagia and morbid obesity (4). In addition to its effect on food intake, leptin deficiency also reduces energy expenditure and decreases fertility. The mutation of leptin or leptin receptor genes also results in very similar phenotype in humans (5, 6)

Basically, the expression of leptin is determined by the amount of adipose tissue (7). Under physiological conditions, serum leptin levels rise when the size of the adipose tissue is increased, and fall during starvation (8). Beside the amount of the adipose tissue, several hormones, cytokines, nutrients and the peripheral nervous system also play important role both in the long- and short-term regulation of circulating leptin levels (9).

These factors can regulate the synthesis and/or the release of leptin. Insulin has been shown to stimulate the leptin gene expression. However, insulin activates the leptin promoter only 48 h after the treatment (10). Interestingly, the incubation of rat adipocytes with insulin for 1-2 hours does not affect the leptin mRNA levels, though stimulate leptin secretion (11). Glucocorticoids also regulate the expression of leptin in a stimulatory fashion (9). Furthermore, several neuropeptides, like melanin concentrating hormone have stimulatory effect on leptin production (12). In contrast, tumor necrosis factor-α decreases the leptin expression (13), while both stimulatory and inhibitory effects of neuropeptide Y (NPY) have been reported (14, 15), suggesting the complexity of the regulation of leptin gene expression.

Short term control of leptin levels occurs primarily through the regulation of leptin secretion. Insulin (11, 16) and noradrenaline (17) are known to be important regulators of this process.

During a short, 24 hour starvation, the circulating levels of leptin dramatically decrease despite the fact that the mass of adipose tissue do not change during this period (18). This happens because of the decrease of leptin secretion from the pool stored in the adipocites. This effect of starvation is mediated by the increased noradrenaline release from the sympathetic innervations of adipose tissue and by the fall of circulating insulin levels. Some authors (9) propose the importance of the rapid secretion of leptin from preformed pools that is stimulated by the rise in insulin and the decrease of

noradrenaline after meal, although serum leptin levels are elevated only 3 hours after meal (19-21). Thus, this mechanism may permit more rapid changes in circulating leptin than would be possible with alterations in *de novo* synthesis.

2.1.3. Gastrointestinal hormones

During ingestion and digestion the brain receives information about the size and quality of meal from mechano- and chemosensitive receptors located along the alimentary tract, but the gastrointestinal tract also signals toward the CNS by secretion of a long list of hormones.

Until now, ghrelin, the only known orexigenic peripheral hormone, is synthesized in the oxyntic cells of the stomach (22). Ghrelin was discovered as an endogenous ligand of the growth hormone secretagogue receptor. However, its potent orexigenic effect was also soon recognized. Both peripheral and central injection of ghrelin cause rapid increase of food intake (23). This effect also sustains during chronic administration and results in weight gain (24). The concentration of ghrelin is the highest just before meal and decreases after food intake (25-28). This decrease is proportional to the amount of ingested food (29, 30). In rats and humans, spikes of ghrelin levels can be observed at the usual meal times, and these periods can be shifted by personal routines (28, 31). Therefore, ghrelin is considered as meal initiating hormone.

Another feeding-related hormone of the gastrointestinal tract is CCK that is widely expressed throughout the gastrointestinal tract but has highest expression in the mucosa of the duodenum and jejunum (32). CCK acts as a short term satiety factor (33, 34). CCK administration decreases the size of meals, but it is compensated by the increase of meal frequency (35). Therefore, chronic CCK administration has no effect on the daily calorie intake (35, 36). Long term administration of CCK also does not result in weight loss (35, 36). Interestingly, CCK may interact with other long term satiety signals, such as leptin and insulin (37). The release of CCK is stimulated by protein and fat ingestion (38, 39). CCK levels start increasing 15 min after food intake, peak at 25 minutes and diminish after 3 hours (38).

Peptide YY (PYY) is synthesized in the endocrine cells of the ileum and the colon (40). After synthesis, the first two aminoacids are rapidly cleaved by dipeptidyl peptidase IV, resulting in the active $PYY_{3–36}$ (41). Administration of PYY_{3-36} reduces

food intake and body weight in both animals and humans (42). Beside its effect on food intake, PYY_{3-36} also reduces gastric emptying, inhibits jejunal and colonic motility and causes intestinal vasoconstriction (42, 43). The level of PYY_{3-36} begins to rise 15 minutes after the start of food intake, suggesting that the upregulation of PYY_{3-36} secretion is independent from the presence of food in the intestinal lumen (42). The highest concentration is achieved after 90 minutes and remains high for 6 hours (44). PYY has been suggested to play critical role in the weight loss after gastric bypass surgery.

Glucagon-like peptide-1 (GLP-1) decreases food intake by enhancing satiety (45, 46). The hormone is synthesized by the L-cells of the distal ileum, and colon, and has short half-life (47, 48). GLP-1 secretion is stimulated by nutrients, gut hormones and intrinsic neuronal signals of the gut (49, 50).

2.2. Vagus nerve

Due to its widespread projection field, the vagus nerve is positioned to mediate peripheral signals from the entire gastrointestinal tract to the CNS. Basically, the vagus nerve mediates two types of information: the sensory information of the mechano- and chemoreceptors, and the effects of certain gastrointestinal hormones.

The vagus nerve innervates all of the visceral organs, including the entire alimentary tract. After ingestion, the presence of the food is detected by the vagal mechanosensors in the mucosa of the gastrointestinal tract (51). In addition, the volume of the ingested meal is sensed by the stretch and tension sensitive receptors located in the external muscle layers of the stomach (52). The vagal afferents in the gastric mucosa also detect locally released hormones, such as leptin and ghrelin (53-57). Though both leptin and ghrelin have receptors in the CNS (58, 59), and can directly act on cells of the hypothalamus (58, 59), it has been shown that the effects of these hormones are partly mediated through the vagus nerve. The secretion of leptin in the wall of stomach is rapidly upregulated by food intake and high dose of exogenous CCK (60). Though the sensory information from the stomach seems to be strictly volumetric, growing body of evidence shows that locally expressed leptin and ghrelin can also modulate appetite and satiation suggesting a more complex regulatory mechanism.

The small intestine also detects the nutrients of the ingested food. The tissue of the upper small intestines are innervated by vagal afferents and detect mechanical touch, stretch and distension, but none of the vagus nerve cross the basal membrane to innervate the epithelial layer, thus the vagal afferents are not able to sense the nutrients directly (61). Several studies suggest that nutrients, particularly lipids and proteins activate vagal afferents via the release of CCK (34, 61, 62). Glucose is a poor stimulator of CCK release, thus the role of another messenger is suggested (61). The importance of the vagus nerve in CCK signaling is proved by the presence of CCK-1 receptors on the surface of the vagal afferents, and by the inability of CCK to influence food intake after vagotomy (63, 64).

In lower part of small intestine, the vagus nerve carries information originating from mechanoreceptors, but also mediates the effects of PYY_{3-36} and GLP-1. Though the receptors of PYY_{3-36} are present in the arcuate nucleus, there is evidence, that the vagus nerve has an important role in the mediation of its anorectic effect, since vagotomy abolishes the anorectic effect of PYY_{3-36} (42, 65).

However, GLP-1 receptors are located in the brainstem, due to the extremely short half-life of GLP-1, it is unlikely that significant amount of peripherally released GLP-1 can reach the brain (66). Though only a small number of GLP-1 receptors was found on vagal afferents, vagotomy abolishes the anorexigenic effects of GLP-1 on food intake suggesting that the vagus nerve also plays critical role in the mediation of the effects of GLP-1 (66).

2.3. Feeding-related sensory regions of the brain

The main sensory regions of the brain, where the peripheral feeding-related signals are integrated, are the arcuate nucleus and the nucleus tractus solitarii (NTS). In addition to the humoral signals, the NTS also receives information from mechano- and chemoreceptors located along the gastrointestinal tract via the vagus nerve (Fig. 1)

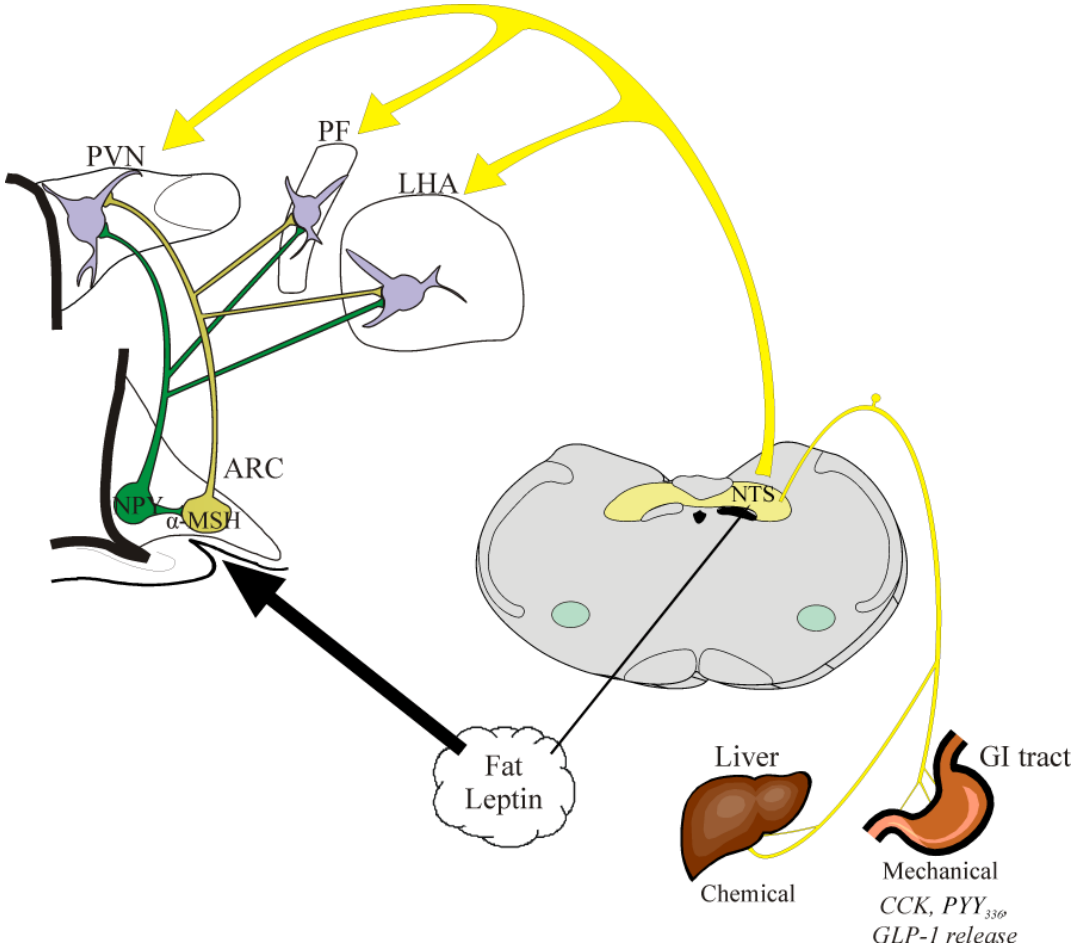

Figure 1. Schematic illustration of the main participants in the regulation of energy homeostasis. Leptin (secreted by adipocites) primarily influences the regulation of energy homeostasis through neurons of the arcuate nucleus (ARC). Leptin exerts opposite effects on the antagonistic feeding-related neuron groups in the arcuate nucleus, since leptin is known to stimulate alpha-melanocyte-stimulating hormone (α-MSH) and inhibit neuropeptide Y (NPY) synthesis in the nucleus. These neurons project to higher order nuclei that are involved in the regulation of food intake (PVN, hypothalamic paraventricular nucleus; PF, perifornical area; LHA, lateral hypothalamic area). Input of gastrointestinal (GI) hormones, such as cholecystokinin (CCK), peptide $YY_{3–36}$ ($PYY_{3–36}$) and glucagon-like peptide-1 (GLP-1) and the signals of mechano- and chemoreceptors located along the GI tract are transmitted through the vagus nerve and sympathetic fibres to the nucleus tractus solitarii (NTS). Since the NTS is also connected with forebrain areas, such as the PVN, the integration of satiety and energy homeostasis information probably involves multiple brains areas.

2.3.1. Arcuate nucleus

The arcuate nucleus is a major central target of peripheral satiety-related hormones. However, it is controversial, how these hormones can enter the nucleus, because of the presence of the blood-brain barrier (BBB) in the arcuate nucleus is disputed. In newborn rodents, the BBB of the arcuate nucleus is not fully developed, therefore, peripheral administration of the excitotoxic monosodium glutamate results in ablation of neurons in this part of the brain (67, 68). In adult animals, however, the arcuate nucleus considered to be inside the BBB. On the other hand, Norsted et al. (69) has shown that some capillaries in the ventromedial part of the arcuate nucleus lack markers of BBB suggesting that peripheral hormones have direct access to this part of the nucleus. Meanwhile, leptin has been shown to enter the arcuate nucleus by saturable transport indicating the presence of transport molecules that can carry the leptin molecules through the BBB (70).

The arcuate nucleus plays pivotal role in the regulation of energy homeostasis. Chemical ablation of the arcuate nucleus causes obese phenotype, and leptin resistance (71-73). The nucleus contains two antagonistic feeding-related neuronal populations. In the lateral part of the arcuate nucleus, two anorexigenic neuropeptides, alpha-melanocyte-stimulating hormone (α-MSH) and cocaine- amphetamine-regulated transcript (CART) are synthesized in the same neuronal population (74, 75). The importance of α-MSH in energy-homeostasis is underlined by the facts that deficiency of proopiomelanocortin (POMC), the precursor of α-MSH, is characterized by early-onset obesity, hyperphagia beside adrenal insufficiency in mice (76). Toxin induced ablation of POMC neuron in transgenic animals leads to hyperphagia and consecutive obesity (77). Additionally, due to the absence of ACTH and peripherally synthesized α-MSH, POMC KO mice have hypocortisolism and altered pigmentation (77). POMC deficiency was also described in humans (78). Due to the lack of POMC neurons, these patients are obese and hyperphagic, while the loss of peripheral POMC expression leads to pale skin and striking red hair (79). Additionally, as peripheral effects, they suffer from hypocortisolemia, prolonged jaundice and susceptibility to the effects of infection (80). The deficiency of melanocortin 4 receptor (MC4R), a centrally expressed receptor of α-MSH, causes similar obesity phenotype (81, 82). MC4R deficiency is one of the most common human monogenic diseases (80). It was reported in 6% of patients with

severe, early-onset obesity (83). These patients have increased fat and lean mass, with accelerated linear growth, as it was described in mice (80). The selective disruption of the other centrally expressed receptor of α-MSH, the melanocortin 3 receptor (MC3R) also leads to altered energy homeostasis. Although MC3R KO mice have normal weight, the lean mass of these animals is decreased that is accompanied by an increase of fat mass (84, 85). Interestingly, double MC3R/MC4R KO mice have greater body weight, than the single MC4R mutants (85). The deficiency of CART also lead to significantly higher body weight without the increase in food consumption, however, only in adult, 40 wk old mice (86). Unfortunately, no CART receptors have been identified so far.

Neurons in the ventromedial part of the nucleus synthesize NPY and agouti-related protein (AGRP) (87, 88). Both neuropeptides are potent orexigenic factors (89-91), and the latter is synthesized exclusively in this part of the brain. The crucial role of the NPY/AGRP neurons was substantiated by toxin-mediated ablation of these neurons in adult transgenic mice resulting in an extremely hypophagic and hypermetabolic phenotype (77, 92). Interestingly, single or double NPY- and/or AGRP-KO mice have normal feeding behavior, normal body weight and maintain a normal response to starvation (93, 94). Moreover, the toxin-mediated ablation of AGRP neurons in newborn mice results in only a slight reduction in body weight and food consumption (92). These data suggest that NPY/AGRP neurons are essential in the regulation of food intake of adult mice, but compensatory mechanisms exists which can replace their role in the developing CNS.

The orexigenic effect of NPY is mediated by both the Y1 and Y5 receptors that are coupled to inhibitory G proteins (95). Interestingly, although the activation of Y1 and Y5 receptors lead to hyperphagia (96, 97), the Y1R-KO and Y5R-KO mice develop late-onset obesity, with increased food intake and adiposity (98). The mechanism leads to this phenotype is currently unknown. The effect of AGRP is mediated by MC3R and MC4R (99). The AGRP acts on these receptors as a competitive antagonist of α-MSH (99, 100).

Both of these energy homeostasis-related neuronal groups of the arcuate nucleus express receptors for peripheral feeding-related signals, such as leptin, ghrelin and insulin (58, 59, 101). Leptin exerts opposite effects on these two neuron populations. It

inhibits the electrophysiological activity and peptide-synthesis of the NPY/AGRP neurons (102-104), while stimulates the synthesis of α-MSH and CART in the anorexigenic neurons, and directly depolarizes these cells (105-107). In fed state, the normal concentration of circulating leptin stimulates the anorexigenic neurons and at the same time inhibits the orexigenic cells. In contrast, during fasting, the fall of leptin levels results in increased expression of NPY and AGRP (102, 108) and decreased production of α-MSH and CART (105, 106). Both changes can be reversed by administration of leptin to fasted animals.

Similarly to leptin, insulin also activates α-MSH/CART neurons (108), primarily through the phosphoinositide 3-kinase (PI3K) pathway (109). Insulin deficiency is associated with increased NPY synthesis, and insulin administration can prevent the fasting-induced increase in NPY expression in the arcuate nucleus neurons (108). Accordingly, the fall of POMC mRNA in response to fasting can be reversed by central insulin injection (108). Interestingly, insulin has no effect on AGRP and CART synthesis (108).

Ghrelin receptors are also expressed on the surface of NPY/AGRP and α-MSH/CART neurons (59), and there is evidence, that the feeding-related neurons of the arcuate nucleus are regulated oppositely by ghrelin and leptin (59).

The orexigenic and anorexigenic neurons of the arcuate nucleus have a greatly overlapping projection field (110). Moreover, it has been shown that axons of the two neuronal groups converge on the very same target neurons (111). This way, the NPY/AGRP and the α-MSH/CART neurons act together on the second-order neurons to regulate food intake and energy expenditure.

2.3.2. Nucleus Tractus Solitarii

The NTS receives inputs from all visceral organs, and serves as the primary central integrator of the vagus nerve-mediated information. The afferent fibers establish an organ-specific projection pattern that determines the role of the NTS subnuclei. The gastrointestinal afferents preferentially terminate in the medial part of the intermediate NTS, but a population of fibers also projects to the medial and commissural parts of the NTS (112).

Several feeding-related neuropeptides are synthesized in these regions of the NTS, such as NPY, CART and pituitary adenylate cyclase activating polypeptide (PACAP) (113-116). Interestingly, the expression of NPY in the NTS is independent from fasting and refeeding, but activated by restricted feeding (117). A distinct neuronal group in the commissural part of the NTS expresses α-MSH (118). These neurons are suggested to regulate energy homeostasis independently from leptin, because leptin is not able to prevent the fasting-induced suppression of POMC mRNA in the NTS (119). In contrast, GLP-1-synthesizing neurons that are located at the ventral edge of the commissural NTS are activated by leptin administration (114). The catecholaminergic neurons of the NTS are divided to the adrenergic C2, and the noradrenergic A2 regions. The vast majority of the adrenergic neurons of the NTS express NPY and CART (113, 120), and a smaller portion of the noradrenergic A2 neurons also synthesize NPY (113).

The vagal afferents provide information about stretch and tension along the gastrointestinal tract and mediate satiety signals, such as CCK, PYY_{3-36} and GLP-1 that are generated during passage of food through the alimentary tract (61). The main role of these signals is the short-term regulation of food intake and energy expenditure (8). Though the processing of the vagus derived information is thought to be the most important function of the NTS, receptors of several feeding-related hormones are also expressed in this region, suggesting that the NTS has a more complex role in the regulation of feeding than a simple switch of meal initiation and termination. For example, leptin receptors are widely expressed in the NTS (121) and leptin has been shown to potentiate the activation of neurons in the NTS by peripheral administration of CCK (122). In addition, amylin has been demonstrated to influence food intake through area postrema-NTS pathway (123).

The NTS has a widespread projection field in the CNS. Though the NTS does not send projections to the periphery, it can influence the regulation of the gastrointestinal tract via the dorsal motor nucleus of vagus (112). The NTS transmits peripheral signals to limbic and hypothalamic structures. Several of its projection fields are linked reciprocally, probably to function as a feedback mechanism (112). Parallel to the direct pathways, the parabrachial nucleus and the C1 region serve as an important relay station to mediate the ascending information from the NTS (112).

2.4. Energy homeostasis-related neurons of the hypothalamic paraventricular nucleus

The hypothalamic paraventricular nucleus (PVN) has a critical role in the maintenance of energy homeostasis. The importance of this nucleus is underlined by earlier studies, in which PVN stimulation resulted in inhibition of food intake, and bilateral PVN lesion caused hyperphagic obesity syndrome (8). The PVN receives information from the feeding-related neurons of the arcuate nucleus and the NTS. It integrates these informations and is connected with higher order neuronal structures, but also send information to the anterior pituitary through projection of hypophysiotropic neurons to the median eminence (8).

The PVN contains two neuronal populations that have critical role in the maintenance of energy homeostasis: the corticotropin-releasing hormone- (CRH) synthesizing neurons are the main central regulators of the hypothalamic-pituitary-adrenal cortex (HPA) axis (124, 125), while the hypophysiotropic thyrotropin-releasing hormone-synthesizing (TRH) neurons govern the thyroid gland through the regulation of thyrotroph cells in the anterior pituitary (126). CRH and TRH regulate energy homeostasis via the HPA and hypothalamic-pituitary-thyroid (HPT) axes, respectively, but both neuropeptides also have central effects on energy homeostasis. Both the hypophysiotropic CRH and TRH neuron populations receive information from several parts of the brain and act as a final common pathway in the regulation of the HPA and HPT axis, respectively (Figs. 2,3).

2.4.1. Hypophysiotropic CRH neurons

CRH neurons primarily regulate energy homeostasis and food intake via the HPA axis but CRH, itself, also has central anorexigenic effects (127). Central injection of CRH decreases food intake (128), while administration of the CRH antagonist, α-helical CRF(9-41), focally into the PVN potentiates the NPY-induced food intake (129).

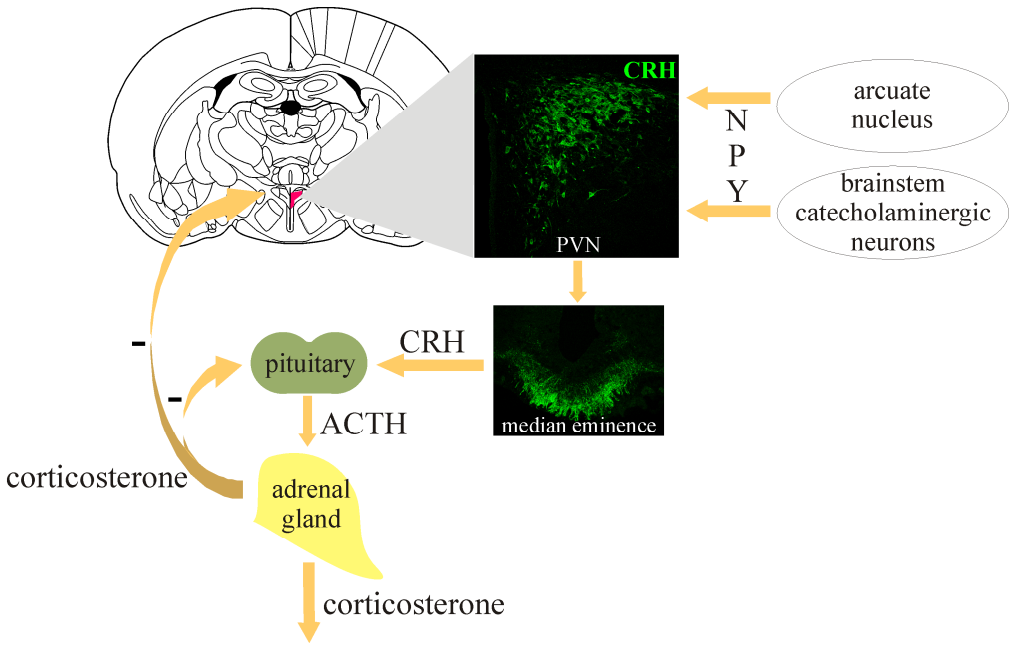

Figure 2. Schematic demonstration of the hypothalamus-pituitary-adrenocortical axis in rats. Corticotropin-releasing hormone (CRH) synthesizing neurons located in the hypothalamic paraventricular nucleus (PVN) project to the median eminence and secrete CRH into the portal capillaries. CRH controls the release of corticosterone through the regulation of adrenocorticotropic hormone (ACTH). Corticosterone exerts negative feedback on the pituitary and the PVN. Neuropeptide Y (NPY) is one of the most important regulators of the hypophysiotropic CRH neurons. The arcuate nucleus and the catecholaminergic neurons of the brainstem are the main sources of the NPY innervation of the PVN, however the rate of their contributions are unknown.

Glucocorticoids, the products of the HPA axis, increase blood-glucose levels. This effect of glucocorticoids is partly achieved by the stimulation of food intake and increase in the transcription of phosphoenolpyruvate carboxykinase in the liver, a key enzyme of the gluconeogenic pathway (130). In addition, glucocorticoids decrease glucose uptake of the skeletal muscles and increase protein degradation. Adenosine monophosphate-dependent kinase (AMPK), which is a sensor of the cellular energy status, is regulated by glucocorticoids in a tissue dependent manner, suggested to be an important mediator of their effects. The glucocorticoid-induced inhibition of AMPK in the hepatic and adipose tissue is involved in the increased deposition of lipids (131). The importance of glucocorticoids is suggested by the fact that a modest increase in the activity of 11β-HDS 1 enzyme (which produces glucocorticoids from their inactive 11-keto forms) results in hyperphagia with increased adiposity, hyperglycemia, glucose intolerance, insulin resistance (132).

Glucocorticoids also influence the CNS. In contrast to their effect on AMPK in adipose tissue, these hormones stimulate AMPK activity in the hypothalamus to increase appetite and calorie intake (131). Glucocorticoids also potentiate the orexigenic effects of NPY, and also stimulate NPY release *in vitro* and in the hypothalamus of female rats *in vivo* (133). Though glucocorticoids stimulate leptin secretion (134), simultaneously reduce the efficacy of leptin to suppress food intake suggesting a complex interaction between leptin and glucocorticoids (133).

The regulation of the HPA axis during fasting is not fully understood. Although the circulating levels of adrenocorticotropic hormone (ACTH) and corticosterone are elevated during fasting (135-137), CRH mRNA level is suppressed in the PVN (111, 138). This discrepancy raises the possibility that during fasting, factors other than CRH activate the peripheral parts of the HPA axis, while the inhibition of the anorexigenic CRH may be important to preserve energy and potentiate the effects of orexigenic signals.

This inhibition of CRH gene expression can be prevented by administration of leptin to fasted animals (58, 139). As leptin administration prevents this fasting induced inhibition of CRH expression even before it normalizes the peripheral glucocorticoid levels, it is unlikely that the leptin induced regulation of CRH gene expression is mediated by the feedback effect of glucocorticoids.

The dense α-MSH/CART and NPY innervations of CRH neurons suggest that leptin may regulate the CRH neurons through the arcuate nucleus-PVN pathway (140, 141). This is further supported by the stimulatory effects of the anorexigenic peptides on the CRH gene expression. Similarly to leptin, central administration of α-MSH can prevent the fasting induced inhibition of CRH gene expression (142) and the stimulatory effect of CART on the CRH neurons has also been demonstrated (143). The direct effect of α-MSH on the CRH neurons is indicated by the presence of MC4R in approximately 30% of the hypophysiotropic CRH neurons (144). Because, more than 50% of CRH neurons are contacted by α-MSH-containing axons (145), the remaining population of the CRH neurons may express MC4R under the detection threshold, or express MC3R.

When the animals are satieted, the level of leptin is elevated in the circulated blood (8). The resulted increase of the synthesis and release of α-MSH and CART may play an important role in the mediation of the effect of leptin on the CRH neurons.

The role of NPY in the regulation of CRH seems to be paradox. Acute icv. administration of NPY elevates CRH mRNA level in the PVN (146, 147), but during fasting when the NPY neurons are activated in the arcuate nucleus and there is an increased NPY release in the PVN, CRH mRNA levels are decreased in the hypophysiotropic neurons (138, 142). This discrepancy suggests that either the NPY neurons of the arcuate nucleus are not involved in the innervation of hypophysiotropic CRH neurons or prolonged administration of NPY may have different effect compared to that observed after acute administration.

The arcuate nucleus is not the only source of the NPY innervation of the PVN (Fig. 2). Other significant sources of this innervation are the catecholamine-producing cells of the brainstem that synthesize either adrenaline (C1–C3 cell groups) or noradrenaline (A1, A2, and A6 cell groups) (113). Using immunohistochemical methods, the adrenergic and noradrenergic neurons can be separated based on their catecholamine-synthesizing enzyme content. The noradrenergic neurons express only dopamine-β-hydroxilase (DBH), an enzyme which synthesizes noradrenaline, while the adrenergic neurons co-express DBH and phenylethanolamine-N-methyltransferase (PNMT), an enzyme that converts noradrenaline to adrenaline.

2.4.2. Hypophysiotropic TRH neurons

Similarly to the HPA axis, the HPT axis also plays critical role in the maintenance of energy homeostasis. The HPT axis is primarily governed by the hypophysiotropic TRH neurons that are located in the medial and periventricular parvocellular subdivisions of the PVN in rats (126, 148).

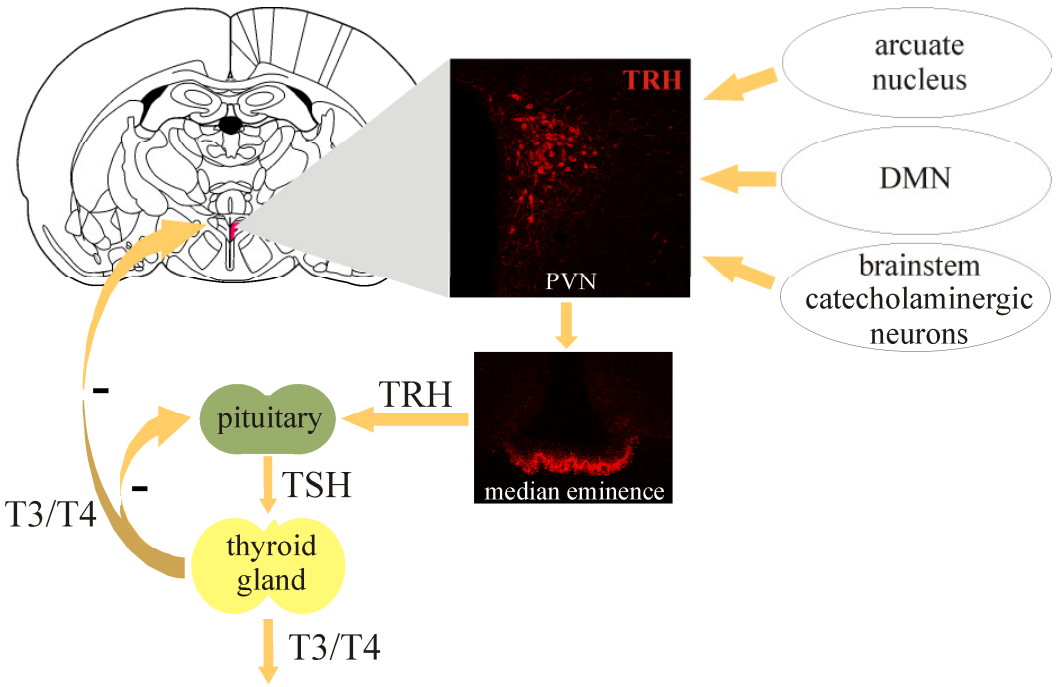

Figure 3. Schematic illustration of the hypothalamic-pituitary-thyroid axis in rats. Thyrotropin-releasing hormone (TRH) synthesizing neurons are residing in the hypothalamic paraventricular nucleus (PVN). TRH is secreted into the portal capillaries of the median eminence, and then stimulate T3/T4 release from the thyroid gland, through the activation of thyrotropin (TSH) secretion in the pituitary. T3/T4 exerts negative feedback on the pituitary and the PVN. The main central regulators of the hypophysiotropic TRH neurons are the arcuate nucleus, the dorsomedial nucleus (DMN) and the catecholaminergic neurons of the brainstem. While the arcuate nucleus and the DMN are probably involved in the mediation of feeding-related signals, brainstem catecholaminergic neurons are responsible for the transmission of the effect of certain stressors, such as cold.

The final products of the HPT axis, the thyroid hormones influence virtually all cells in the body and well-known to regulate energy homeostasis through their influence on the basal metabolic rate and adaptive thermogenesis. In most tissues, thyroid hormones raise the metabolic rate by increasing the number and size of mitochondria in the target cells, stimulating the synthesis of enzymes in the respiratory chain, increasing membrane Na^+/K^+ ATP-ase concentration and membrane Na^+ and K^+ permeability (149). In the complete absence of thyroid hormone, the basal metabolic rate decreases by approximately 30%, while hyperthyroidism is associated with an increase in metabolic rate and acceleration of practically all metabolic pathways (150). Chronic treatment of animals with thyroid hormones leads to an increased heat production, while

hypothyroidism has the opposite effect (151). The thermogenic effects of the thyroid hormones are primarily exerted in the brown adipose tissue (BAT) and in muscles by increasing the activity of the uncoupling proteins (UCP-1 and UCP-3, respectively) that dissociate the respiratory chain, thus the mitochondrial combustion is uncoupled from ATP synthesis (151, 152).

Hyperthyroidism is associated with increased appetite that is suggested to compensate the elevated energy expenditure (153). Interestingly 5-10% of hyperthyroid individuals have sufficiently increased appetite to gain weight, despite the stimulated catabolic processes. These data raise the possibility that thyroid hormones regulate food intake directly, not just through a compensatory mechanism. This hypothesis is supported by the data showing that peripheral administration of 3,5,3'-triiodothyronine (T3) stimulates the expression of immediate early genes in the ventromedial nucleus (VMN) known to play role in the regulation of energy homeostasis (154). Moreover, T3 injection directly into the VMN leads to a four-fold increase of food intake in the first hour after injection (154), suggesting the importance of the VMN in the mediation of thyroid hormone-induced food-intake.

One of the major regulatory mechanisms over HPT axis is the negative feedback effect of thyroid hormones that is critical to maintain euthyroid hormone levels in the circulating blood (155). Thyroid hormones inhibit both the gene expression and the posttranslational processing of proTRH in hypophysiotropic neurons, but have no effect on other proTRH-synthesizing neuronal groups of the forebrain (156, 157). Moreover, low level of circulating thyroid hormones is accompanied by increased proTRH gene expression and increased synthesis of prohormone convertase enzymes, which are essential in the maturation of TRH, in the PVN (158).

Under certain circumstances, the setpoint for feedback inhibition of hypophysiotropic TRH neurons can be altered by neuronal inputs to achieve the necessary increase or decrease of the metabolic rate and adapt to the changing physiological or pathophysiological conditions (155). For example, the fasting induced inhibition of the HPT axis is mediated by the arcuato-paraventricular pathway, while the cold-induced activation of the axis is mediated through the adrenergic innervations of the TRH neurons (155).

The afferents of the hypophysiotropic TRH neurons arise from at least three different brain regions: the arcuate nucleus, the hypothalamic dorsomedial nucleus, and the catecholaminergic neurons of the brainstem (Fig 3) (155).

The arcuate nucleus is a crucial regulator of the hypophysiotropic TRH neurons, since the ablation of the arcuate nucleus abolishes response of the hypophysiotropic TRH neurons to fasting and leptin administration (73).

Both anorexigenic and orexigenic neuron populations of the arcuate nucleus send projections to the TRH neurons (111). All TRH neurons in the PVN are innervated by CART, but only 34 % of the TRH neurons in the medial and 70 % in the periventricular subdivision of the PVN is juxtaposed to α-MSH containing boutons (111). The explanation of this discrepancy is that CART neurons of the brainstem contribute to more than 60 % of the CART innervation of the TRH neurons in the PVN, while all of the α-MSH innervations of these cells originate from the arcuate nucleus (159). Practically all of the TRH neurons receive NPY and AGRP innervation and these fibers establish symmetrical synapses on the soma and dendrites of the TRH neurons (160). About 80 % of the NPY innervation of the TRH neurons originates from the arcuate nucleus, and these neurons co-express AGRP (160). Nevertheless, all of the TRH neurons that are innervated by α-MSH/CART axons also receive projections from the NPY/AGRP neurons (111).

Both α-MSH and CART have an activating effect on TRH gene expression (111, 120, 161, 162). Moreover, the decreased level of TRH mRNA in the PVN can fully restored by the central administration of α-MSH or CART to fasting animals (111, 120). Since all melanocortin receptors are coupled in a stimulatory fashion to cAMP (163), α-MSH administration dramatically increases the phosphorylation of cAMP response element binding protein (CREB) in TRH neurons located in the PVN (164). Since the TRH promoter contains a cAMP response element, CREB phosphorylation increases TRH transcription (165). It is further supported by the data that the mutation of CREB binding site in the TRH promoter markedly decreases the stimulatory effect of α-MSH on TRH expression (166). In contrast, CART receptors and the signaling mechanism by which CART activates the TRH neurons are unknown.

In contrast to the anorexigenic peptides, NPY has potent inhibitory effects on the TRH neurons. Central administration of this peptide to fed animals results in central

hypothyrioidism characterized by decreased TRH gene expression in the PVN and fall of peripheral thyroid hormone levels (167). In addition, physiological studies demonstrated that both Y1 and Y5 receptors mediate the effects of NPY on the HPT axis (168), and the presence of Y1 receptor has been demonstrated on the surface of the TRH neurons (169, 170). The effect of AGRP on the hypophysiotropic TRH neurons is similar to NPY, AGRP administration to fed animals also results in a central hypothyroidism (171). AGRP acts on the MC4R and MC3R and serves as an inverse agonist of α-MSH on these receptors (99, 100, 172). As AGRP does not alter the HPT axis in MC4R KO mice, it is suggested that this peptide primarily inhibit TRH expression via the MC4R (173).

The effects of the anorexigenic and orexigenic peptides of the arcuate nucleus converge on the hypophysiotropic TRH neurons and interact at several levels. This is supported by the fact that each α-MSH/CART innervated TRH neurons receive and NPY/AGRP projections (111). Moreover, α-MSH and AGRP act on the very same melanocortin receptors of the TRH neurons (99, 100, 172). These peptides also interact at the level of the second messengers. Since the melanocortin receptors are linked to G_S proteins that stimulate the cAMP-CREB second messenger pathway (163) and the Y1 and Y5 receptors are coupled to G_I proteins (95), known to decrease cAMP levels, CREB seems to be the final common pathway in the signalling of α-MSH, AGRP and NPY. This is supported by the data that central administration of NPY reduces the α-MSH-induced CREB phosphorylation in the TRH neurons (174).

In addition to the PVN, the arcuate nucleus also sends projections to the dorsomedial nucleus (DMN) (175). This nucleus contains a dense network of α-MSH and AGRP fibers (176, 177). Using tract tracing methods it was demonstrated that the vast majority of the TRH neurons residing in the PVN receive innervation arising from the DMN (178). Since a remarkable portion of the PVN projecting neurons in the DMN is contacted by α-MSH-containing boutons, it is possible that the DMN acts as an alternative pathway in the mediation of the effects of leptin on the hypophysiotropic TRH neurons (155).

The axon terminals originating from the catecholaminergic neurons of the brainstem contribute to approximately 20% of all synapses on TRH neurons in the PVN (179). Both DBH and PNMT-synthesizing catecholaminergic axons have been shown to

establish asymmetric synapses with the TRH neurons in the PVN, suggesting their excitatory function (180). Although this massive innervation would indicate that the brainstem catecholaminergic neurons have a widespread role in the regulation of TRH neurons, until now, the only known role of this neuron population in the regulation of TRH neurons is the mediation of cold-induced activation of the hypophysiotropic TRH neurons.

Several neuropeptides are co-synthesized in the catecholaminergic neurons of the brainstem that projects to the PVN. These neuropeptides may modulate the effects of catecholamines on their target neurons. NPY, which is known to inhibit the TRH neurons, is synthesized in the vast majority of the adrenergic neurons, while only a smaller portion of the noradrenergic neurons co-express NPY (113). The other catecholamine co-transmitters are expected to stimulate TRH gene expression, such as CART, which is expressed in the adrenergic C1-3 regions of the brainstem (115) and PACAP that is synthesized in the C1 region (116). The difference in the neuropeptid content of the adrenergic and noradrenergic neurons would suggest distinct role of the catecholaminergic neuron populations in the regulation of the TRH neurons. Nevertheless, the rate of adrenergic and noradrenergic innervation was not described, moreover, the existence of the noradrenergic input was not proved.

2.4.3. Non-hypophysiotropic TRH neurons located in the anterior parvocellular subdivision of the PVN

In addition to the hypophysiotropic TRH neuron population located in the periventricular and medial parvocellular subdivisions of the PVN, this nucleus also houses non-hypophysiotropic TRH neurons (126, 148). These cells are situated in the anterior, ventral, lateral parvocellular subdivisions and in the dorsal cap of the PVN (181). The TRH mRNA expression of the non-hypophysiotropic TRH neurons is independent from the negative feedback effect of the thyroid hormones (156, 157). In the anterior parvocellular subdivision of the PVN (aPVN) the non-hypophysiotropic TRH neurons are densely innervated by axons containing feeding-related neuropeptides, such as α-MSH, CART, NPY, AGRP and galanin-like peptide, suggesting that the aPVN TRH neurons play a role in the regulation of energy homeostasis (111, 177). Since these neurons do not project to the median eminence, it is likely that TRH

released from these neurons exerts its effects independently from the HPT axis. However, the pathways and the projections by which the TRH neurons in the aPVN may regulate energy homeostasis are unknown.

The perifornical area houses another non-hypophysiotropic TRH neuron population in the close proximity of the aPVN. As in contrast to the TRH neurons of the aPVN, the preifornical TRH neurons express enkephalin and urocortin 3, it is suggested that these two TRH neurons populations are functionally different (182, 183). However, the well known role of urocortin 3 in the regulation of energy homeostasis suggests that these neurons may also play role in the central regulation of energy homeostasis (184, 185).

3. Specific aims

1. Determine the relative contribution of the arcuate nucleus and the brainstem catecholaminergic neurons in the NPY innervation of the hypophysiotropic CRH neurons

2. Examine the effect of chronic NPY administration on the CRH gene expression of the hypophysiotropic neurons

3. Elucidate the relative contribution of the brainstem adrenergic and noradrenergic neurons in the innervation of the hypophysiotropic TRH neurons

4. Reveal the efferent projections of the TRH neurons located in the aPVN

4. Materials and Methods

4.1. Animals

All experiments were carried out on adult male Wistar (TOXI-COOP KKT, Budapest, Hungary) and Sprague-Dawley rats (Taconic Farms, Germantown, NY) weighing 260-400 g, housed under standard environmental conditions (light between 0600 and 1800 h, temperature 22 ± 1 °C, rat chow and water *ad libitum*). All experimental protocols were reviewed and approved by the Animal Welfare Committee at the Institute of Experimental Medicine of the Hungarian Academy of Sciences and Tufts-New England Medical Center.

4.2. Tissue preparation for immunocytochemistry

Because colchicine-treatment is necessary to visualize the perikarya and dendrites of hypophysiotropic CRH and TRH neurons and our preliminary studies indicated that a low dose of colchicine (40 µg/animal) does not alter the staining pattern of DBH, PNMT, AGRP, or NPY axons in the PVN, we used colchicine-treated rats for our studies (4.5.2.; 4.5.5.; 4.7.2.; 4.8.2.). The animals were deeply anesthetized with ketamine-xylazin (ketamine: 50 mg/kg body weight; xylazine: 10 mg/kg body weight, ip) and injected icv. with 40 µg colchicine in 2 µl 0.9% saline under stereotaxic control. After 20 h, the animals were transcardially perfused.

Depending on the optimal conditions of the used antisera, different fixative solutions were used for transcardial perfusion of the animals. In all experiments, the first step was a quick perfusion of the animals with 20 ml 0.01 M phosphate buffered saline (PBS, pH 7.4), which was followed sequentially by 100 ml 2% paraformaldehyde/4% acrolein in 0.1 M PB (pH 7.4) and 50 ml 2% paraformaldehyde (PFA) in the same buffer in experiments 4.5.2. and 4.5.4.; or 100 ml 3% paraformaldehyde/1% acrolein in 0.1 M phosphate buffer (PB, pH 7.4) and 50 ml 3% paraformaldehyde in the same buffer in experiment 4.8.2.; or 150 ml 4% paraformaldehyde in 0.1 M PB (pH 7.4) in experiments 4.5.5., 4.6.2., 4.7.1. and 4.8.1.. The brains were rapidly removed, and blocks containing the hypothalamus were cryoprotected in 30% sucrose in 0.01 M PBS (pH 7.4) overnight

at 4 ºC and snap frozen on dry ice. Serial 30 µm thick coronal sections were cut through the PVN on a freezing microtome (Leica Microsystems, Wetzlar, Germany), collected in freezing solution (30% ethylene glycol, 25% glycerol, 0.05 M PB) and stored at –20 ºC until used.

4.3. Section preparation for immunocytochemistry

The basic preparation method is described in this section; the specific steps used in the different experiments are delineated in the description of each experiment. If the perfusion solution of the animals contained acrolein, the sections were treated with 1% sodium borohydride in distilled water for 30 min and washed in PBS until the sections sank to the bottom of washing dish. If the animals were perfused only with PFA, this step was omitted. Then the sections were treated with 0.5% Triton X-100/0.5% H_2O_2 in PBS for 20 min. To reduce nonspecific antibody binding, the sections were treated with 2% normal horse serum in PBS for 20 min. Between treatments, the sections were washed in PBS for 30 min (3 x 10 min). The sections were then incubated in a mixture of primary antibodies for 3 days at 4 ºC. The used primary and secondary antibodies and fluorochrome-conjugated reagents (listed in Table 1.) were diluted in PBS that contained 2% normal horse serum and 0.2% sodium azide. The sections were mounted onto glass slides and coverslipped with Vectashield (Vector Laboratories, Burlingame, CA) mounting medium.

Table 1. Summary of the antibodies and reagent used in different experiments

	Used primary antibodies	*Dilution*	*Fluorochrome*
4.5.2. Quadruple-labeling immunofluorescence for DBH, PNMT, NPY, and CRH			
	murine monoclonal antibody to **DBH** (Cat# MAB308, Millipore, Billerica, MA)	1:150	CY^3
	rabbit anti-**PNMT** serum (gift from Martha C. Bohn, Northwestern University Medical School, Chicago, IL)	1:500	FITC
	sheep anti-**NPY** serum (gift from István Merchenthaler)	1:8,000	CY^5
	guinea-pig anti-**CRH** serum (Peninsula Laboratories Inc., San Carlos, CA)	1:3,500	AMCA

4.5.3. Validation of the arcuate nucleus ablation			
	sheep anti-**NPY** serum (gift from István Merchenthaler)	1:100,000	Ni-DAB
4.5.4. Triple-labeling immunofluorescence for DBH, NPY, and CRH			
	murine monoclonal antibody to **DBH** (Cat# MAB308, Millipore)	1:150	CY^3
	sheep anti-**NPY** serum (gift from István Merchenthaler)	1:8,000	CY^5
	guinea-pig anti-**CRH** serum (Peninsula Laboratories Inc.)	1:3,500	AMCA
4.5.5. Triple-labeling immunofluorescence for AGRP, NPY, and CRH			
	rabbit anti-**AGRP** serum (H-003-57; Phoenix Pharmaceuticals, Inc., Burlingame, CA)	1:2,500	CY^3
	sheep anti-**NPY** serum (gift from István Merchenthaler)	1:8,000	CY^5
	guinea-pig anti-**CRH** serum (Peninsula Laboratories Inc.)	1:3,500	AMCA
4.7.2. Triple-labeling immunofluorescence for DBH, PNMT, and proTRH			
	murine monoclonal antibody to **DBH** (Cat# MAB308, Millipore)	1:1,000	CY^3
	rabbit anti-**PNMT** serum (gift from Martha C. Bohn)	1:1,000	FITC
	rabbit anti-**proTRH** serum (178-199) (gift from Éva Rédei, Northwestern University, Chicago, IL)	1: 2,500	CY^5
	sheep anti-**TRH** serum (generated in our laboratory)	1:8,000	CY^5
4.8.1. Anterograde tract-tracing experiments			
	rabbit anti-**PHAL** serum (Vector Laboratories)	1:5,000	Ni-DAB
	goat anti-**PHAL** serum (Vector Laboratories)	1:1,000	FITC
	rabbit anti-**proTRH** serum (178-199) (gift from Éva Rédei)	1:2,500	CY^3
4.8.2. Retrograde tract-tracing experiments			
	goat anti-**CTB** serum (List Biological Laboratories, Campbell, CA)	1:10,000	FITC
	rabbit anti-**TRH** serum (No. 31; a gift from Dr. Ivor M. Jackson, Brown Medical School, Providence, RI)	1:2,500	CY^3

4.4. Image analysis of immunofluorescent preparations

Both quadruple-labeled and triple-labeled sections were examined using a Radiance 2100 confocal microscope (Bio-Rad Laboratories, Hemel Hempstead, UK).

The settings of the confocal microscope were the follows: laser excitation lines, 405 nm for AMCA, 488 nm for FITC, 543 nm for CY^3, and 637 nm for CY^5; dichroic/emission filters, 420–480 nm for AMCA, 560/500–530 nm for FITC, 650/565–625 nm for CY^3, and a 660-nm-long pass filter for CY^5. Images captured through a x20 objective are less than 2.1 µm thick, whereas images captured through the x60 oil lens are less than 0.8 µm thick. The series of optical slices were recorded with a 2.0 µm and 0.6 µm Z step, for x20 and x60 objectives, respectively. The series of optical sections were merged and displayed with LaserVox (Bio-Rad Laboratories) and Image Pro Plus (Media Cybernetics Inc., Bethesda, MD) software and an IBM-compatible personal computer. All presented images represent single optical slices.

4.5. Methodologies applied in studies examining the NPY-immunoreactive innervation of the CRH neurons in the PVN of rats

4.5.1. Ablation of the arcuate nucleus with neonatal monosodium glutamate treatment

To ablate the NPY neurons of the arcuate nucleus, a chemical lesion of this region was performed by monosodium glutamate (MSG) treatment. Six neonatal wistar rats were injected subcutan with MSG solution (dissolved in distilled water), using a treatment paradigm adapted from Légrádi and Lechan (186): on postnatal days 2 and 4, at a dose of 2 mg/g body weight, and on postnatal days 6, 8, and 10, at a dose of 4 mg/g body weight. Control animals were treated with the same volume of saline. The animals were studied as adults when they reached a body weight of 280–320 g.

4.5.2. Quadruple-labeling immunofluorescence for DBH, PNMT, NPY, and CRH

To elucidate the putative contribution of noradrenergic and adrenergic cell groups of the brainstem in the NPY-immunoreactive (IR) innervation of hypophysiotropic CRH neurons, quadruple-labeling immunocytochemistry was performed on every third hypothalamic sections of animals possessing an intact arcuate nucleus. After

pretreatment of sections described above, additional 10 min incubation in 0.5% Triton X-100 was applied to further improve the antibody penetration. The sections were then incubated in the following mixture of primary antibodies for 3 days at 4 °C: murine monoclonal antibody to DBH (Cat# MAB308, Millipore, Billerica, MA) at 1:150, guinea pig anti-CRH serum (Peninsula Laboratories Inc., San Carlos, CA) at 1:3500, sheep anti-NPY serum (gift from István Merchenthaler) at 1:8000, and rabbit anti-PNMT serum (a gift from Martha C. Bohn, Northwestern University Medical School, Chicago, IL) at 1:500. After rinses in PBS, the sections were incubated in a mixture of secondary antibodies for 1 day at 4 °C. The secondary antibodies were as follows: CY^3-conjugated donkey anti-mouse IgG (Jackson ImmunoResearch, West Grove, PA) at 1:200 dilution, biotinylated donkey anti-guinea pig IgG (Jackson Immunoresearch) at 1:250 dilution, CY^5-conjugated donkey anti-sheep IgG (Jackson Immunoresearch) at 1:100 dilution, and fluorescein isothiocyanate (FITC)-conjugated donkey anti-rabbit IgG (Jackson Immunoresearch) at 1:50 dilution. The sections were then rinsed in PBS and incubated in 7-amino-4-methyl-coumarin-3-acetic acid (AMCA)-conjugated avidin D (Vector Laboratories), diluted at 1:250 for 1 day at 4 ºC.

4.5.3. Validation of the arcuate nucleus ablation

The effectiveness of the chemical ablation of the arcuate nucleus was assessed by examination of hypothalamic sections from intact and MSG-treated rats (Fig.9). The sections were incubated in sheep anti-NPY serum (gift from István Merchenthaler) at 1:100,000 for 1 day at 4 ºC. After rinsing in PBS, the sections were incubated first in biotinylated donkey anti-rabbit IgG (Jackson Immunoresearch) diluted to 1:500 and, after additional washes in PBS, in avidin-biotin complex (ABC, 1:1000; Elite Kit, Vector Laboratories) for 1 h. The peroxidase reaction was developed in 0.05 M Tris buffer (pH 7.6) containing 0.025% diaminobenzidine and 0.0036% H_2O_2. Animals with more than three to five NPY cells per section were excluded from further studies. The effectiveness of the ablation was also confirmed by Nissl-staining.

4.5.4. Triple-labeling immunofluorescence for DBH, NPY, and CRH

To elucidate the effects of the ablation of the NPY containing neurons of the arcuate nucleus on the NPY-containing innervation of the CRH neurons, triple-labeling immunofluorescence was performed on every third hypothalamic section of control and MSG-treated rats. Antisera against DBH, NPY, and CRH were used following the immunocytochemical protocol described above for quadruple labeling (4.5.2.) except that the PNMT immunolabeling was excluded.

4.5.5. Triple-labeling immunofluorescence for AGRP, NPY, and CRH

To further determine the relative contribution of the AGRP/NPY neurons of the arcuate nucleus in the NPY innervation of the CRH neurons, a triple-labeling immunofluorescence was performed on every third hypothalamic section of animals with an intact arcuate nucleus. The sections were pretreated according to the method described above. Sections were incubated in a cocktail of primary antisera that contained antibodies against NPY, CRH, and rabbit anti-AGRP serum (1:2500, H-003-57; Phoenix Pharmaceuticals, Inc., Burlingame, CA) for 3 days at 4 ºC. For secondary labeling, CY^3-conjugated donkey anti-mouse IgG (Jackson ImmunoResearch, West Grove, PA) at 1:200 dilution CY^5-conjugated donkey anti-sheep IgG (Jackson Immunoresearch) at 1:100 dilution and biotinylated donkey anti-guinea pig IgG (Jackson Immunoresearch) at 1:250 dilution was used, followed by AMCA-conjugated avidin D (Vector Laboratories) dilution at 1:250 dilution for 1 day at 4 ºC.

4.5.6. Image analysis of triple and quadruple labeled preparations

From each brain, at least four sections were analyzed from different rostrocaudal levels of the medial parvocellular subdivision of the PVN in which hypophysiotropic CRH neurons reside. The atlas by Paxinos and Watson (187) was used to identify the subdivisions of the PVN (Fig.4.)

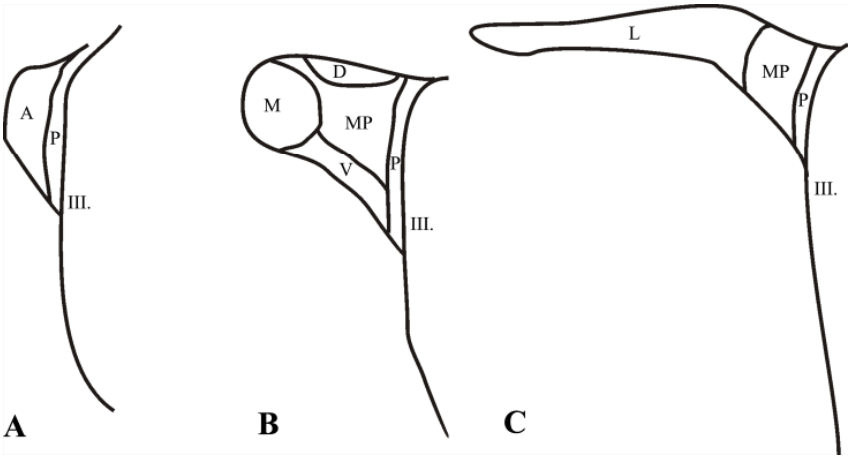

Figure 4. Schematic illustration of the subdivisions in the PVN at rostral (**A**), mid (**B**), and caudal (**C**) levels of the nucleus. A, Anterior parvocellular subdivision; D, dorsal parvocellular subdivision; L, lateral parvocellular subdivision; M, magnocellular division; MP, medial parvocellular subdivision; P, periventricular parvocellular subdivision; V, ventral parvocellular subdivision.

Serial optical sections of 180 x 180 µm areas covering the entire medial parvocellular subdivision of the PVN were recorded with a x60 oil lens in each section. The sections subjected to quadruple-labeling immunofluorescence were scanned in two steps such that two, consecutive scans were recorded from each area. The first scan was for FITC, CY^3, and CY^5 and the second scan was for AMCA. The sections subjected to triple-labeling immunofluorescence were scanned in one step for CY^3, CY^5, and AMCA.

Perikarya and proximal dendrites of the CRH neurons were traced through the optical slices, and the different types of boutons juxtaposed to the CRH neurons were counted. The regional heterogeneity of AGRP-IR boutons were analyzed with one-way ANOVA followed by Newman-Keuls test. $P < 0.05$ was considered significant. All data are presented as mean ± SEM.

To illustrate the images of the quadruple-labeled preparations, the three basic colors (red, green, and blue) were used to show pairs of triple-colored images of the same field in adjacent figures. Thus, CRH-, DBH-, and PNMT-immunoreactivities are displayed in one image, whereas CRH-, DBH-, and NPY-immunoreactivities are shown in the second image. Accordingly, DBH- and CRH-immunoreactivities are displayed in *red* and *blue*, respectively, in both images, whereas the *green* represents either PNMT- or NPY-immunoreactivity. Therefore, DBH/PNMT- and DBH/NPY-IR double-labeled axons appear *yellow* due to red and green color mixing.

Boutons that contained only DBH-immunoreactivity without PNMT-immunoreactivity were considered noradrenergic, whereas fibers containing both DBH- and PNMT-immunoreactivity were considered adrenergic axons. To examine the regional differences in the AGRP-IR innervation of the CRH neurons, the CRH neurons were analyzed at rostral, mid, and caudal levels of the PVN. The mid level was further divided into dorsal and ventral compartments (Fig.5).

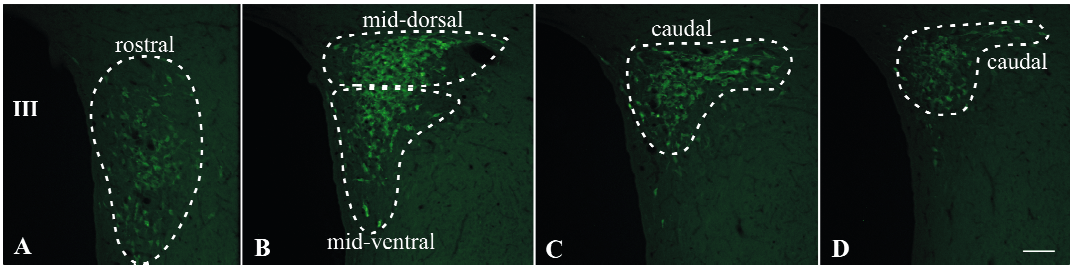

Figure 5. Distribution of CRH neurons in the PVN. Localization of the CRH cells in four different rostrocaudal planes of the PVN. **A**, Rostral population, -1.6 mm from Bregma; **B**, middorsal and midventral populations, -1.8 mm from Bregma; **C** and **D**, caudal population, -2.0 and -2.2 mm from Bregma. Scale bar, 100 μm.

4.6. Methods used to study the effects of chronic NPY administration on the CRH gene expression in rats

4.6.1. Animal preparation for central NPY infusion

Adult male Sprague-Dawley rats were implanted with a 22-gauge stainless steel guide cannula (Plastics One Inc., Roanoke, VA) into the lateral cerebral ventricle under stereotaxic control (coordinates from Bregma anterior to posterior, –0.8; lateral, –1.2; dorsal to ventral, –3.8) through a burr hole in the skull under anesthesia. The cannula was secured to the skull with three stainless steel screws and dental cement and temporarily occluded with a dummy cannula. Bacitracin ointment was applied daily to the interface of the cement and the skin. One week after icv cannulation, under general anesthesia, an osmotic minipump (Alzet model 1003D; Alza Pharmaceuticals, Palo Alto, CA) was implanted sc between scapulae and connected with polyethylene tubing to a 28-gauge needle that was permanently inserted into and extended 1 mm below the external guide cannula. The animals had free access to food and were divided in two groups. The osmotic minipumps delivered artificial cerebrospinal fluid (140 mM NaCl,

3.35 mM KCl, 1.15 mM $MgCl_2$, 1.26 mM Ca Cl_2, 1.2 mM Na_2HPO_4, 0.3 mM NaH_2PO_4, 0.1% BSA, pH 7.4) (group 1, n = 8), or 10 µg/24 h NPY (Peninsula) (group 2, n = 7) in artificial cerebral spinal fluid for 3 d at a rate of 1 µl/h. These doses have been previously shown to induce pronounced orexigenic activity when administered centrally (167). The weight of the animals and food intake were monitored daily.

4.6.2. Tissue preparation for in situ hybridization histochemistry

Tissue blocks containing the hypothalamus were cryoprotected in 20% sucrose in PBS at 4 ºC overnight and then frozen on dry ice. Serial, 18 µm thick coronal sections through the rostrocaudal extent of the PVN were cut on a cryostat (Reichert-Jung 2800 Frigocut-E) and adhered to Superfrost/Plus glass slides (Fisher Scientific Co., Pittsburgh, PA) to obtain four sets of slides, each set containing every fourth section through the PVN. Cannula placement was confirmed by light microscopic examination, and animals with cannulas outside the lateral ventricle were excluded from further study. The tissue sections were desiccated overnight at 42 ºC and stored at -80 ºC until prepared for *in situ* hybridization histochemistry.

4.6.3. In situ hybridization histochemistry for CRH

Every fourth section of the PVN was hybridized with a 976-bp single-stranded [^{35}S]UTP-labeled cRNA probe for CRH as previously described (188). Specificity of the probe for CRH mRNA has been demonstrated in previous studies (189). The hybridization was performed under plastic coverslips in a buffer containing 50% formamide, a 2-fold concentration of standard sodium citrate, 10% dextran sulfate, 0.5% sodium dodecyl sulfate, 250 µg/ml denatured salmon sperm DNA, and 6 x 10^5 cpm radiolabeled probe for 16 h at 56 ºC. Slides were dipped into Kodak NTB2 autoradiography emulsion (Eastman Kodak, Rochester, NY), and the autoradiograms were developed after 2 wk of exposure at 4 ºC.

4.6.4. Image analysis of CRH in situ hybridization

Autoradiograms were visualized under dark-field illumination using a COHU 4910 video camera (COHU, Inc., San Diego, CA). The images were captured with a PCI frame grabber board (Scion Corp., Frederick, MD) and analyzed with a Macintosh G3

computer using Scion Image. Background density points were removed by thresholding the image, and integrated density values (OD x area of distribution of silver grains on each side of the PVN) were measured in four consecutive sections for each animal, which represent the majority of neurons containing CRH mRNA in the PVN. The integrated density values were summed to yield total integrated density values for each animal, and the means and SEM of the total integrated density values were calculated for each experimental group. Nonlinearity of radioactivity in the emulsion was evaluated by comparing density values with a calibration curve created from autoradiograms of known dilutions of the radiolabeled probes immobilized on glass slides in 2% gelatin fixed with 4% formaldehyde and exposed and developed simultaneously with the *in situ* hybridization autoradiograms.

4.7. Methodologies applied in the study of catecholaminergic innervation of the TRH neurons in the PVN of rats

4.7.1. Tissue preparation for immunocytochemistry

Colchicine-treated rats (40 µg/animal) were used for the visualization of proTRH neurons. The same tissue preparation protocol was used as described above (4.2.), the animals were perfused transcardially with 150 ml of 4% paraformaldehyde in 0.1 M PB (pH 7.4).

4.7.2. Triple-labeling immunofluorescence for DBH, PNMT, and proTRH

To elucidate the relative contribution of noradrenergic and adrenergic cell groups of the brainstem to the catecholaminergic innervation of hypophysiotropic TRH neurons, triple-labeling fluorescent immunocytochemistry was performed on every fourth section of the hypothalamus. The pretreatments were the same as described above (4.3.). The sections were then incubated first in the following mixture of primary antibodies for 3 days at 4 °C: murine monoclonal antibody to DBH (Cat# MAB308, Millipore) at 1:1000 and rabbit anti-PNMT serum (gift from Martha C. Bohn) at 1:1000. After rinses in PBS, the sections were incubated in biotinylated donkey anti-rabbit IgG, 1:250 (Jackson Immunoresearch) overnight. After further washing in PBS the sections were incubated in rabbit anti-proTRH serum (178-199) (gift from Éva Rédei, Northwestern

University, Chicago, IL) at 1:2500 for 2 days. After rinses in PBS, the sections were incubated in a mixture of fluorochrome-conjugated reagents for one day at 4 °C. The fluorescent markers were as follows: FITC-conjugated Streptavidin (Jackson Immunoresearch) at 1:300 dilution, CY^3-conjugated donkey anti-mouse IgG (Jackson Immunoresearch) at 1:200 dilution and CY^5-conjugated donkey anti-rabbit IgG (Jackson Immunoresearch) at 1:100 dilution.

Although rabbit antiserum was used for the detection of both the PNMT- and proTRH-IR structures, because PNMT antiserum and biotinylated donkey anti-rabbit IgG was applied before the use of rabbit anti-proTRH serum, the avidin-conjugated FITC labeled only the PNMT-IR structures. CY^5-conjugated anti-rabbit IgG labeled both PNMT- and proTRH-IR elements, but PNMT-containing neurons are not present in the PVN, therefore, all CY5-labeled perikarya in the PVN were proTRH-IR perikarya. Similar approach was successfully used in our earlier studies (111, 160).

To further improve the specificity of the immunostaining, the triple-labeling was also performed with a recently generated sheep TRH antiserum (190). Immunolabeling was performed as described above just the rabbit proTRH serum was replaced with the sheep TRH antiserum at 1:8000 dilution.

4.7.3. Image analysis for TRH, DBH and PNMT labeling

The triple-labeling immunofluorescence was scanned in one step for FITC, CY^3 and CY^5. Perikarya and proximal dendrites of the proTRH neurons were traced through the optical slices, and the different types of boutons juxtaposed to proTRH neurons were counted.

To illustrate images of the triple-labeled preparations, proTRH-, DBH- and PNMT-immunoreactivities were displayed by using the three basic colors (red, green, and blue). DBH- and PNMT-immunoreactivities are displayed in *red* and *green*, respectively, while *blue* represents proTRH-immunoreactivity. Therefore, DBH/PNMT double-labeled axons appear *yellow* due to red and green color mixing.

Boutons that contained only DBH-immunoreactivity without PNMT-immunoreactivity were considered noradrenergic, whereas fibers containing both DBH- and PNMT-immunoreactivity were considered adrenergic axons. To examine the regional differences in the catecholaminergic innervation of the TRH neurons, the

region where the hypophysiotropic TRH neurons reside were divided into two parts: medial and lateral (Fig. 6.). The regional heterogeneity of catecholaminergic boutons were analyzed with Student T-test. $P < 0.05$ was considered significant. Data are presented as mean ± SEM.

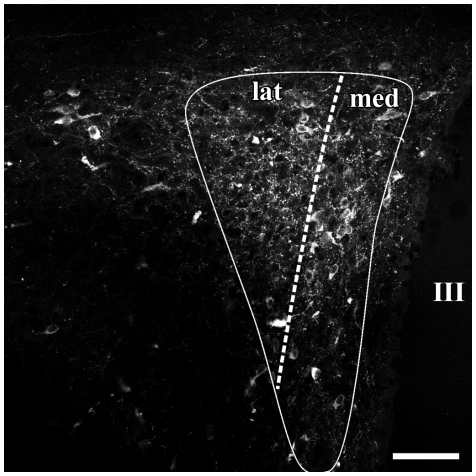

Figure 6. Photomicrograph of TRH-immunoreactivity in the PVN illustrates the medial and lateral parts of the medial parvocellular subdivision of the PVN used for quantification of the DBH- and PNMT-containing innervation of the TRH neurons. med: medial part of the medial parvocellular subdivision, lat: lateral part of the medial parvocellular subdivision, III: third ventricle. Scale bar, 100 μm

4.8. Methods applied in studies examining the efferent projections of the TRH neurons located in the aPVN

4.8.1. Anterograde tract-tracing experiments

The anterograde tracer, PHAL (Vector Laboratories), was injected by iontophoresis into the region of aPVN of 17 animals. Rats were anesthetized i.p. with ketamine-xylazine and their heads positioned in a stereotaxic apparatus with Bregma and lambda in the horizontal plane. Through a burr hole in the skull, a glass micropipette (20 μm outer tip diameter) filled with 2.5% PHAL in 0.01 M PB at pH 8.0 was lowered into the brain at stereotaxic coordinates corresponding to the aPVN based on the atlas of Paxinos and Watson (187). The tracer was deposited by iontophoresis for 11-15 minutes (6 μA positive current, pulsed on-off at 7-second intervals) using a constant-current

source (Stoelting, Wood Dale, IL). Rats were allowed to survive for 9-14 days and then perfused transcardially as described above (4.2.)

Single-labeling immunohistochemistry for PHAL was performed to evaluate the injection sites, using rabbit PHAL antiserum (Vector Laboratories) at 1:5,000, for 1 day at room temperature. After washing in PBS, sections were incubated in biotinylated donkey anti-rabbit IgG (Jackson Immunoresearch) at 1:500 for 2 hours at room temperature. After further rinsing in PBS, the sections were incubated in ABC (Vector Laboratories) at 1:1,000 dilution for 1 hour. After rinses in PBS, the tissue-bound peroxidase activity was visualized by 0.05% diaminobenzidine and 0.15% nickel ammonium sulfate with 0.005% H_2O_2 in 0.05 M Tris buffer at pH 7.6. The sections were counterstained with 1% cresyl-violet, mounted onto glass slides, and coverslipped with DPX mounting medium.

Sections from four animals with injection sites in the aPVN/perifornical area were used for double-labeling immunofluorescence to identify the axons that contain both PHAL- and pro-TRH-immunoreactivity. After standard pretreatment as described above (2.2.), sections were incubated in a mixture of primary antisera: goat anti-PHAL (Vector Laboratories) at 1:1,000 and rabbit anti-pro-TRH 178-199 peptide, diluted 1:2,500 (gift from Dr. Éva Rédei, Northwestern University, Chicago, IL) for 2 days at 4°C. After washes in PBS, sections were immersed in a cocktail of biotinylated donkey anti-sheep IgG at 1:500 (Jackson Immunoresearch) and CY^3-conjugated donkey anti-rabbit IgG (Jackson Immunoresearch; 1:200) and incubated for 2 hours at room temperature. After being rinsed with PBS, sections were transferred into ABC (Vector Laboratories) at 1:1,000 for 2 hours. The sections were rinsed in PBS and then amplified with biotinylated tyramide using the TSA amplification kit (Perkin Elmer Life and Analytical Sciences, Waltham, MA). After further washes, the sections were incubated in FITC-conjugated Streptavidin (1:300; Vector Laboratories) for 2 hours and mounted onto glass slides. To facilitate identification of brain nuclei, sections were coverslipped with Vectashield Mounting Medium with DAPI (Vector Laboratories).

4.8.2. Retrograde tract-tracing experiments

The retrograde tracer cholera toxin β subunit (CTB; List Biological Laboratories, Campbell, CA) was injected into specific brain regions where the majority of

PHAL/pro-TRH-containing, double-labeled axons were found in the anterograde tract-tracing experiment. Animals were anesthetized i.p. with ketamine-xylazine and their heads mounted in a stereotaxic apparatus as described above (4.8.1.). At stereotaxic coordinates corresponding to each target region, a glass micropipette with 20 μm outer tip diameter filled with 0.5% CTB was lowered into the brain through a burr hole. CTB was iontophoresed by a 6 μA positive current, pulsed on-off at 7 second intervals over 10-15 minutes for each injection. After a 6-10 day transport time, animals were anesthetized and stereotaxically injected with 60 μg colchicine into the lateral cerebral ventricle to enhance the immunocytochemical detection of TRH in cell bodies. After 20 hours of survival, the animals were deeply anesthetized and perfused (4.2.). The brains were removed, immersed in 30% sucrose for 1-2 days, and frozen on dry ice and 25 μm thick coronal sections were cut on a freezing microtome into one-in-four series of sections.

The location of CTB injection sites and the distribution of CTB-containing TRH neurons in the aPVN and perifornical area were studied in double-immunolabeled sections. Sections were incubated in the mixture of goat anti-CTB serum (List Biological Laboratories) at 1:10,000 and rabbit anti-TRH serum (No. 31; a gift from Dr. Ivor M. Jackson, Brown Medical School, Providence, RI) at 1:2,500 for 2 days at 4°C. After washes in PBS, the sections were immersed in a mixture of biotinylated donkey anti-sheep IgG 1:500 (Jackson Immunoresearch) and CY^3-conjugated donkey anti-rabbit IgG (Jackson Immunoresearch; 1:200) and incubated for 2 hours at room temperature. After rinsing with PBS, sections were incubated in ABC (Vector Laboratories) at 1:1,000 for 2 hours. The sections were rinsed in PBS and subjected to biotinylated tyramide amplification for 15 minutes as described above (4.8.1.). After further washes, the sections were incubated in fluorescein DTAF-conjugated streptavidin (1:300; Vector Laboratories) for 2 hours, mounted onto glass slides, and coverslipped with Vectashield (Vector Laboratories).

4.8.3. Image and data analysis of the tract-tracing experiments

Double-labeled fluorescent preparations were examined with a Zeiss AxioImager M1 epifluorescent microscope (Carl Zeiss AG, Göttingen, Germany). To facilitate identification of double-labeled axons and cell bodies, sections were examined under

fluorescent illumination through Zeiss Filter Set 23: excitation 475-495 and 540-552 nm, beam splitter 500 and 560 nm, emission 515-530 and 580-630 nm. For unequivocal detection of the signals of individual fluorochromes and for taking images, the following filter sets were used: for fluorescein DTAF, excitation filter of 450-490 nm, beam splitter of 495 nm, and emission filter of 500-550 nm; for CY^3, excitation of 538-562 nm, beam splitter of 570 nm, and emission filter of 570-640 nm. Images were captured either with the Zeiss AxioImager M1 microscope using AxioCam MRc 5 digital camera (Carl Zeiss AG) and AxioVision 4.6 software (Carl Zeiss AG) or with a Radiance 2100 confocal microscope (Bio-Rad Laboratories). Confocal images were taken using the setup described above (4.4). To enhance visibility of double-labeled PHAL/pro-TRH and CTB/TRH cell bodies, consecutive optical sections (from 3 to 12) were projected into one image with ImageJ image analysis software (http://rsb.info.nih.gov/ij/download/src/). Brightfield images of the PHAL injection sites were captured with a Zeiss AxioImager M1 microscope (Carl Zeiss AG). Adobe Photoshop 7.0 (Adobe Systems Incorporated, San Jose, CA) and an IBM-compatible personal computer were used to create composite images and to modify brightness and contrast of the images.

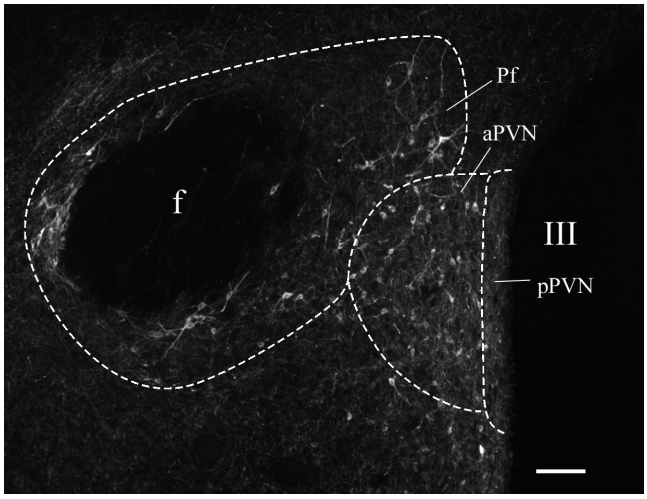

Figure 7. Photomicrograph of the rostral-mid level of the aPVN, where perifornical TRH neurons are in close proximity to the border of the aPVN. Scale bar, 100 μm.

PHAL/pro-TRH-containing axon terminals and en passant boutons were considered in the analysis as projections of aPVN or perifornical TRH neurons. Line drawings representing the distribution of double-labeled PHAL/pro-TRH-IR fibers and CTB/TRH-IR neurons were made in Corel Draw 11 (Corel Corporation, Ottawa, Ontario, Canada). Cell counts of CTB/TRH-IR neurons in the aPVN and perifornical area were counted in one-in-four series of 25 μm thick sections from each brain with successful CTB injections. In sections of the CTB-injected brains, the aPVN and the perifornical area were identified by the distribution, shape, and orientation of the TRH-IR neurons (Fig. 7).

4.9. Antibody characterization

The specificity of sheep anti-NPY serum (gift of Dr. István Merchenthaler) was demonstrated by the loss of immunoreactivity after preadsorption of the diluted antiserum with an excess of synthetic NPY peptide (1 μg/ml) (data not shown).

According to descriptions of the manufacturers, the PHAL antiserum was produced by hyperimmunization of goat with purified PHAL, and specific antibodies to PHAL were isolated by affinity chromatography on PHAL-agarose columns, whereas the CTB antiserum forms an immunoprecipitin band against a 0.5 mg/ml solution of CTB. Because PHAL and CTB are normally not present in the brain, the specificities of PHAL and CTB antisera were verified by the lack of any labeling in brain sections from animals that were not injected with PHAL and CTB.

The specificity of the following antibodies was described previously: murine a-DBH (Cat# MAB308, Millipore) (191); rabbit a-PNMT (gift from Martha C. Bohn) (192); guinea pig a-CRH (Peninsula Laboratories Inc.) (145); rabbit a-AGRP (Phoenix Pharmaceuticals Inc.) (193); rabbit a-proTRH (gift from Éva Rédei) (194); sheep a-TRH (190).

5. Results

5.1. Origin of the NPY-IR innervation of the CRH neurons in the PVN of rats

5.1.1. Involvement of the brainstem noradrenergic and adrenergic cell groups in the NPY-immunoreactive innervation of CRH neurons

NPY-, DBH- and PNMT-IR axons densely innervated the parvocellular subdivisions of the PVN (Fig. 8A). However, the distribution of the three fiber networks showed regional differences (Fig. 8A). NPY-IR axons and slightly less intensely DBH-IR axons inundated the ventral parvocellular subdivision, whereas the PNMT-IR axons were rare in this location (Fig. 8A). Furthermore, NPY-IR axons more densely innervated the periventricular parvocellular subdivision and the medial part of the medial parvocellular subdivision than PNMT-IR or DBH-IR fibers (Fig. 8A).

The area of the medial parvocellular subdivision, where the majority of the hypophysiotropic CRH neurons are located, was heavily innervated by all three afferent systems (Fig. 8A). As expected, the vast majority of PNMT-IR axons were also labeled for DBH (Fig. 8, A2, B2, and C2). The majority of adrenergic (PNMT-IR) and a subpopulation of noradrenergic (DBH-IR but not PNMT-IR) axons also showed NPY-immunoreactivity (Fig. 8, B and C). In the area of hypophysiotropic CRH neurons, the density of catecholaminergic NPY-IR fibers was much higher than the density of single-labeled NPY-IR axons (Fig. 8B). However, in the ventral and most caudal parts of the medial parvocellular subdivision, single-labeled NPY-IR fibers exceeded the density of catecholaminergic NPY-IR fibers (Fig. 8C).

NPY/PNMT-IR axon varicosities were found in juxtaposition to the vast majority of CRH neurons (94.2 ± 1.1%) (Fig. 8, B and C). An average of 5.5 ± 0.4 NPY/PNMT boutons per CRH cell was observed. Noradrenergic NPY/DBH-IR boutons were also found juxtaposed to the 82.8 ± 6.2% of CRH neurons with an average of 3.5 ± 0.8 NPY/DBH boutons per cell (Fig. 8, B and C). Table 2 shows the results of the quantitative analysis.

Table 2. Quantitative analysis of quadruple-labeling immunofluorescence (PNMT/DBH/NPY/CRH) in intact rats

Type of NPY-IR bouton	Percentage of CRH neurons contacted (%)	Average number of NPY-IR varicosities per innervated CRH neuron	Percentage of all NPY-IR boutons in contact with CRH neurons (%)
Single-labeled NPY	89.0 ± 5.3	5.3 ± 0.8	36.6 ± 3.1
DBH/NPY	82.8 ± 6.2	3.5 ± 0.8	22.2 ± 3.0
PNMT/DBH/NPY	94.2 ± 1.1	5.5 ± 0.4	41.2 ± 5.6
All NPY	100	12.9 ± 2.0	100

Of all NPY-containing axon varicosities located on the surface of CRH neurons, 41.2 ± 5.6% contained both PNMT- and DBH-immunoreactivity, whereas 22.2 ± 3.0% were only DBH-IR. An additional 36.6 ± 3.1% of NPY-IR axon varicosities were only single-labeled, indicating that these fibers do not originate from catecholaminergic sources. However, the single-labeled NPY-IR fibers were found in juxtaposition to 89.0 ± 5.3% of CRH neurons. These single-labeled NPY-IR axon varicosities were unevenly distributed and more frequently contacted the most posterior CRH neurons, and the CRH neurons located laterally and in the ventral part of the medial parvocellular subdivision (Fig. 8, B and C). Conversely, 86.5 ± 5.6% of PNMT-IR boutons and 47.8 ± 12.0% of DBH-IR, PNMT-immunonegative boutons on the surface of CRH neurons contained NPY.

With respect to the catecholaminergic boutons on the surface of CRH neurons, 48.5 ± 6.2% contained DBH but not PNMT, suggesting that these varicosities produce noradrenaline, whereas 51.6 ± 6.2% contained both DBH and PNMT, indicating their adrenergic phenotype.

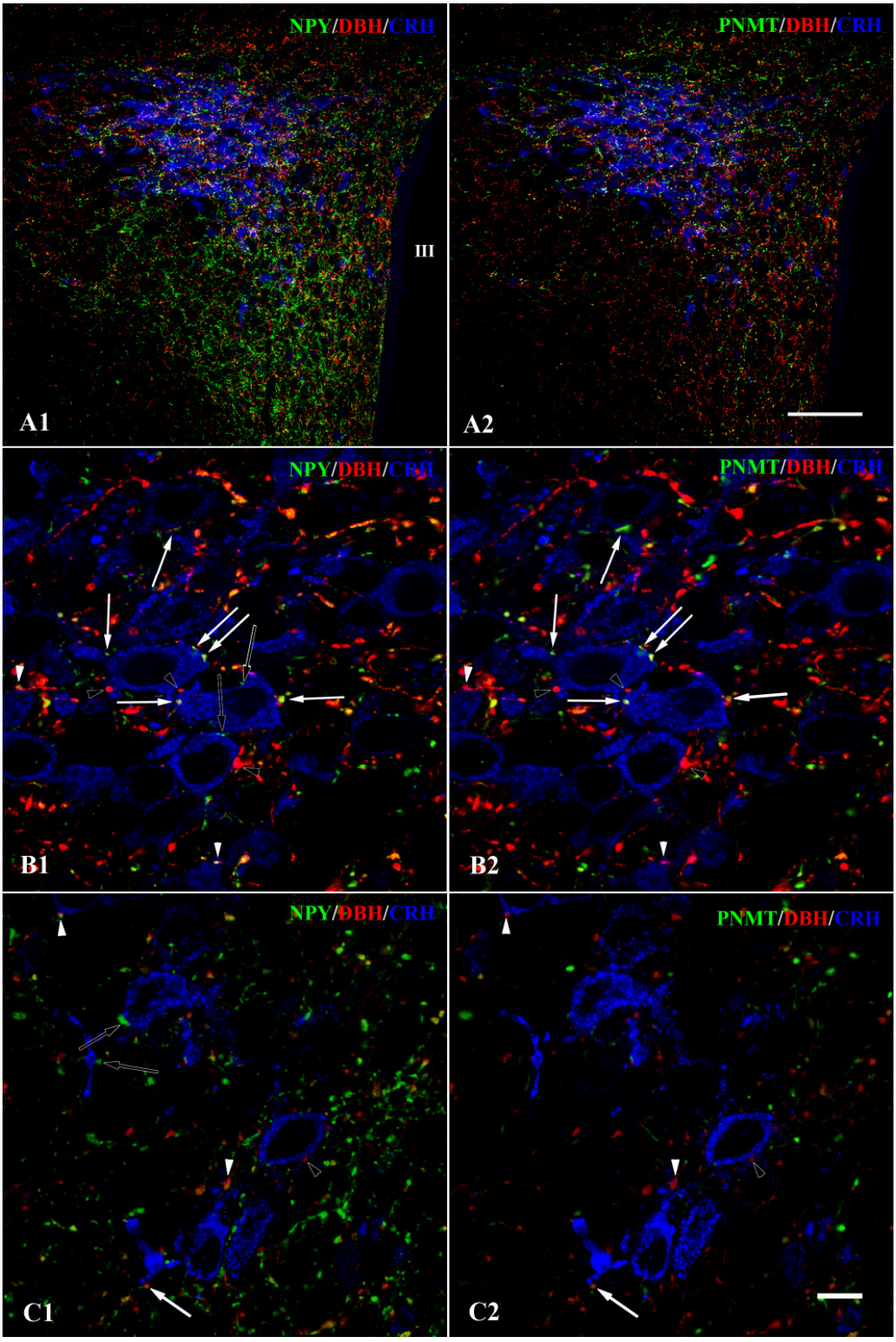
NPY/DBH/CRH
III
A1
PNMT/DBH/CRH
A2
NPY/DBH/CRH
B1
PNMT/DBH/CRH
B2
NPY/DBH/CRH
C1
PNMT/DBH/CRH
C2

Figure 8. Distribution of, DBH, PNMT, and NPY axons and CRH perikarya in the PVN of intact rats. **A1** and **A2**, Low-magnification confocal images of the same field demonstrate the distribution of NPY (*green*), DBH (*red*), and CRH (*blue*) (**A1**) and PNMT (*green*), DBH (*red*), and CRH (*blue*) (**A2**) containing elements in the PVN. **A1**, NPY-IR is present in DBH-IR axons in the area of CRH neurons. Note that single-labeled NPY-IR axons, which contain only NPY without DBH-IR, are much less dense in the region of CRH neurons, whereas a dense, single-labeled NPY-IR network is present in the ventral parvocellular subdivision and in the ventral part of the medial parvocellular subdivision. **A2**, CRH neurons in the medial parvocellular subdivision are embedded in a dense network of adrenergic fibers. Noradrenergic (DBH-IR but not PNMT-IR) fibers appear *red*, adrenergic fibers (both DBH- and PNMT-IR) appear *yellow*. **B** and **C**, High-magnification images of the same field demonstrate the uneven distribution of NPY-IR boutons juxtaposed to CRH neurons in the dorsal (**B1** and **B2**) and the ventral (**C1** and **C2**) parts of the medial parvocellular subdivision of the PVN. Note that whereas single-labeled NPY-IR boutons are relatively rare in the dorsal part of the medial parvocellular subdivision (**B1** and **B2**), these noncatecholaminergic NPY fibers are more frequently seen in the ventral part of the subdivision (**C1** and **C2**). *White arrow*, NPY/DBH/PNMT-IR; *white arrowhead*, DBH/NPY-IR; *open arrow*, single-labeled NPY boutons; *open arrowhead*, single-labeled DBH-IR boutons juxtaposed to CRH neurons. III, Third ventricle. Scale bars, 100 µm (shown in **A2**) for **A1** and **A2** and 10 µm (shown in **C2**) for **B1**, **B2**, **C1**, and **C2**.

5.1.2. Effect of arcuate nucleus ablation on the NPY-IR innervation of CRH neurons

Immunostaining against NPY in MSG-treated animals demonstrated that the vast majority of NPY-IR cells in the arcuate nucleus were ablated (Fig. 9). Only a small number of NPY-IR neurons remained intact in the most caudal part of the arcuate nucleus.

Catecholaminergic axons more densely inundated the medial parvocellular subdivision, and fewer catecholaminergic/NPY-IR fibers were found in the ventral and caudal parts of this subdivision (Fig. 10A1). In the ventral part of the medial parvocellular subdivision where the density of the single-labeled NPY axons was the heaviest in intact rats, only sparse remaining fibers were found in MSG-treated animals (Fig. 10, A2 and A3). In triple-labeled preparations, the density of single-labeled NPY axons dramatically decreased throughout the PVN. Only 2.3 ± 0.3 single-labeled NPY boutons were found juxtaposed to CRH neurons, and these boutons comprised only 8.2 ± 2.3% of the total number of NPY varicosities. The vast majority (91.8 ± 2.3%) of the NPY boutons on the surface of the CRH neurons also contained DBH-immunoreactivity (Fig. 10, A2 and A3). Table 3 shows the results of the quantitative analysis.

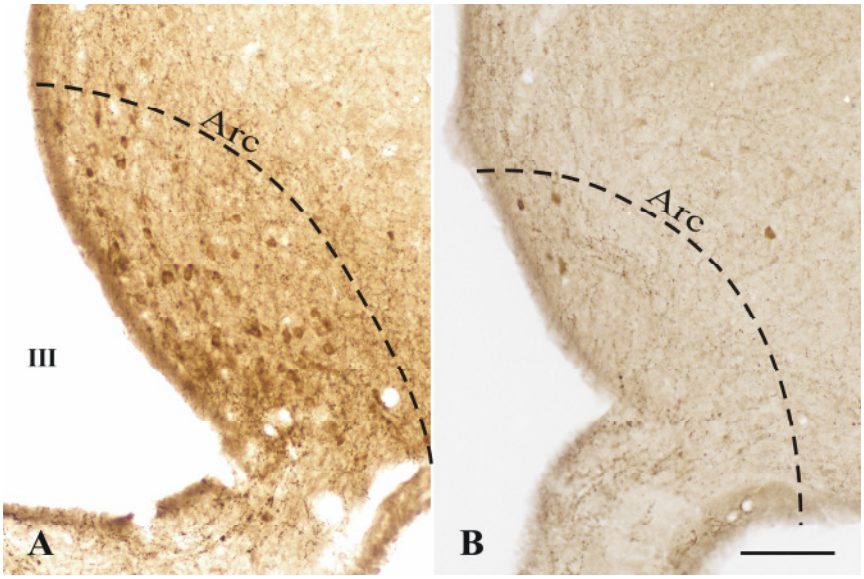

Figure 9. Effect of chemical ablation of the arcuate nucleus on NPY-IR neurons of the arcuate nucleus. **A**, Distribution of NPY-IR neurons in the arcuate nucleus of control rats; **B**, neonatal MSG treatment results in a dramatic reduction of NPY perikarya and almost complete disappearance of NPY fibers in the arcuate nucleus. Arc, Arcuate nucleus; III, third ventricle. Scale bar, 100 μm.

Table 3. Quantitative analysis of triple-labeling immunofluorescence (DBH/NPY/CRH) in MSG-treated rats

Type of NPY-IR bouton	Percentage of CRH neurons contacted (%)	Average number of NPY-IR varicosities per innervated CRH neuron	Percentage of all NPY-IR boutons in contact with CRH neurons (%)
Single-labeled NPY	67.3 ± 11.3	2.3 ± 0.3	8.2 ± 2.3
DBH/NPY	100	19.2 ± 1.6	91.8 ± 2.3
All NPY	100	20.8 ± 1.4	100

5.1.3. Relative involvement of the arcuate nucleus in the NPY-IR innervation of CRH neurons

AGRP/NPY-IR fibers arising from the arcuate nucleus densely innervated the parvocellular subdivisions of the PVN (Fig. 10B1). The distribution of the AGRP/NPY fibers was similar to the distribution of single-labeled NPY-IR fibers in the quadruple-labeling studies: the dorsal part of the medial parvocellular subdivision of the PVN was less intensely innervated, whereas the ventral part of the medial parvocellular subdivision was covered by a dense network of AGRP-IR axons (Fig. 10, B1 and B2). Quantitative analysis of the regional heterogeneity of the AGRP innervation showed that

in the caudal region, significantly more AGRP boutons were juxtaposed to CRH neurons than in the other regions of the parvocellular division (Fig. 10B3). The relative contribution of AGRP/NPY-IR varicosities to the innervation of the CRH neurons was significantly higher in the midventral region than in the middorsal region but significantly lower than in the caudal region. Table 4 shows the regional heterogeneity in the density of the AGRP-IR boutons juxtaposed to the hypophysiotropic CRH neurons. The topography of the analyzed regions is shown in Fig. 5.

Double-labeled NPY/AGRP-IR axon varicosities were found in juxtaposition to the vast majority of CRH neurons (94.3 ± 0.7%) (Fig. 10, B2 and B3). An average of 7.1 ± 0.3 NPY/AGRP boutons per CRH cell was observed. Of all NPY-containing axon varicosities on the surface of CRH neurons, 33.7 ± 1.9% contained AGRP-immunoreactivity. Table 5 shows the results of the quantitative analysis.

Table 4. Regional heterogeneity of NPY-IR and AGRP/NPY-IR innervation in the PVN of intact rats

Type of NPY-IR bouton	Average number of NPY-IR varicosities per CRH neuron	AGRP/NPY-IR boutons (%)
Rostral		
AGRP/NPY	5.5 ± 1.3	32.6 ± 4.8
All NPY	17.9 ± 4.9	
Middorsal		
AGRP/NPY	4.9 ± 0.2	23.9 ± 0.7
All NPY	20.5 ± 0.6	
Midventral		
AGRP/NPY	8.1 ± 1.4	38.4 ± 3.1[2]
All NPY	20.8 ± 1.8	
Caudal		
AGRP/NPY	12.4 ± 1.7[123]	51.2 ± 2.9[123]
All NPY	24.2 ± 2.9	

[1] Significantly different from the rostral subdivision.

[2] Significantly different from the middorsal subdivision.

[3] Significantly different from the midventral subdivision.

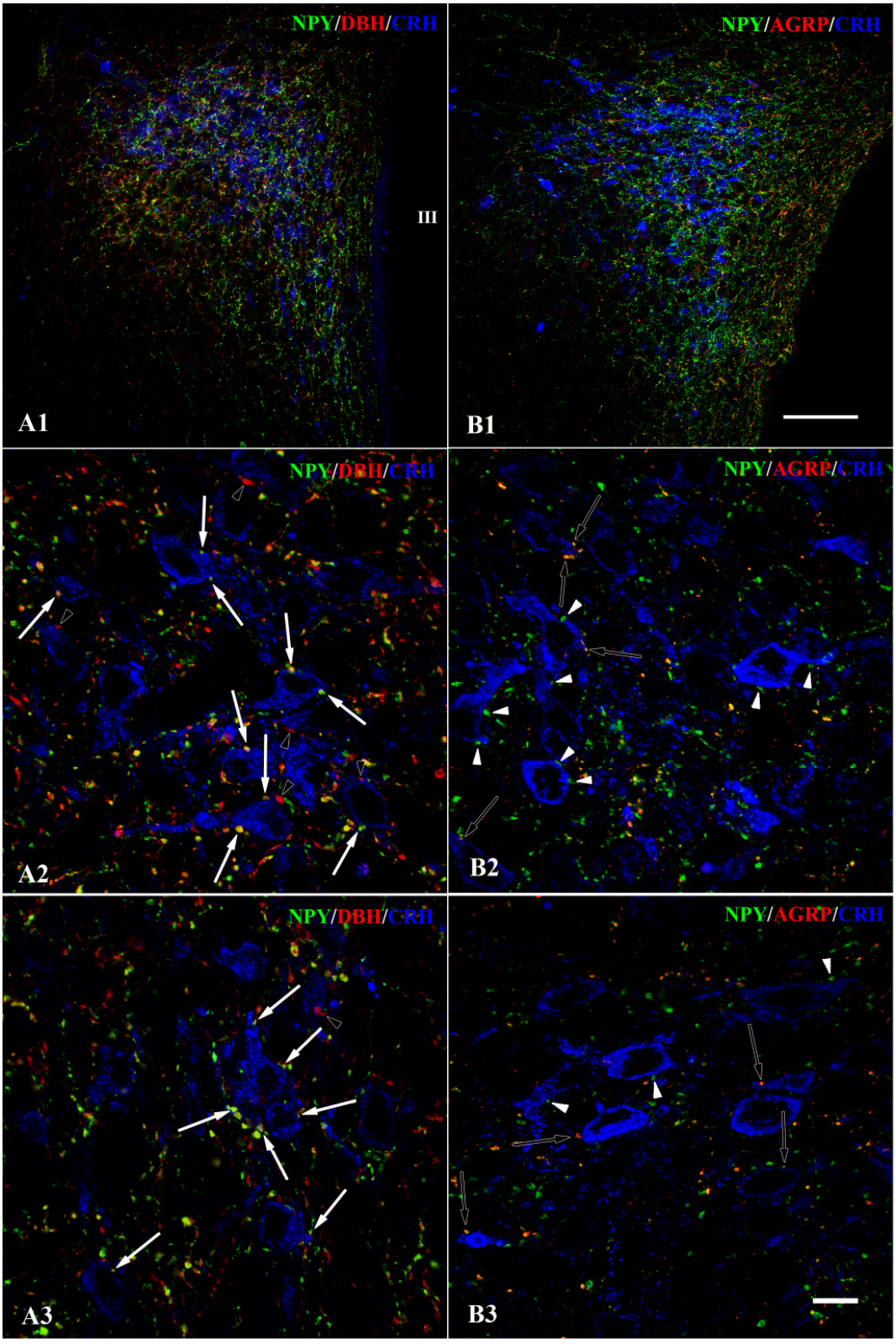
NPY/DBH/CRH
III
A1
NPY/AGRP/CRH
B1
NPY/DBH/CRH
A2
NPY/AGRP/CRH
B2
NPY/DBH/CRH
A3
NPY/AGRP/CRH
B3

Figure 10. Involvement of the arcuate nucleus neurons in the NPY innervation of the CRH neurons in the PVN. **A1**–**3**, Low-power magnification image illustrates the distribution of NPY-IR (*green*), DBH-IR (*red*), and CRH-IR (*blue*) elements in the PVN of MSG-treated rats. **A1**, DBH-IR is present in the vast majority of NPY-IR fibers (*yellow*), suggesting that these fibers originate from the catecholaminergic neurons of the brainstem. Note the dramatic reduction in the ventral part of the parvocellular division in the density of single-labeled NPY fibers after the chemical ablation of the arcuate nucleus (compare Fig 4A1). **A2** and **A3**, High-level magnification images demonstrate NPY-IR varicosities juxtaposed to the CRH neurons in different parts of the parvocellular division in MSG-treated rats. Note that the vast majority of the NPY-IR boutons contain DBH-IR. In the dorsal part of the medial parvocellular subdivision (**A2**), more intensive catecholaminergic innervation is seen compared with the ventral part (**A3**). **B1**, Low-power magnification image illustrates the distribution of AGRP-IR (*red*), NPY-IR (*green*), and CRH-IR (*blue*) elements in the PVN of intact rats. Note that a dense AGRP-IR network is present in the ventral part of the medial parvocellular subdivision, whereas single-labeled NPY-IR fibers mainly innervate the dorsal part (**B1**). **B2** and **B3**, High-power magnification images demonstrate NPY- and AGRP-IR varicosities juxtaposed to the CRH neurons. The majority of the boutons contain only NPY-IR in the dorsal part of the medial parvocellular subdivision, suggesting that these fibers arise from the brainstem (**B2**). In the images taken from the caudal part of the PVN, a notable portion of the NPY-IR varicosities contain AGRP, identifying the arcuate nucleus as source of origin (**B3**). *White arrow*, DBH/NPY-IR; *open arrow*, AGRP/NPY-IR; *white arrowhead*, single-labeled NPY boutons; *open arrowhead*, single-labeled DBH boutons juxtaposed to CRH neurons. III, Third ventricle. Scale bars, 100 μm (shown in **B1**) for **A1** and **B1** and 10 μm (shown in **B3**) for **A2**, **A3**, **B2**, and **B3**.

Table 5. Quantitative analysis of triple-labeling immunofluorescence (AGRP/NPY/CRH) in intact rats

Type of NPY-IR bouton	Percentage of CRH neurons contacted (%)	Average number of NPY-IR varicosities per innervated CRH neuron	Percentage of all NPY-IR boutons in contact with CRH neurons (%)
AGRP/NPY	94.3 ± 0.7	7.1 ± 0.3	33.7 ± 1.9
Single-labeled NPY	100	14.1 ± 0.9	66.4 ± 1.9
All NPY	100	21.3 ± 0.9	100

5.2. Effects of chronic NPY administration on the CRH gene expression in rats

NPY-treated animals consumed significantly more food (control *vs.* NPY, 64.2 ± 1.8 *vs.* 119.07 ± 5.6 g) and gained considerably more weight than controls (control *vs.* NPY, 14.8 ± 1.2 *vs.* 31.00 ± 5.3%) during the 3 days of infusion.

In control animals, neurons containing CRH mRNA were readily visualized by *in situ* hybridization histochemistry, symmetrically distributed in the medial parvocellular subdivision of the PVN on both sides of the third ventricle (Fig. 11A). A 3 day central infusion of NPY resulted in a uniform decrease in the hybridization signal over the CRH neurons throughout the anterior-posterior extent of the PVN (Fig. 11B). By image analysis, the mean of integrated density values of CRH mRNA in the PVN of NPY-treated animals was approximately 30% of that of the control animals (control *vs.* NPY, 77.1 ± 15.9 *vs.* 23.9 ± 2.7 integrated density units).

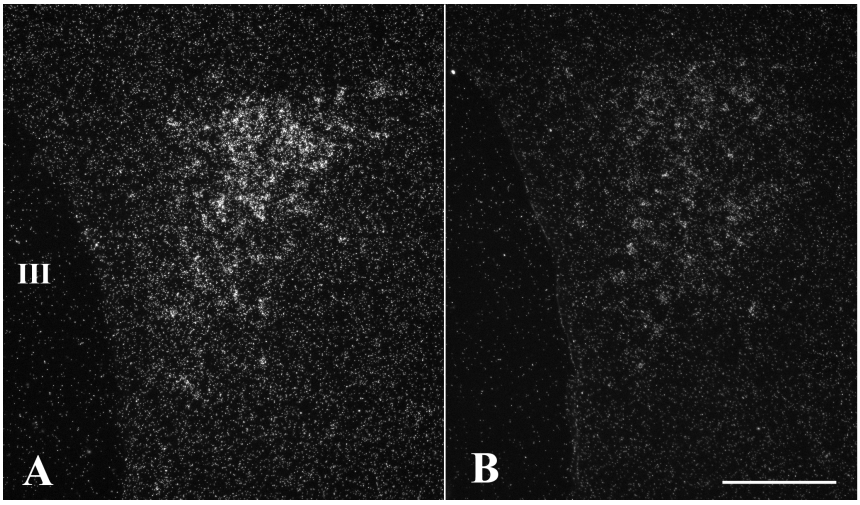

Figure 11. Effect of central NPY administration on CRH mRNA in the PVN. Dark-field illumination micrographs depicting CRH mRNA expression in the parvocellular division of the PVN in control rats (**A**) and in rats receiving an icv infusion of 10 µg/d NPY for 3 d (**B**). Note the marked reduction in the accumulation of silver grains over the PVN in NPY-treated animals compared with controls. III, Third ventricle. Scale bar, 200 µm.

5.3. Catecholaminergic innervation of the TRH neurons in the PVN of rats

Both single-labeled DBH-IR and DBH/PNMT-IR axon varicosities were found in juxtaposition to the vast majority of proTRH-IR neurons (97.8 ± 0.7% and 100%, respectively) (Fig. 12B-D). An average of 7.4 ± 1.0 single-labeled DBH-IR boutons per TRH cell was observed while 11.8 ± 0.6 PNMT-IR boutons were juxtaposed to TRH neurons (Table 6). The relative contribution of noradrenergic axons to the catecholaminergic innervation of the hypophysiotropic TRH neurons was 36.5 ± 1.2%. Adrenergic axons formed the remaining two thirds (63.5 ± 1.2%) of the catecholaminergic innervation of TRH neurons (Table 6). The results of the quantitative analysis showed that there were significantly more PNMT-IR varicosities juxtaposed to the TRH neurons in the lateral part of the medial parvocellular subdivision of the PVN compared to the medial part of this subdivision. Table 7 displays the regional heterogenity.

Table 6. Quantitative analysis of triple-labeling immunofluorescence (DBH/PNMT/TRH) in rats

Type of catecholaminergic axons	Percentage of contacted proTRH neurons (%)	Average number of catecholaminergic varicosities per innervated proTRH neuron	Percentage of all catecholaminergic boutons in contact with proTRH neurons (%)
single DBH	97.8±0.7	7.4±1.0	36.5±1.2
DBH/PNMT	100	11.8±0.6	63.5±1.2
all catecholaminergic	100	19.8±2.2	100

Table 7. Regional heterogeneity of DBH-IR and DBH/PNMT-IR innervation of TRH neurons in the PVN of rats

Type of catecholaminergic axons	Average number of DBH varicosities per proTRH neuron	DBH boutons (%)
Medial part of medial parvocellular subdivision		
single DBH	7.0±0.7	38.2±0.9*
DBH/PNMT	11.3±1.0*	
all catecholaminergic	18.4±1.7	
Lateral part of medial parvocellular subdivision		
single DBH	6.3±0.9	29.5±2.2*
DBH/PNMT	14.7±0.6*	
all catecholaminergic	21.0±1.5	

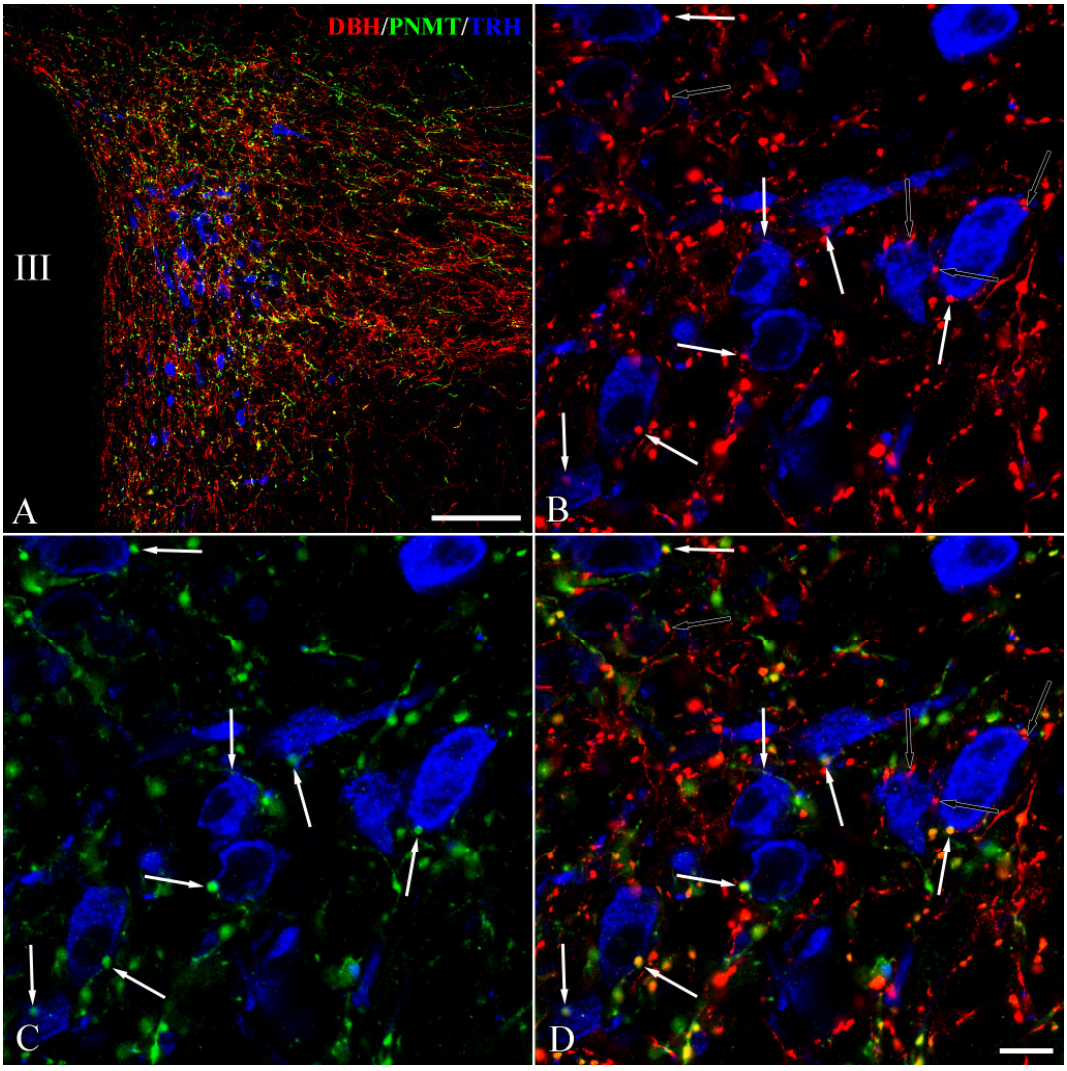

Figure 12. Relationship between DBH- (red) and PNMT-IR (green) axons and TRH-containing neurons (blue) in the PVN. Low power magnification image (**A**) of the PVN illustrates that TRH-synthesizing neurons are embedded in a dense network of DBH- and double-labeled DBH/PNMT-IR (yellow) axons. High magnification confocal images of the same field (**B**-**D**) demonstrate DBH- (**B**) and PNMT-IR (**C**) varicosities on the surface of TRH-containing neurons (blue) in the medial parvocellular subdivision of the PVN. The composite image (**D**) demonstrate that both noradrenergic (DBH-IR only, red, open arrows) and DBH/PNMT-IR, adrenaline-synthesizing axons (yellow, white arrows) establish contacts with the TRH neurons. III, Third ventricle. Scale bars, 100 μm for A 10 μm for (**B**–**D**).

5.4. Efferent projections of the TRH neurons located in the aPVN

5.4.1. Localization of PHAL injection sites

To map the projection fields of the TRH neurons residing in the aPVN, PHAL was injected into this subnucleus of the PVN. In four animals, the core of the injection site covered the aPVN. In two of the four brains, cases 116 and 117, the PHAL injection site was centered halfway between the fornix and the third ventricle, corresponding to the lateral border of the aPVN (Fig. 13A,B). In these cases, the large cores of PHAL injections substantially overlapped with the location of TRH neurons in both the aPVN and the perifornical area. In case 124, PHAL was injected adjacent to the third ventricle, resulting in an injection site almost entirely confined to the aPVN and the anterior part of the periventricular parvocellular subdivision of the PVN (pPVN; Fig. 13C). In case 125, the PHAL injection site covered the ventral part of the aPVN and the adjacent area (Fig. 13D).

5.4.2. Distribution of double-labeled PHAL/proTRH-IR fibers projecting from the aPVN/perifornical area (cases 116 and 117)

The distribution of PHAL/proTRH fibers was very similar in both cases. PHAL/proTRH fibers were found primarily on the ipsilateral side, but some scattered double-labeled fibers were also observed on the contralateral side in every major projection area. The contralateral projection was most profound in the lateral septal nucleus. The distribution pattern of PHAL/proTRH axons in case 117 is illustrated in Figure 14, while the relative density of double-labeled fibers in brain areas is summarized in Table 8.

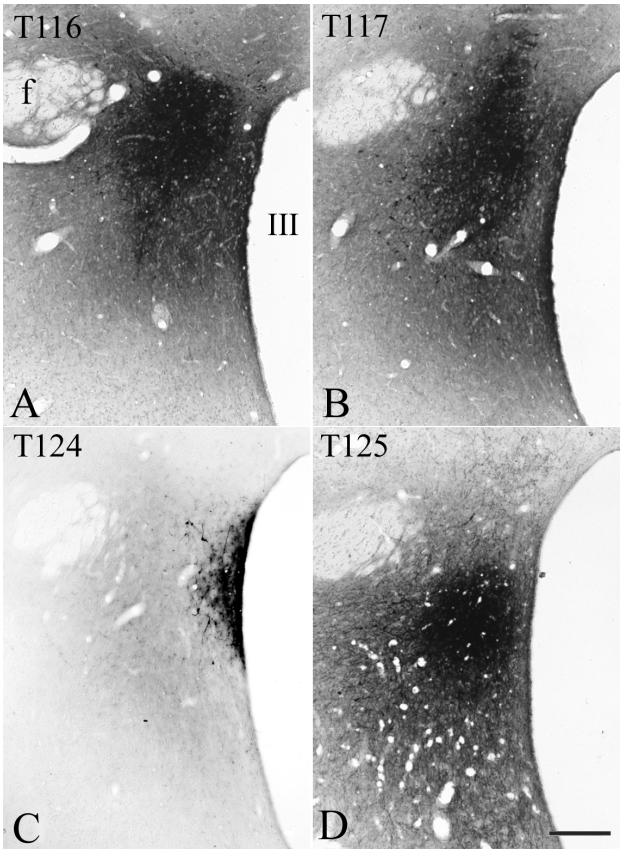

Figure 13. A-D: Localization of PHAL injection sites in four brains used in the anterograde tracing experiment. Scale bar, 250 μm.

Table 8. Subjective evaluation of the density of PHAL/proTRH-IR fibers in cases 116 and 117

Regions	Density of PHAL/proTRH fibers
Hypothalamus and preoptic region	
Anterior hypothalamic area	**
Anterodorsal preoptic nucleus	***
Anteroventral periventricular nucleus	**
Arcuate nucleus	*****
Arcuate nucleus-ventromedial nucleus border	***
Dorsomedial nucleus	***
Dorsomedial nucleus-ventromedial nucleus border	****
Lateral hypothalamic area	**
Lateroanterior hypothalamic nucleus	*
Medial preoptic area	**
Medial preoptic nucleus	***
Medial tuberal nucleus	****
Paraventricular nucleus	*
Periventricular nucleus	**
Posterior hypothalamic area	*
Retrochiasmatic area	****
Strial part of the preoptic area	**
Suprachiasmatic nucleus	*
Supramammillary nucleus	*
Supraoptic nucleus	*
Tuber cinereum area	****
Ventral premammillary nucleus	***
Ventral tuberomammillary nucleus	*
Ventromedial nucleus	*****
Thalamus	
Lateral habenular nucleus, medial part	*
Mediodorsal thalamic nucleus	*
Paraventricular thalamic nucleus	***
Reuniens thalamic nucleus	*
Amygdala, hippocampus, substantia innominata	
Amygdalohippocampal area	*****
Anterior cortical amygdaloid nucleus	*
Basomedial amygdaloid nucleus, anterior part	*
Basomedial amygdaloid nucleus, posterior part	*
Bed nucleus of the stria terminalis, intraamygdaloid division	***
Central amygdaloid nucleus, capsular part	*
Central amygdaloid nucleus, medial division	***
Dentate gyrus	***
Field CA1 of hippocampus	*
Field CA3 of hippocampus	***
Fimbria of the hippocampus	**

Lateral amygdaloid nucleus, ventromedial part	*
Medial amygdaloid nucleus, anterodorsal part	****
Medial amygdaloid nucleus, posterodorsal part	*****
Medial amygdaloid nucleus, posteroventral part	*****
Piriform cortex	*
Posterolateral cortical amygdaloid nucleus	*
Posteromedial cortical amygdaloid nucleus	*
Substantia innominata	***
Substantia innominata, basal part	**
Bed nucleus of the stria terminalis and septum	
Bed nucleus of the stria terminalis, lateral division	*
Bed nucleus of the stria terminalis, lateral division, dorsal part	*
Bed nucleus of the stria terminalis, lateral division, intermediate part	*
Bed nucleus of the stria terminalis, lateral division, ventral part	***
Bed nucleus of the stria terminalis, medial division, anterior part	*****
Bed nucleus of the stria terminalis, medial division, posterior part	*****
Bed nucleus of the stria terminalis, medial division, posterointermediate	****
Bed nucleus of the stria terminalis, medial division, posterolateral part	*****
Bed nucleus of the stria terminalis, medial division, ventral part	***
Lateral septal nucleus, dorsal part	*
Lateral septal nucleus, intermediate part	***
Lateral septal nucleus, ventral part	*****
Parastrial nucleus	*
Stria terminalis	*
Other telencephalic regions	
Anterior olfactory nucleus, medial part	*
Anterior olfactory nucleus, posterior part	*
Dorsal endopiriform nucleus	*
Islands of Calleja, major island	*
Medial septal nucleus	*
Nucleus of the horizontal limb of the diagonal band	*
Nucleus of the vertical limb of the diagonal band	*
Ventral pallidum	*
Zona limitans	**
Mesencephalon and hindbrain	
Lateral parabrachial nucleus, central part	*
Lateral periaqueductal gray	*
Periaqueductal gray	*
Ventral tegmental area	*
Ventrolateral periaqueductal gray	*

5.4.3. Hypothalamus and preoptic region

The density of PHAL/proTRH-IR fibers was moderate in the preoptic region and anterior hypothalamus (Fig. 14E-G). Double-labeled fibers were distributed broadly in these areas, extending to the medial preoptic nucleus (Fig. 15C), anterodorsal preoptic nucleus, strial part of the preoptic area, periventricular nucleus, anteroventral periventricular nucleus, posterior part of the medial preoptic area, and most anterior portions of the anterior hypothalamic area. Laterally, the dorsal part of the lateral hypothalamic area also contained PHAL/proTRH fibers.

More caudally in the hypothalamus, a high density of double-labeled axons was found throughout the retrochiasmatic area and the rostrocaudal extent of the arcuate nucleus (Fig. 14H-K). Most double-labeled fibers were distributed in the dorsomedial part of the arcuate nucleus, whereas a moderate density of fibers was observed in the lateral part of the nucleus, with only scattered fibers in its ventromedial part. In the dorsomedial part, the double-labeled fibers were oriented mainly rostrocaudally and frequently established large varicosities (Fig. 15A).

Large number of PHAL/proTRH-IR axons was found in the ventromedial nucleus (Fig. 14H,I). The double-labeled fibers were distributed primarily in the dorsomedial and medial parts of the nucleus. Several fibers ran parallel to the coronal plane and established several varicosities (Fig. 15E). Many double-labeled axons were also seen immediately rostral to the ventromedial nucleus, in the medial part of the subparaventricular zone. Several varicose PHAL/proTRH-IR axons were present between the arcuate and the ventromedial nuclei and between the borders of the ventromedial and dorsomedial nuclei.

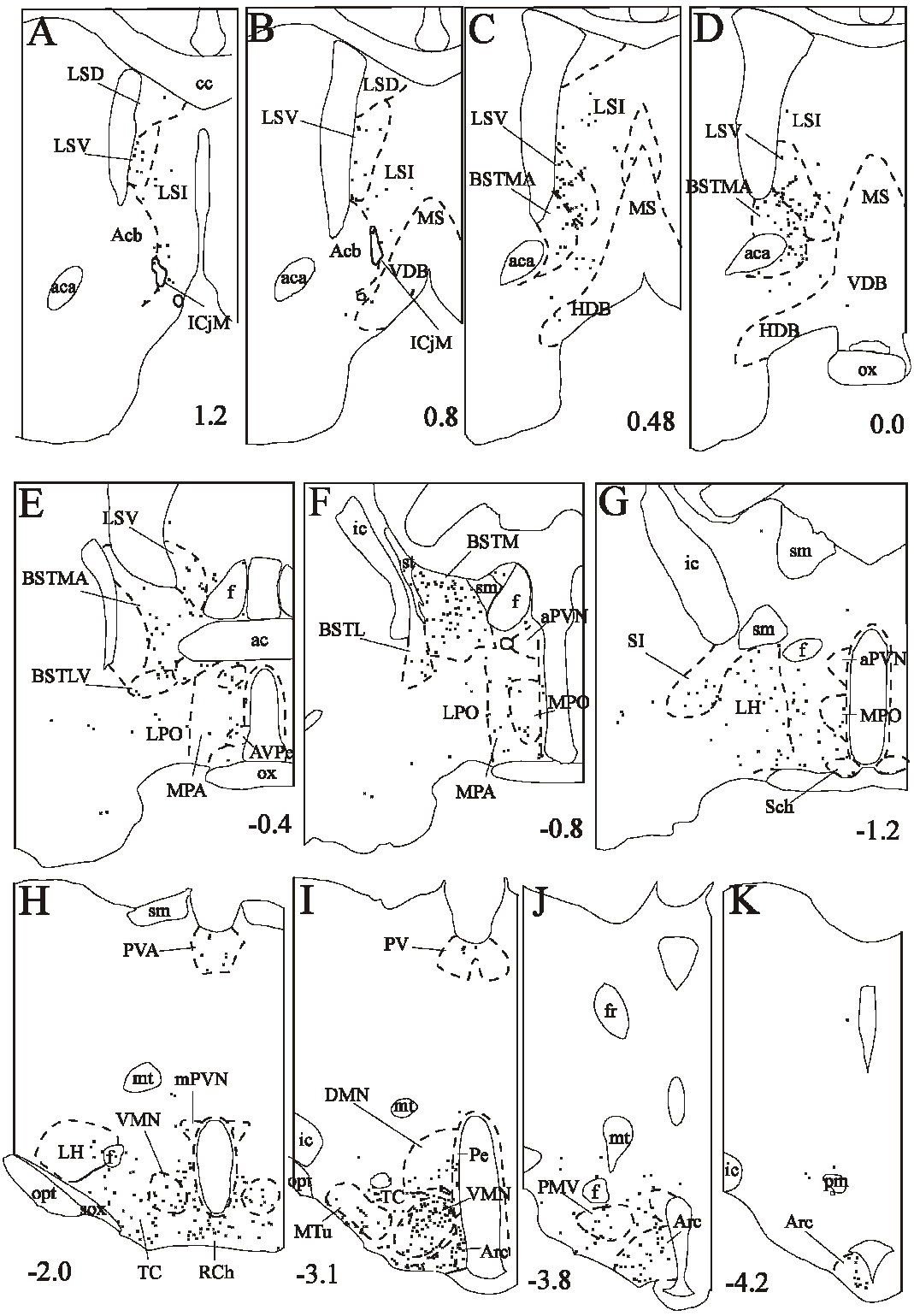
A
LSD
cc
LSV
LSI
Acb
aca
ICjM
1.2
B
LSD
LSV
LSI
MS
Acb
VDB
aca
ICjM
0.8
C
LSV
LSI
BSTMA
MS
aca
HDB
0.48
D
LSV
LSI
BSTMA
MS
aca
VDB
HDB
ox
0.0
E
LSV
BSTMA
f
ac
BSTLV
LPO
AVPe
ox
MPA
-0.4
F
ic
BSTM
st
sm
f
aPVN
BSTL
LPO
MPO
MPA
-0.8
G
ic
sm
SI
sm
f
aPVN
LH
MPO
Sch
-1.2
H
sm
PVA
mt
mPVN
VMN
LH
f
opt
aox
TC
RCh
-2.0
I
PV
DMN
mt
ic
Pe
opt
TC
VMN
MTu
Arc
-3.1
J
fr
mt
PMV
f
Arc
-3.8
K
ic
pm
Arc
-4.2

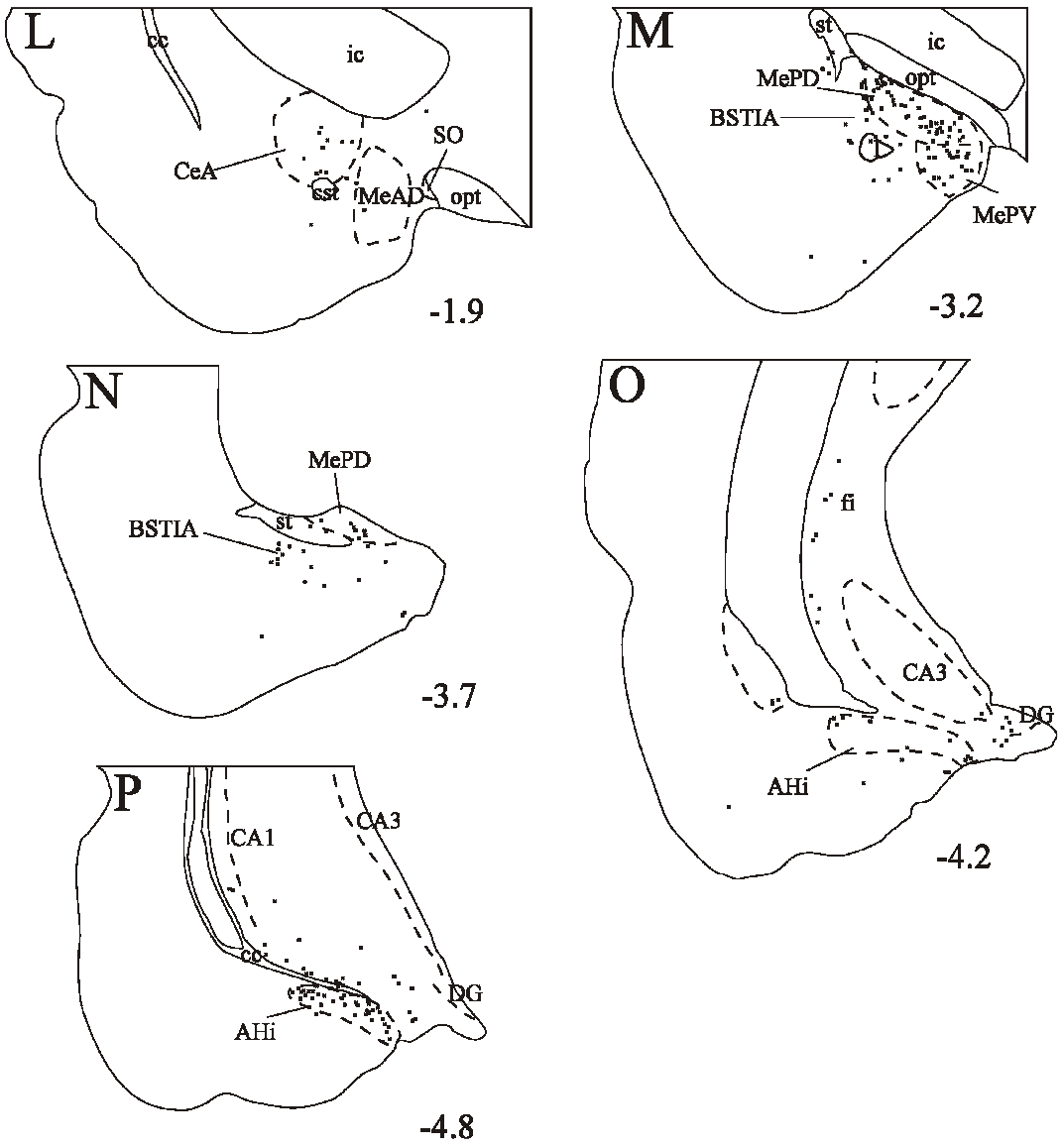

Figure 14. A-P: Schematic drawings of sections from case 117 illustrate the distribution of PHAL/proTRH-IR axons. Crosses represent double-labeled fiber segments. Numbers indicate the approximate anteroposterior distance of sections in mm from the bregma. Regions of the amygdala and hippocampus are shown in **L**-**P**.

Double-labeled fibers were also observed in the ventromedial part of the dorsomedial nucleus (Figs. 14I, 15B), rostral to the level of the compact part. More caudally, some double-labeled fibers were present in the compact and the ventral parts of the dorsomedial nucleus.

Several PHAL/proTRH-IR fibers were distributed in a broad region ventral to the fornix (Fig. 14H-J). This region included the tuber cinereum area, the medial tuberal

nucleus (Fig. 15F), and the ventral premammillary nucleus. PHAL/proTRH-IR fibers were also found close to the ventral surface of the hypothalamus.

Beside these major hypothalamic areas, scattered PHAL/proTRH fibers were seen in several other hypothalamic nuclei, namely, the lateroanterior hypothalamic nucleus, suprachiasmatic nucleus, supraoptic nucleus, paraventricular nucleus, posterior part of the lateral hypothalamic area, posterior hypothalamic area, ventral tuberomammillary nucleus, and supramammilary nucleus.

5.4.4. Thalamus and epithalamus

A moderate density of PHAL/proTRH-IR fibers was found in the paraventricular nucleus of the thalamus, throughout its rostrocaudal extent (Figs. 14H,I, 15D). These fibers mainly ran parallel to the coronal plane. Scattered PHAL/proTRH-IR axons were present in the nucleus reuniens, mediodorsal nucleus, and lateral habenular nucleus.

5.4.5. Substantia innominata, amygdala, and hippocampus

Some varicose double-labeled fibers and mediolaterally running, thin PHAL/proTRH axons that established a few boutons were observed in the substantia innominata (Figs. 14G, 15M). Varicose PHAL/proTRH-IR fibers were present in the medial and capsular parts of the central amygdaloid nucleus (Figs. 14L, 15L), especially between anteroposterior levels 1.7 and 2.2 mm caudal to the Bregma.

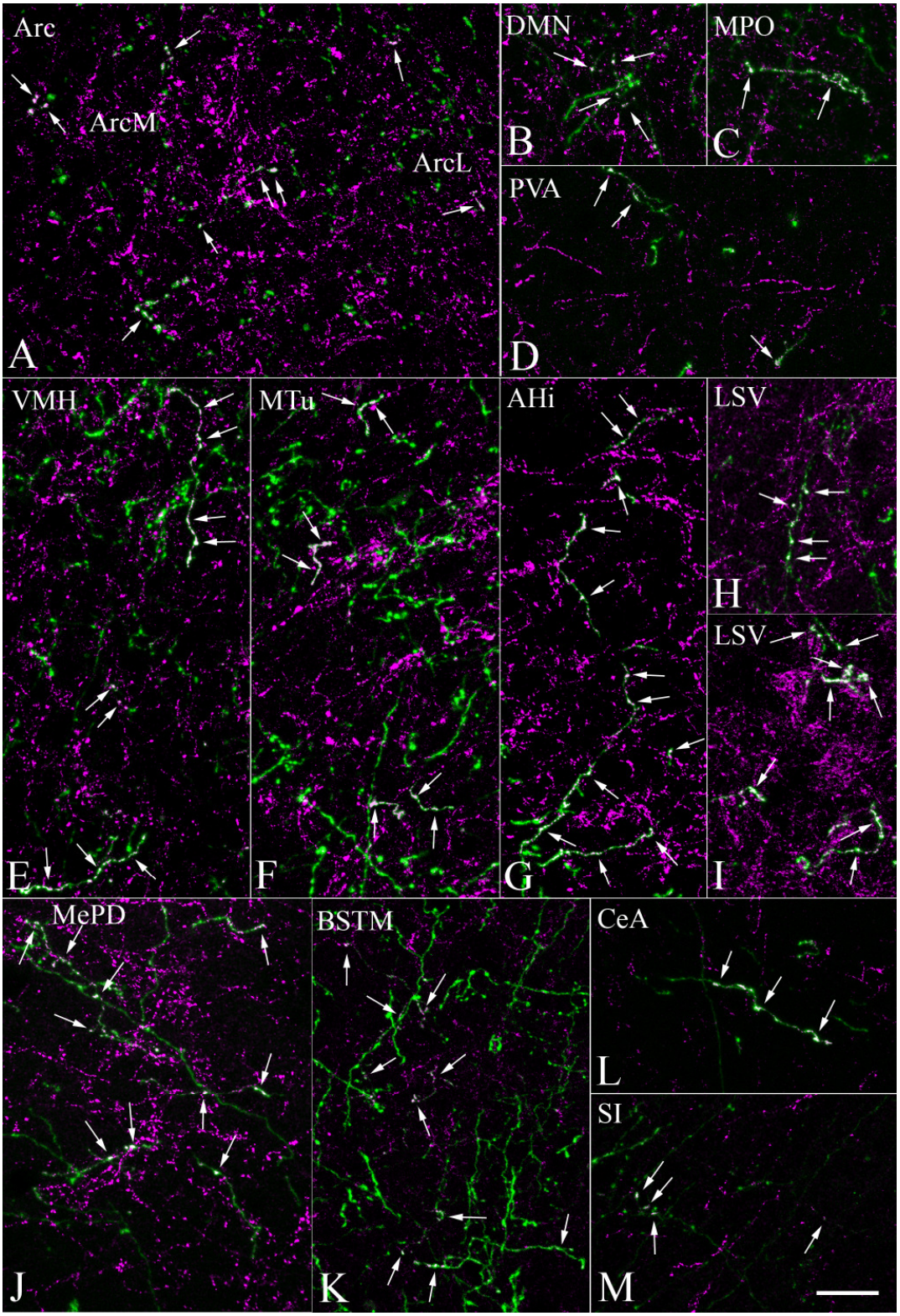
Arc
ArcM
ArcL
A
DMN
B
MPO
C
PVA
D
VMH
E
MTu
F
AHi
G
LSV
H
LSV
I
MePD
J
BSTM
K
CeA
L
SI
M

Figure 15. Double immunofluorescent staining demonstrates the presence of proTRH (magenta) in PHAL-containing (green) axons in different brain regions. Double-labeled axons (arrows) are indicated by the composite white color. Images represent five to twelve 1-μm-thick confocal optical sections projected into one plane for better visualization of segments of double-labeled fibers. Images demonstrate PHAL/proTRH-containing fibers present in the arcuate nucleus (**A**), dorsomedial nucleus (**B**), medial preoptic nucleus (**C**), paraventricular thalamic nucleus (**D**), ventromedial hypothalamic nucleus (**E**), medial tuberal nucleus (**F**), posteromedial part of amygdalohippocampal area (**G**), lateral septal nucleus on the ipsilateral and contralateral sides (**H,I**), posterodorsal part of the medial amygdaloid nucleus (**J**), medial division of the bed nucleus of the stria terminalis (**K**), central amygdaloid nucleus (**L**), and substantia innominata (**M**). Scale bar, 20 μm.

A high density of varicose PHAL/proTRH-IR axons was found in the medial amygdaloid nucleus, primarily in the posterodorsal and posteroventral subnuclei (Fig. 14M,N). These fibers were highly varicose, and many long fibers could be seen running parallel to the coronal plane (Fig. 15J). A moderate density of double-labeled fibers was also present in the intraamygdaloid division of the bed nucleus of the stria terminalis (Fig. 14M). More caudally, several PHAL/proTRH-IR axons were observed in a dense network of proTRH-IR fibers located in the amygdalohippocampal transition area (Fig. 11P). These PHAL/proTRH axons ran parallel to the coronal plane and established several medium-size to large varicosities (Fig. 15G). Several double-labeled axons were found in a discrete group of varicose proTRH-IR fibers medial to the amygdalohippocampal transition area near the dentate gyrus (Fig. 14O). PHAL/proTRH fibers were also present diffusely in the ventral hippocampus. Scattered PHAL/proTRH fibers were present in several areas, including the anterior cortical amydaloid nucleus, posteromedial and posterolateral cortical amygdaloid nuclei, basomedial amygdaloid nucleus, piriform cortex, ventromedial part of the lateral amygdaloid nucleus, and fimbria of the hippocampus.

5.4.6. Bed nucleus of the stria terminalis and septum

PHAL/proTRH fibers were found in several divisions of the bed nucleus of the stria terminalis. Many of these fibers could be followed for a long distance, indicating the coronal orientation of the fibers. A high density of double-labeled fibers was present throughout the medial division (Figs. 14C-F, 15K). Among the nuclei of the lateral division, only the ventral and the posterior part contained significant numbers of

double-labeled fibers (Fig. 14E,F). In the stria terminalis, passing PHAL/proTRH fibers establishing some boutons were observed. In the lateral septal nucleus, proTRH-IR fibers established an extremely dense fiber network, frequently forming basket-like structures around the surface of perikarya and completely ensheathed dendrites. Varicose PHAL/proTRH-IR axons were densely distributed in the ventral part of the lateral septal nucleus, some of them forming basket-like shapes (Figs. 14A-E, 15H,I). The intermediate part of the lateral septal nucleus contained a moderate number of double-labeled fibers (Fig. 14B-D); in its medial part, double-labeled axons frequently ran dorsally, establishing a few en passant boutons. The dorsal part of the lateral septal nucleus contained only scattered double-labeled fibers in its most anterior portions.

5.4.7. Other forebrain regions

Scattered double-labeled fibers were found in the ventral pallidum, medial septal nucleus, nucleus of the horizontal limb of the diagonal band, nucleus of the vertical limb of the diagonal band, major island of Calleja, posterior part of the anterior olfactory nucleus, and the area adjacent dorsomedially to the dorsal endopiriform nucleus.

5.4.8. Midbrain and hindbrain

Some scattered PHAL/proTRH-IR fibers could be observed in the periaqueductal gray, lateral and ventrolateral periaqueductal gray, ventral tegmental area, and central part of the lateral parabrachial nucleus.

5.4.9. Cases 124 and 125

Despite the apparently limited spread of the tracer outside the aPVN, the distribution pattern of PHAL/proTRH axons in case 124 was very similar to that in cases 116 and 117, with only slight differences in the density of double-labeled fibers in some regions. In case 125, the general distribution of double-labeled axons showed similarities to the pattern seen in the brains described above. However, generally, fewer PHAL/proTRH axons were observed in all regions, and only sparse double-labeled axons were present in the medial amygdaloid nucleus, dorsomedial nucleus, and substantia innominata. No PHAL/proTRH fibers were observed near the dentate gyrus or in the ventral hippocampus.

5.4.10. Distribution of retrogradely labeled TRH-IR cell bodies in the aPVN and perifornical area

To differentiate between the projection sites of TRH neurons residing in the aPVN and perifornical area, the retrograde tracer CTB was injected into brain regions where a high or moderate density of the PHAL/proTRH-IR fibers was observed in the anterograde tracing experiment. Representative CTB injection sites are shown in Figure 16. CTB/TRH-IR neurons in the aPVN and perifornical area were found primarily ipsilateral to the injection sites, with fewer double-labeled neurons on the contralateral side. The retrogradely labeled TRH neurons in the aPVN and perifornical region were counted in each brain with a successful CTB injection. The data are summarized in Table 9. Moderate to high numbers of CTB-containing TRH neurons in the aPVN were found after CTB injections into the arcuate nucleus (Figs. 17A, 19A), dorsomedial nucleus (Figs. 17C, 19B), medial preoptic area (Figs. 17D, 19E), caudal tuber cinereum area (Figs. 18D, 19D), ventral premammillary nucleus, anterior and posterior parts of the medial division of the BNST (Figs. 18A,B, 19J), paraventricular nucleus of the thalamus (Figs. 18E, 19G), central amygdaloid nucleus (Figs. 18F, 19K), and ventral part of the lateral septal nucleus (Fig. 19H). Only a few CTB/TRH-IR neurons, fewer than 10/animal, were found in the aPVN after CTB injections into the ventromedial nucleus, medial amygdaloid nucleus, and amygdalohippocampal area. Moderate to high numbers of CTB-containing TRH neurons were present in the perifornical area after CTB injections into the ventral part of the lateral septal nucleus (Figs. 18G, 19H), ventromedial nucleus (Figs. 17B, 19C), dorsomedial nucleus (Figs. 17C, 19B), medial preoptic region (Figs. 17D, 19E), medial amygdaloid nucleus (Fig. 19F), amygdalohippocampal area (Figs. 17E, 19I), ventral premammillary nucleus, and posterior part of the medial division of the BNST (Figs. 18A,C, 19J). The greatest number of retrogradely labeled perifornical TRH neurons was observed after CTB injection into the ventral part of the lateral septal nucleus. Only rare (fewer than 10/animal) perifornical TRH neurons contained CTB when injections were made into the arcuate nucleus, paraventricular nucleus of the thalamus, central amygdaloid nucleus, caudal part of the tuber cinereum area, and anterior part of the medial division of the BNST.

In all of the CTB-injected brains, very few TRH neurons in hypophysiotropic parts of the PVN contained CTB. In the medial and periventricular parvocellular subdivisions, 10 or more CTB-IR TRH neurons/animal were found in only two cases: after CTB injection into the medial preoptic region (10 neurons) and the dorsomedial nucleus (12 neurons).

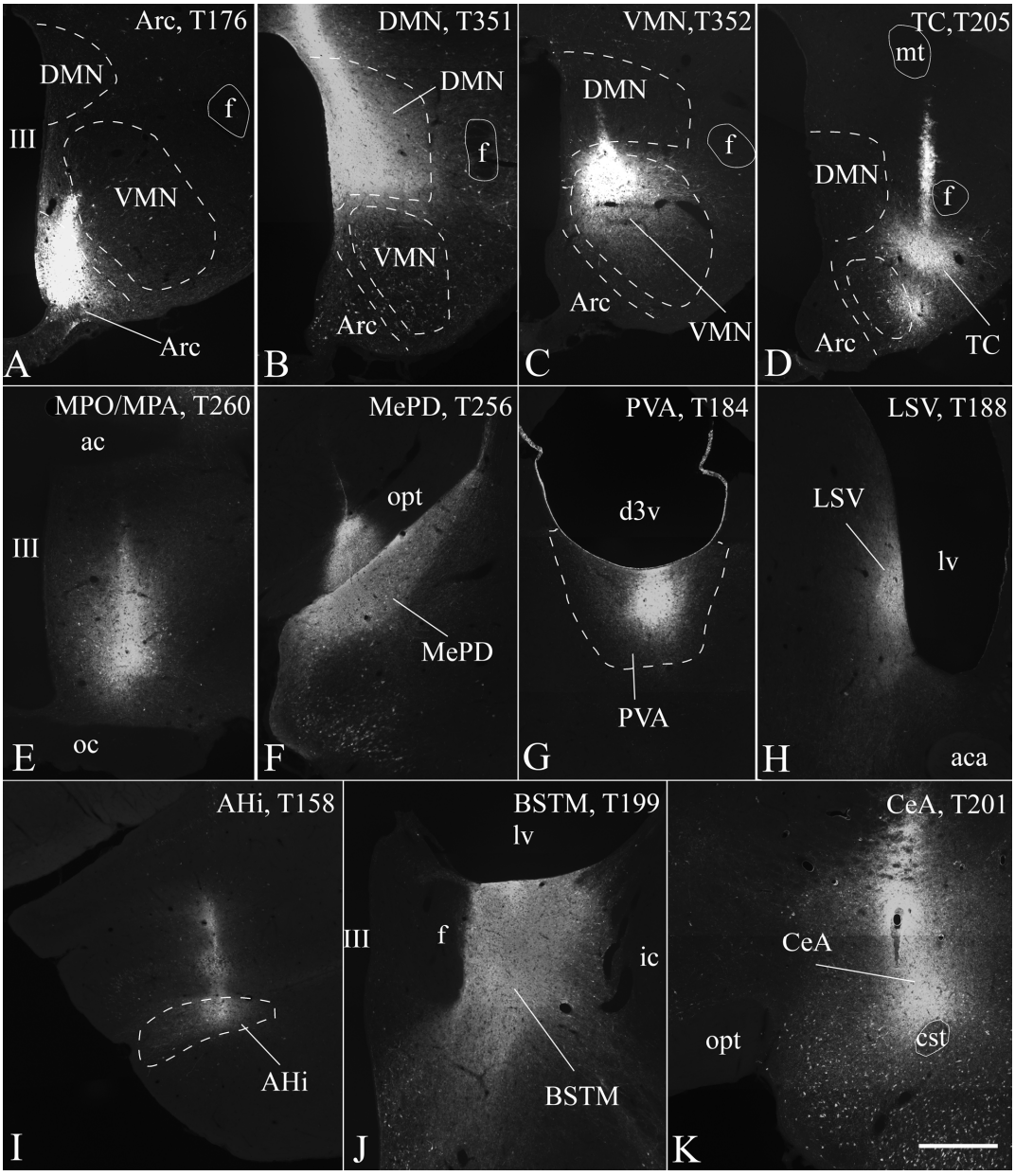

Figure 16. Cores of CTB injection sites centered in the arcuate nucleus (**A**), dorsomedial nucleus (**B**), dorsomedial part of the ventromedial nucleus (**C**), caudal part of the tuber cinereum area (**D**), medial preoptic nucleus/medial preoptic area (**E**), posterodorsal part of the medial amygdaloid nucleus (**F**), paraventricular nucleus of the thalamus (**G**), ventral part of the lateral septal nucleus (**H**), amygdalohippocampal area (**I**), posterior medial division of the BNST (**J**), and central amygdaloid nucleus (**K**). Case numbers are indicated in the images. Scale bar, 500 μm.

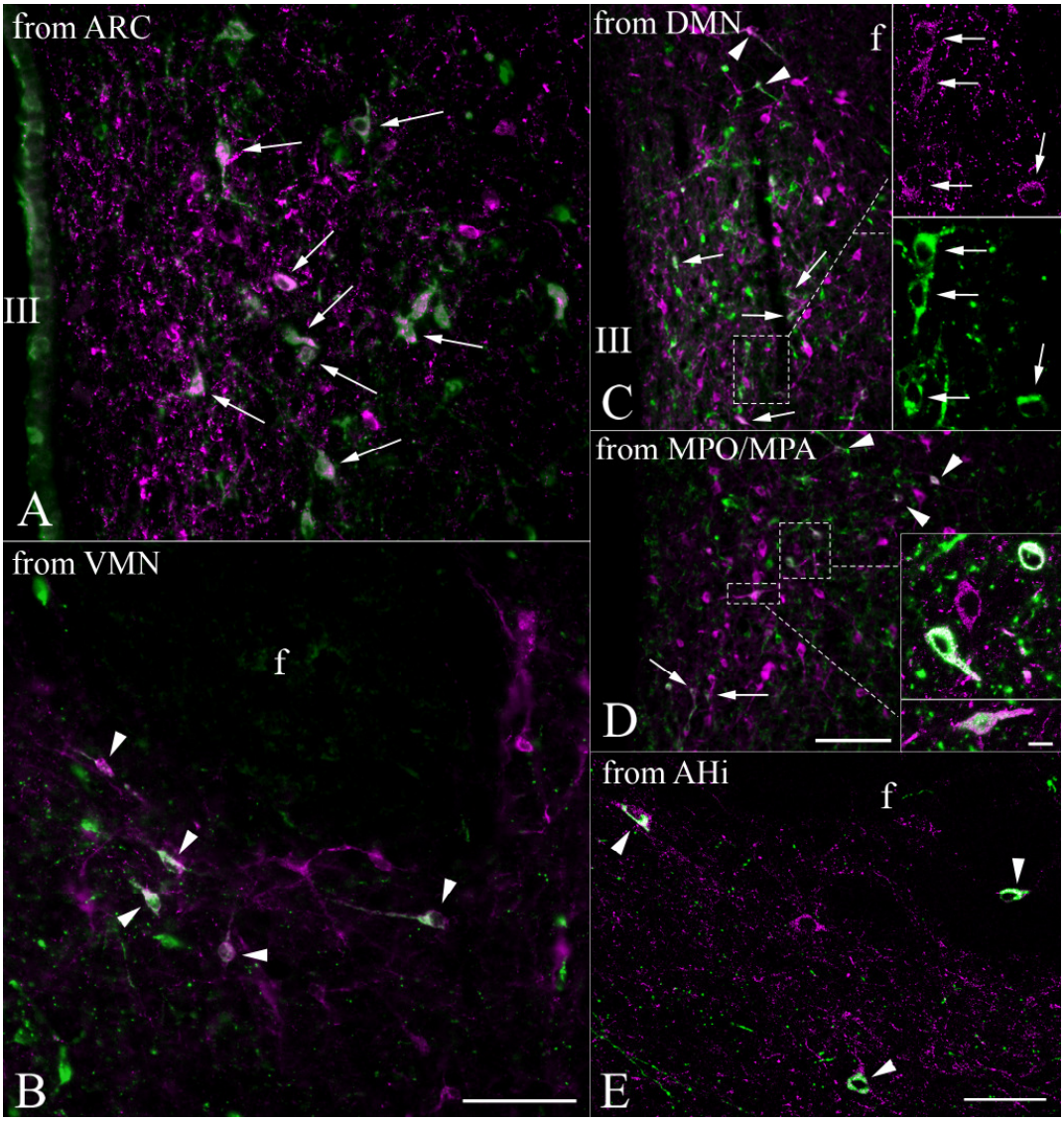

Figure 17. Double immunofluorescence demonstrates the presence of CTB (green) in TRH-IR (magenta) perikarya in the aPVN and perifornical area of brains previously injected with CTB into the arcuate nucleus (ARC; **A**), ventromedial nucleus (VMN; **B**), dorsomedial nucleus (DMN; **C**), medial preoptic nucleus/medial preoptic area (MPO/MPA; **D**), and amygdalohippocampal area (AHi; **E**). Arrows point to CTB/TRH-IR neurons in the aPVN; arrowheads indicate CTB/TRH-IR neurons of the perifornical cell group. High-magnification confocal images of single 1-µm-thick optical sections were taken of framed areas in **C** and **D** and are shown as **insets**. Inset in **C** shows TRH and CTB labeling in separate images to facilitate identification of double-labeled perikarya. Scale bars, 50 µm in **B** (applies to **A**,**B**); 100 µm in **D** (applies to **C**,**D**); 50 µm in **E**; 10 µm in insets.

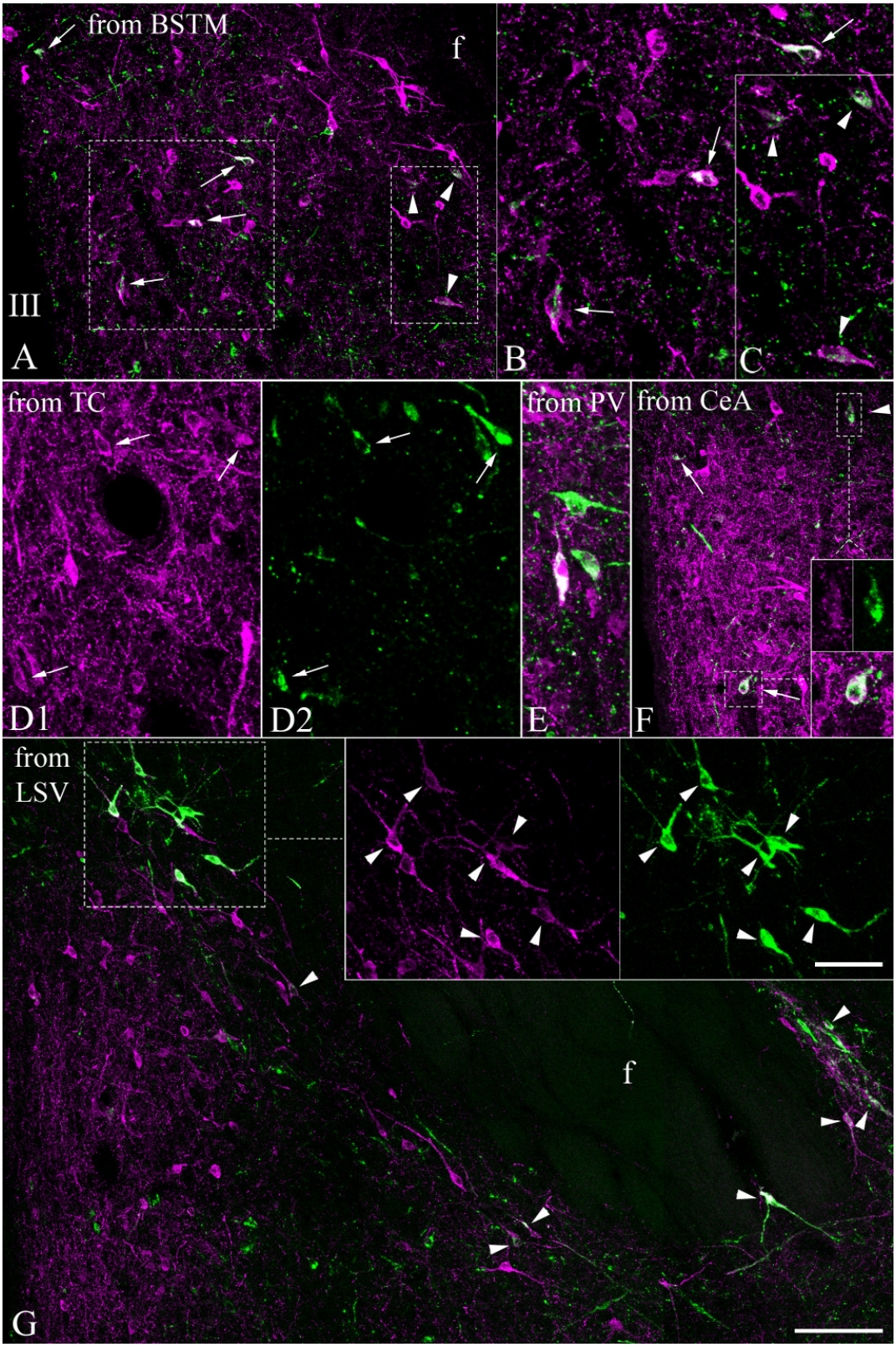
from BSTM
f
III
A
B
C
from TC
D1
D2
from PV
E
from CeA
F
from
LSV
f
G

Figure 18. Double immunofluorescence demonstrates the presence of CTB (green) in TRH-IR (magenta) perikarya in the aPVN and perifornical area of brains previously injected with CTB into the bed nucleus of the stria terminalis, posterior medial division (BSTM; **A-C**), caudal part of the tuber cinereum area (TC; **D1,2**), paraventricular nucleus of the thalamus (PV; **E**), central amygdaloid nucleus (CeA; **F**), and ventral part of the lateral septal nucleus (LSV; **G**). Images were made by projecting four to seven consecutive 2-µm-thick confocal optical slices into one plane. Arrows point to CTB/TRH-IR neurons in the aPVN; arrowheads indicate CTB/TRH-IR neurons of the perifornical cell group. Framed areas in **A** are magnified and shown in **B** and **C**, framed areas in **F** and **G** are magnified and shown in **insets**. To facilitate identification of double-labeled cells, TRH and CTB labelings of the same fields are shown in separate images in **D1** and **D2**, in the upper inset pair in **F**, and in the inset in **G**. Scale bars, 100 µm in **G** (applies to **A**,**F**,**G**); 50 µm for **B**-**E**, insets in **F**; 50 µm in insets in **G**.

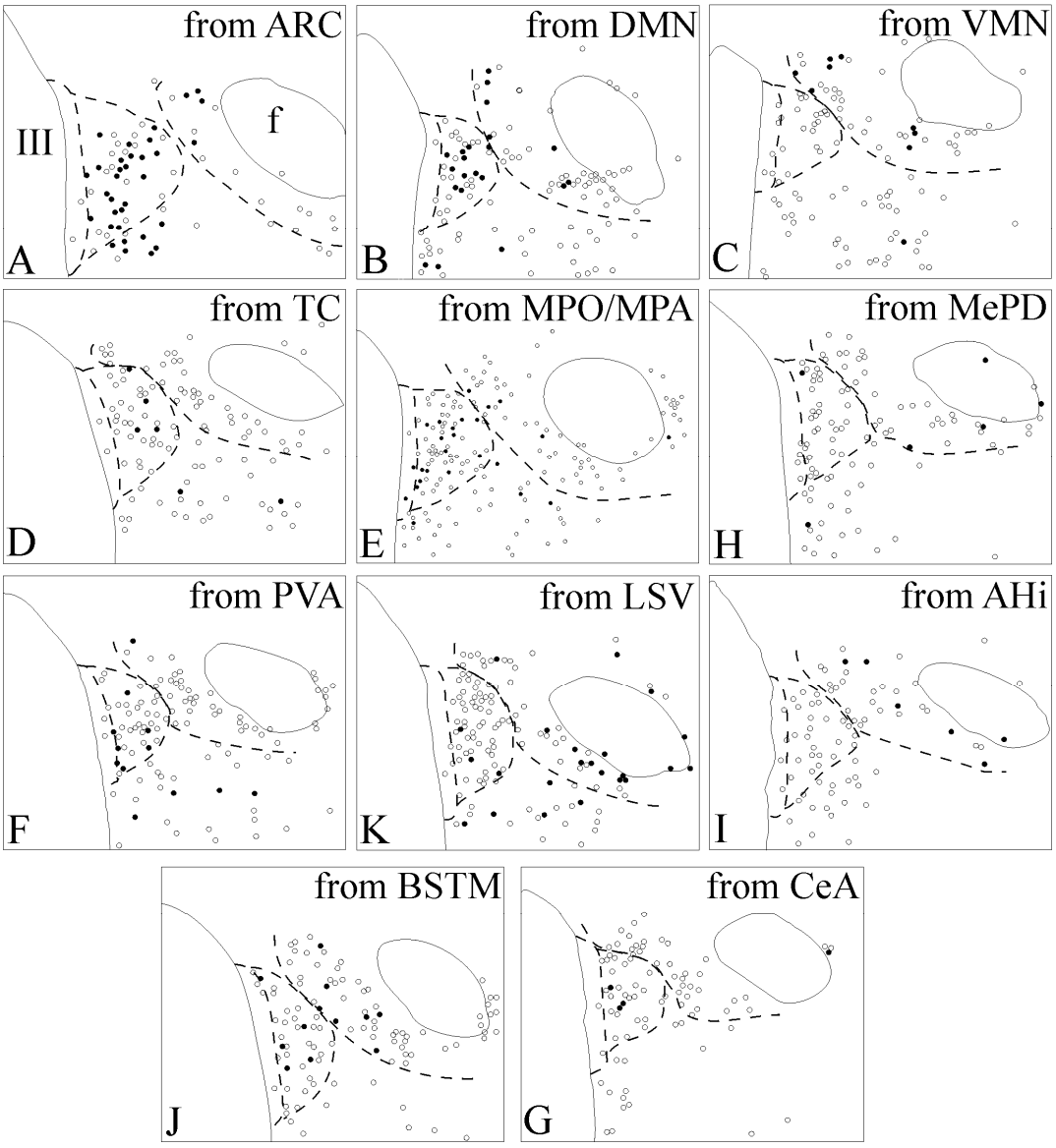

Figure 19. Schematic representation of retrogradely labeled TRH neurons in the aPVN and perifornical area following CTB injections into the arcuate nucleus (ARC; **A**), dorsomedial nucleus (DMN; **B**), ventromedial nucleus (VMN; **C**), caudal tuber cinereum area (TC; **D**), medial preoptic nucleus/medial preoptic area (MPO/MPA; **E**), medial amygdaloid nucleus (MePD; **F**), paraventricular nucleus of the thalamus (PVA; **G**), ventral part of the lateral septal nucleus (LSV; **H**), amygdalohippocampal area (AHi; **I**), bed nucleus of the stria terminalis, posterior medial division (BSTM; **J**), and central amygdaloid nucleus (CeA; **K**). The corresponding injection sites are illustrated in Figure 13. Open circles, single-labeled TRH neurons; solid circles, CTB/TRH double-labeled neurons. Dashed lines indicate the approximate borders of the periventricular parvocellular subdivision of the PVN, aPVN, and perifornical TRH cell group.

Table 9. Quantification of retrogradely labeled TRH neurons in the aPVN and perifornical area

Site of CTB injection	Case	Number of CTB/TRH-IR cells in the		
		aPVN[1]	perifornical area	
			in the level of the aPVN	caudal to the aPVN[2]
Arcuate nucleus, medial part	T176	45	5	0
Dorsomedial hypothalamic nucleus	T351	64	31	12
Ventromedial hypothalamic nucleus, dorsomedial part	T352	6	31	10
Ventromedial hypothalamic nucleus, ventromedial part	T177	4	22	3
Caudal part of the tuber cinereum area	T205	22	2	2
Ventral premammillary nucleus	T214	30	5	6
Medial preoptic nucleus / medial preoptic area	T260	43	31	5
Paraventricular thalamic nucleus	T183	15	1	1
Paraventricular thalamic nucleus	T184	25	2	2
Lateral septal nucleus, ventral part	T188	12	85	44
Lateral septal nucleus, ventral part / medial division of the BNST, anterior part	T197	28	60	18
Anterior and posterolateral part of the medial division of the BNST	T198	13	0	0
Medial division of the BNST, posterior part	T199	18	17	2
Central amygdaloid nucleus	T201	11	6	1
Medial amygdaloid nucleus, posterodorsal part	T256	6	10	2
Medial amygdaloid nucleus, posterodorsal part	T257	1	12	3
Medial amygdaloid nucleus, posteroventral part	T254	2	11	4
Amygdalohippocampal area	T155	1	11	5
Amygdalohippocampal area	T158	1	13	2

CTB/TRH neurons were counted in every fourth section on both the ipsilateral and contralateral sides

[1] included the CTB/TRH neurons in the periventricular parvocellular subdivision adjacent to the aPVN

[2] CTB/TRH neurons in the posterior part of the perifornical TRH cell group, located caudally to the antero-posterior level of the aPVN

6. Discussion

6.1. Origin of the NPY-IR innervation of the CRH neurons in the PVN of rats

Our data demonstrate that the three main sources of the NPY-IR innervation of hypophysiotropic CRH neurons are the arcuate nucleus and the noradrenergic and adrenergic neuronal populations of the brainstem (Fig. 20).Other regions may have only a minor role in the NPY innervation of these cells.

Approximately two thirds of the NPY innervation of CRH neurons of the PVN originate from the brainstem: 41% from adrenergic, and 22% from noradrenergic neurons. The adrenergic NPY innervation of the PVN originates from the C1–3 regions of the medulla, where the vast majority of the adrenergic neurons are known to co-synthesize NPY and project to the medial parvocellular subdivision of the PVN (113, 195). The noradrenergic/NPY innervation of the PVN originates from the A1, A2, and A6 noradrenergic cell populations of the brainstem (113). The noradrenergic A1 region contains the largest population of the NPY-synthesizing DBH neurons that innervate the PVN, but it projects primarily to the magnocellular division and sends only scattered NPY fibers to the parvocellular subnuclei (196). Only 15% of the noradrenergic neurons of the A2 region contains NPY-immunoreactivity (113), but these neurons innervate the parvocellular subnuclei of the PVN including the medial parvocellular subdivision (196). The A6 region (locus coeruleus) also contains an NPY-synthesizing noradrenergic subpopulation that projects to the PVN, but the locus coeruleus projects primarily to the periventricular parvocellular subdivision and sends only scattered fibers to the medial parvocellular subdivision (196). Accordingly, because the CRH neurons are largely localized in the medial parvocellular subdivision of the PVN, we assume that the noradrenergic/NPY innervation of the CRH neurons mainly originates from the A2 region, and the A1 and A6 regions contribute only in a minor way to this innervation. Several lines of data indicate that the brainstem catecholaminergic neurons contribute to the activation of HPA axis during glucoprivation, infection and inflammation.

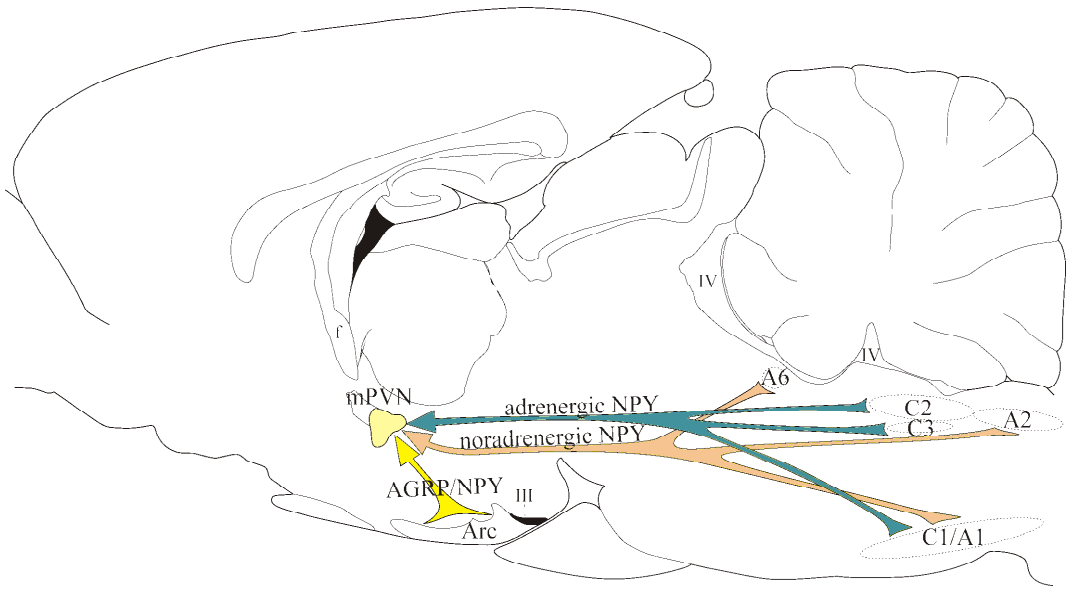

Figure 20. Schematic figure illustrates the main sources of the neuropeptide Y (NPY) innervation of the hypophysiotropic corticotropin-releasing hormone neurons, which are localized in the parvocellular subdivision of the hypothalamic paraventricular nucleus (PVN). Three neuron populations contribute unequally to this innervation, the arcuate nucleus (Arc), the adrenergic (C1-3) and the noradrenergic (A1, A2, A6) neurons of the brainstem. f, fornix; III, third ventricle; IV, fourth ventricle,

One of the known functions of the brainstem catecholaminergic neurons is the mediation of the neuronal response to glucoprivation, and several lines of evidence indicate that the catecholaminergic neurons of the brainstem innervating the PVN are activated by glucoprivation. Glucoprivation increases c-fos expression in the C1–3 regions (197), significantly increases NPY mRNA level in the C1–3 and A1 regions (198), and stimulates DBH gene expression in the C1, A1, and A2 regions (199). Because glucoprivation activates CRH neurons in the PVN and increases circulating corticosterone levels that can be prevented by the ablation of the catecholaminergic projection neurons to the PVN (200), it is presumed that brainstem catecholamine neurons are important for this response. It has also been shown that brainstem catecholamine neurons are necessary for increased food intake in response to hypoglycemia (201-204).

Brainstem catecholaminergic neurons also contribute to activation of the HPA axis in response to infection and inflammation. After the systemic administration of interleukin-1 (IL-1), c-fos expression was observed in neurons of C1, C2, A1, and A2

regions projecting to the PVN, and lesioning these regions decreased the number of the IL-1-activated CRH neurons in the PVN (205, 206). Moreover, the CRH mRNA increase induced by IL-1 or bacterial lipopolysaccharide was markedly attenuated by transection of ascending brainstem pathways (205, 207).

On the basis of these data, therefore, it is conceivable that catecholaminergic NPY neurons may contribute to the activating effects of hypoglycemia and immune stress on hypophysiotropic CRH neurons. In support of this possibility, the acute icv administration of NPY markedly stimulates CRH neurons (146, 147, 174). Although CRH neurons are directly innervated by NPY axons, and contain Y1 receptors (208), the stimulatory effects of NPY on CRH gene activity could be mediated indirectly because all NPY receptors are coupled to inhibitory G proteins (95). In support of this possibility, Pronchuk *et al.* (209) demonstrated that acutely administered NPY markedly suppresses the GABAA-mediated inhibitory postsynaptic currents in neurons in the PVN, suggesting that NPY may stimulate CRH neurons by disinhibition of the GABA-ergic tone. In addition, CRH neurons are embedded in a network of Y1-IR fibers, suggesting a presynaptic location of Y1 receptor in the afferents of CRH neurons (140).

To determine the origin of the noncatecholaminergic NPY axons that innervate CRH neurons in the PVN, we performed triple-labeling immunocytochemistry on sections of arcuate nucleus-ablated rats. MSG treatment eradicated the vast majority of arcuate nucleus including the NPY-IR neurons, leading to a marked decrease in the number of NPY-IR axons lacking DBH-immunoreactivity that were in contact with hypophysiotropic CRH neurons. In addition, triple-labeling immunocytochemistry using AGRP as a marker for NPY axons of arcuate nucleus origin showed that 34% of the NPY boutons in contact with CRH neurons contained AGRP and that 94% of hypothalamic CRH neurons were contacted by these NPY/AGRP fibers. However, most of the NPY axons originating from the arcuate nucleus tended to innervate ventromedially and caudally located CRH neurons in the PVN. In the caudal parts of the PVN, more than half of the NPY boutons juxtaposed to CRH neurons contained AGRP-immunoreactivity. These data not only assign an important role for the arcuate nucleus in the NPY-IR innervation of the CRH neurons in the PVN, but because of the regional heterogeneity of the arcuate innervation pattern, they also raise the possibility of functional segregation of paraventricular CRH neurons.

6.2. Effect of chronic NPY administration on the CRH gene expression of rats

Despite the fasting induced marked activation of NPY neurons in the arcuate nucleus, and the direct connection between the CRH neurons and the NPY neurons of the arcuate nucleus, CRH gene expression in the PVN decreases during fasting (111, 138). This would suggest an inhibitory effect of NPY on the CRH gene expression. Given the observations that NPY can increase circulating levels of ACTH, corticosterone (210), and CRH mRNA levels in the PVN (146, 147) as well as phosphorylate CREB in the nucleus of CRH neurons in the PVN (174), an inhibitory effect of NPY on CRH neurons would seem paradoxical. However, in contrast to the studies in the literature where the effect of an acute increase of NPY concentration was studied, NPY expression and release is chronically elevated during fasting (138).

To determine whether chronically elevated levels of NPY may regulate CRH synthesis during fasting, we examined the effect of a 3 day, continuous, central infusion of NPY on CRH gene expression in the PVN. In contrast to the acute effect of NPY, the chronic administration of NPY over 3 days by continuous infusion resulted in a marked reduction in CRH mRNA in the PVN. Because all NPY receptors are coupled to inhibitory G proteins (95), we presume that the effect of chronic NPY administration is exerted directly on these neurons to decrease cAMP synthesis through the activation of one or more NPY receptors. Since similarly to our experiment, NPY release is increased for a prolonged period during fasting, based on our results, we hypothesize that the activation of the NPY neurons of the arcuate nucleus plays important role in the mediation of the fasting.

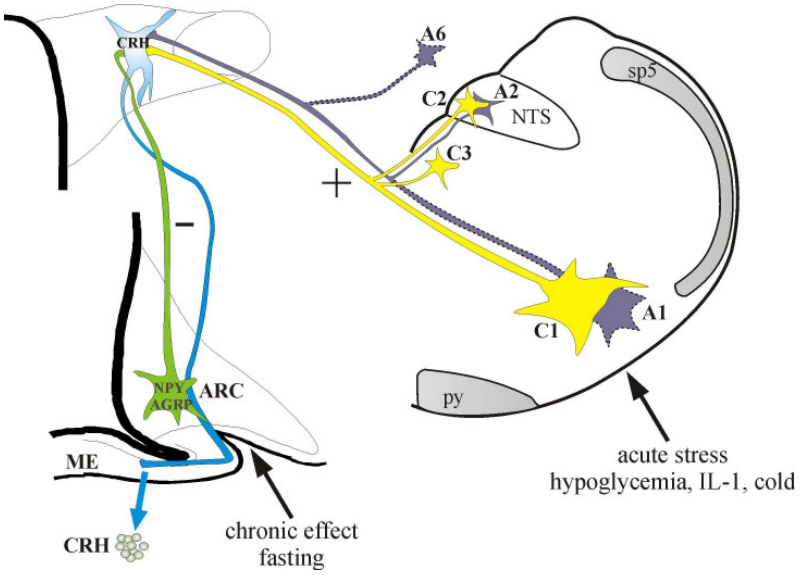

Figure 21. Schematic drawing illustrates the hypothesized role of neuropeptide Y (NPY) in the regulation of the hypophysiotropic corticotrophin-releasing hormone (CRH) neurons. During fasting, the prolonged increase of NPY from terminals of the arcuate nucleus inhibits the CRH neurons in the PVN. In contrast, the acute increase of NPY-release from the catecholaminergic neurons of the brainstem caused by such stressors as hypoglycemia, inflammation and cold results in stimulation of hypophysiotropic CRH neurons. ARC, arcuate nucleus; ME, median eminence; py, pyramidal tract; NTS, nucleus tractus solitarius; sp5, spinal trigeminal tract

As the brainstem catecholaminergic NPY neurons are activated by acute stressors, such as infection, cold and inflammation, these stressors may induce an acute increase of NPY release in the PVN that stimulate the CRH neurons. Due to the lack of NPY receptors, which are coupled in a stimulatory fashion to CRH expression, we propose that this stimulation is an indirect effect. It is conceivable that the increased level of NPY may facilitate the stimulatory effects of catecholamines on the CRH neurons (Fig. 21).

6.3. Catecholaminergic innervation of the TRH neurons in the PVN of rats

We have shown that approximately two thirds of the catecholaminergic innervation of the TRH neurons arises from adrenergic neurons, while the remaining one third originates from noradrenergic neurons. These data demonstrate that, similarly as it was observed in case of the hypophysiotropic CRH neurons, the catecholaminergic innervation of the hypophysiotropic TRH neurons originates from both adrenergic and noradrenergic neurons.

The adrenergic C1-3 regions and the noradrenergic A1, A2 and A6 regions contribute to the catecholaminergic innervation of the PVN. Since among the noradrenergic regions, only the A2 region sends dense projection to the medial parvocellular part of the PVN, we suggest that the catecholaminergic innervation of the hypophysiotropic TRH neurons arises from the C1-3 and A2 regions of the brainstem (Fig. 22).

DBH is present in the synaptic vesicles and synthesizes noradrenaline in the terminals of both the noradrenergic and adrenergic neurons (211). In contrast PNMT is present in the cytoplasm of the PNMT-containing terminals, therefore, the adrenaline-synthesis of these terminals is dependent on the noradrenaline concentration in the cytoplasm (211). The synthesized adrenaline is transported then into the synaptic vesicles (211). The cytoplasmic noradrenaline pool at least partly originates from reuptake of the released noradrenaline (211). Therefore, under basal condition, when these neurons may contain primarily noradrenaline, the released transmitter may act primarily on β1 and/or α1 adrenergic receptors (211). However, after repeated firing when the reuptake of catecholamines is increased, these neurons may contain primarily adrenaline and act on α2 adrenergic receptors (211). All adrenergic receptors are G protein coupled receptors, but use different classes of G proteins (212). The α1 receptors are coupled to G_Q proteins and result in increased intracellular Ca^{2+} levels (212). The α2 receptors are coupled to G_I proteins and therefore, inhibit cAMP synthesis (212). Beta adrenergic receptors are coupled to G_S proteins and stimulate the synthesis of cAMP (212). Therefore, noradrenergic neurons and adrenergic neurons may exert different effects on their postsynaptic targets.

The action of catecholamines on the TRH neurons may also be modified by co-released transmitters. NPY has a potent inhibitory effect on TRH neurons (167, 174), but it is known that NPY can also affect catecholaminergic neurons by increasing the number of the presynaptic α2 catecholaminergic receptors (213). An inhibitory presynaptic action of NPY has also been reported in which NPY can decrease the synaptic activity of A1 catecholaminergic terminals by acting on Y2 presynaptic receptors (214).

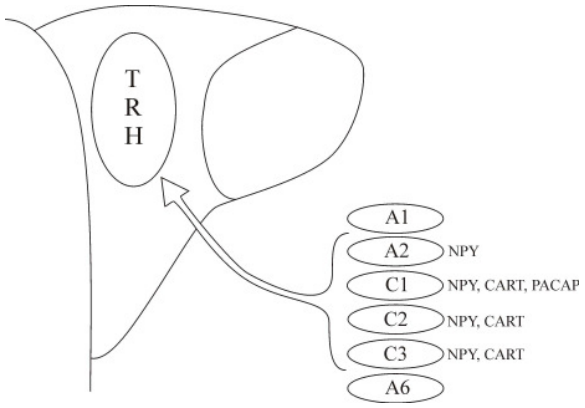

Figure 22. Schematic illustration of the catecholaminergic innervation of the hypophysiotropic TRH neurons. The medial and parvocellular subdivision in the hypothalamic paraventricular nucleus, where the hypophysiotropic thyrotropin-releasing hormone (TRH) neurons reside receive dense innervation from the adrenergic C1-3 and the noradrenergic A2 region. As an important co-transmitter NPY is expressed in these regions, while CART is also synthesized in the adrenergic neuron groups and pituitary adenylate cyclase activating polypeptide (PACAP) is expressed in the C1 region. These co-transmitters may modify the actions of catecholamines and contribute to to the mediation of diverse physiological effects.

Other co-transmitters of the catecholaminergic neurons, such as CART and PACAP, also regulate the TRH neurons in the PVN, possibly by potentiating the effects of catecholamines on these neurons (120, 215, 216). CART is mainly expressed in adrenergic C1-3 regions (115, 217). Approximately half of the CART-IR innervation of the TRH neurons derives from the adrenergic neurons of the C1-3 region, suggesting that these regions are of considerable importance in the regulation of the TRH neurons (159). Although CART increases the TRH mRNA level in the PVN (120), both the CART receptor and the signaling mechanism are unknown. PACAP is expressed in the

C1 region and stimulates the transcription of the TRH gene (215, 216) probably through the phopshorylation of CREB but experimental confirmation is needed. Finally, a subgroup of noradrenergic neurons of the A6 co-expresses galanin (218).

The only known physiological condition in which catecholaminergic neurons regulate the TRH neurons is cold stress (219-223). Though there is still no morphological evidence for the existence of adrenergic receptors on the surface of TRH neurons, a large amount of pharmacological data that support the effects of catecholamines on TRH neurons. For example, the cold-induced stimulation of TSH secretion does not occur within the first 10 days after birth in the rat when the hypothalamic catecholamine innervation is still immature. In addition, pharmacological depletion of the catecholaminergic system in adult rats can prevent the effect of cold on the HPT axis. The administration of α-adrenoreceptor antagonists leads to the same result. Furthermore, Perello et al. (220) have recently demonstrated that cold-induced proTRH biosynthesis and TRH-release can be blocked by centrally administered β-adrenoreceptor and α-adrenoreceptor antagonists, respectively. It is likely that adrenergic receptors are present on TRH neurons, since β-adrenoreceptor antagonists can block CREB phosphorylation in the TRH neurons (220), a factor which strongly enhances proTRH synthesis (166, 216). Cold-induced TRH release might also be mediated by α1-adrenoreceptors located on TRH axon terminals in the median eminence, because α1-adrenoreceptor agonist infusion into the median eminence can increase TRH secretion (224). Interestingly, however, c-fos expression has not been described in catecholaminergic neurons after cold exposure (225). Therefore, application of other activation markers will be necessary to determine whether adrenergic or noradrenergic cell groups or both mediate the effects of cold exposure on hypophysiotropic TRH neurons.

6.4. Efferent projections of the TRH neurons located in the aPVN

We revealed the major efferent projection sites of the nonhypophysiotropic population of TRH neurons located in the aPVN by using combined anterograde and retrograde tract-tracing methods. Additionally, we identified the main projection fields of an adjacent population of TRH neurons located in the perifornical area (Fig. 23).

Although the two TRH neuronal populations partially overlap, their projection fields differ substantially, suggesting different physiological roles for these two cell populations. As a common trait, both cell groups innervate hypothalamic and extrahypothalamic forebrain nuclei and do not send a substantial projection to the hindbrain, suggesting that they regulate homeostatic and behavioral functions at the level of the hypothalamus and the limbic forebrain. Table 10. summarizes the identified projection fields of TRH neurons located in the aPVN or in the perifornical area.

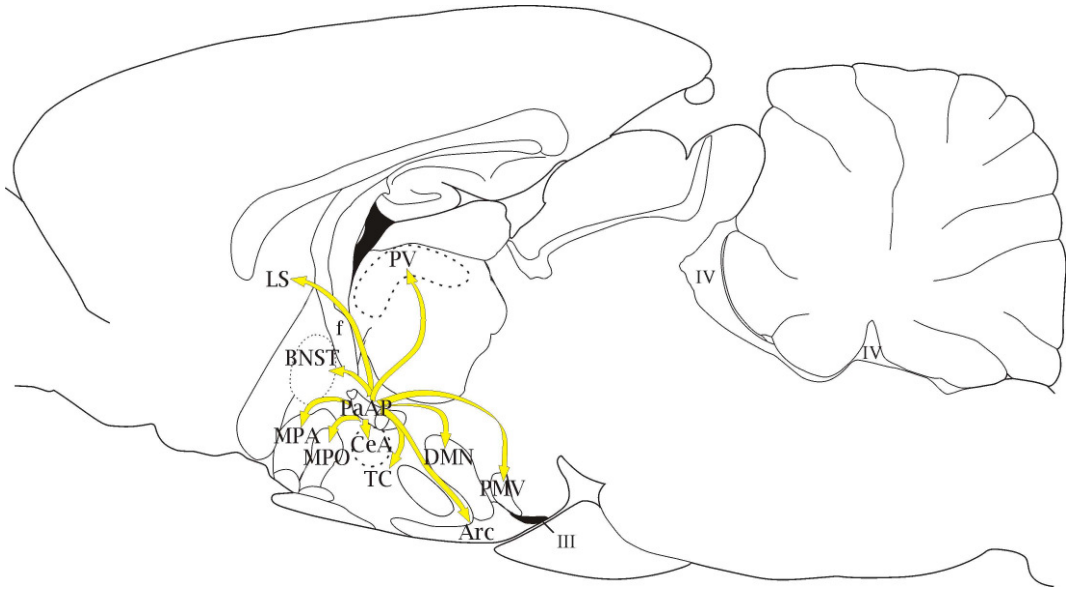

Figure 23. Schematic map demonstrates the main projections of the non-hypophysiotropic thyrotropin-releasing hormone (TRH) neurons localized in the anterior parvocellular subdivision of the hypothalamic paraventricular nucleus (aPVN). The projection fields of the aPVN TRH neurons suggests that this TRH neuron group plays role in the regulation of energy homeostasis (Arc, arcuate nucleus; DMN, dorsomedial nucleus), feeding behaviour (CeA, central amygdaloid nucleus; BNST, bed nucleus of stria terminalis; LS, lateral septum; PV, paraventricular nucleus of the thalamus), arousal (PV) thermoregulation (DMN), prolactin synthesis (Arc) and possibly sexual behaviour (MPA, medial preoptic area; MPO, medial preoptic nucleus). TC, tuber cinereum; III, third ventricle; IV, fourth ventricle; f, fornix; intermittent lines represent nuclei located outside this sagittal level of the brain.

6.4.1. Technical considerations

Mapping the projection fields of TRH neurons residing in the aPVN by anterograde tract-tracing was complicated by the small volume of the aPVN and the close proximity of perifornical TRH neurons. Indeed, even PHAL injections that appeared to be

confined to the aPVN without spreading into the perifornical area resulted in a qualitatively similar topography of PHAL/pro-TRH fibers compared with those cases in which PHAL injection sites spread both into the aPVN and the medial part of the perifornical area. These data raise the possibility that perifornical TRH neurons may concentrate PHAL from the area of the aPVN through dendrites that might penetrate the aPVN. Therefore, it was necessary to conduct retrograde tracing experiments to distinguish between the genuine projection sites of TRH neurons residing in the aPVN and perifornical area.

CTB injections into brain regions where a relative abundance of PHAL/pro-TRH axons was found revealed distinct projection sites of TRH neurons residing in the aPVN or in the perifornical area, although common projection fields were also found. The extent of the projections from the aPVN and perifornical group to each specific area cannot be quantitatively compared, but the arcuate nucleus would appear to be the primary target of the aPVN, whereas the lateral septal nucleus appears to be the primary target of perifornical TRH neurons. In the anterograde tracing experiment, a high density of PHAL/pro-TRH fibers was observed in the arcuate nucleus, and large numbers of TRH neurons in the aPVN but not the perifornical area were labeled retrogradely from the arcuate nucleus. In contrast, the ventral part of the lateral septal nucleus contained a high density of PHAL/pro-TRH fibers, and, after CTB injection, large numbers of TRH neurons in the perifornical area but not the aPVN were retrogradely labeled. Projections of perifornical TRH neurons to the lateral septal area were also reported earlier by Ishikawa et al. (226) and Merchenthaler (227).

It should be noted that CTB was injected into most of the regions where a high to moderate density of anterogradely labeled pro-TRH-containing fibers was observed, but it was beyond the scope of this study to inject CTB into regions where only a low density of PHAL/TRH fibers was observed. Thus, it is conceivable that there might be additional brain areas that receive functionally significant but less dense innervation of TRH-containing axons originating from the aPVN and/or perifornical areas. Furthermore, PHAL injections covered only the medial part of the perifornical TRH cell group. Thus, there may be additional projection sites of this cell group that were not observed in our study.

6.4.2. Functional implications

There is essentially nothing known about the biological significance of TRH neurons located in the aPVN. Nevertheless, the robust innervation of these cells by NPY/AGRP and α-MSH/CART neurons of the arcuate nucleus (111, 177) is indicative of the possibility that aPVN TRH neurons may be tightly regulated by feeding-related neuronal afferents and integrated into the energy-control system. Indeed, TRH is well known to regulate appetite, and when injected into the brain it consistently reduces food intake and the time spent interacting with food in all animals species studied (228-233). This includes a reduction in food intake in *ad lib*-feeding animals, in animals that have been subjected to a fast and reintroduced to food, and in models of stress-induced eating. Given that the major projection fields of aPVN TRH neurons include the arcuate and dorsomedial nuclei, two critical integrating centers in the brain involved in the regulation of food intake (234), it is conceivable that the anorectic actions of TRH could be mediated through one or both of these areas. In addition, the presence of projection fields of aPVN TRH neurons to extrahypothalamic areas such as the paraventricular thalamic nucleus, central amygdaloid nucleus, bed nucleus of the stria terminalis, and ventral part of the lateral septal nucleus may integrate the regulation of appetite and satiety with other components of the energy regulatory system. For example, projections to the paraventricular thalamic nucleus may induce arousal (235) and, hence, increase locomotor activity, now considered an important component of energy homeostasis (236). Projections to the bed nucleus of the stria terminalis and central amygdaloid nucleus may contribute to feeding behavior (237-239) and/or induce gastric contractility (240).

Nevertheless, the major projection field of aPVN TRH neurons in the arcuate nucleus is primarily the dorsomedial part of the nucleus, a region not generally associated with the regulation of food-related signals, but rather with the regulation of prolactin secretion via dopamine-producing neurons of the tuberoinfundibular system (241). TRH has a well-known effect on prolactin secretion, potently releasing prolactin from anterior pituitary lactotrophs (242). However, pro-TRH 178–199, a non-TRH peptide derived from the posttranslational processing of the TRH prohormone (243), also has a potent effect on prolactin secretion by decreasing the expression of the dopamine-synthesizing enzyme, tyrosine hydroxylase, when injected into the arcuate

nucleus (244). Thus, TRH neurons may have a dual action on prolactin secretion, through both direct effects on lactrotrophs and indirect effects by inhibiting the tuberoinfundibular dopaminergic system.

By projecting to the preoptic area, aPVN TRH neurons may also be involved in the regulation of thermogenesis. Injection of TRH into the preoptic area inhibits heat-sensitive neurons and activates cold-sensitive neurons (245). This action results in increased body temperature through peripheral vasoconstriction, increased metabolic heat production, and shivering (246). Thus, it is intriguing to consider the possibility that activation of aPVN TRH neurons following a meal may contribute to the generation of diet-induced thermogenesis in coordination with other TRH mediated responses associated with meal termination. Alternatively, this projection pathway may be involved in the adaptation response to cold stress, given that animals exposed to a cold environment increase TRH gene expression in all PVN regions, including the aPVN (221). Thus, it is possible that cold-sensitive TRH neurons in the PVN increase heat production not only by increasing peripheral thyroid hormone levels (223, 247) but also by regulating preoptic neurons that increase heat production via activation of the sympathetic nervous system (248).

Projections of aPVN TRH neurons to the dorsomedial nucleus could also contribute to some of the well-recognized autonomic effects of centrally administered TRH (243), particularly those involved in the regulation of the cardiovascular and respiratory systems. Activation of the DMN increases heart rate, and vasomotor activity and induces hyperventilation (249, 250), responses that are highly reminiscent of the central actions of TRH (243). Many of the central effects of TRH on the autonomic system, however, are thought to be exerted directly on the brainstem (243) and/or through projections of TRH-producing neurons in the medullary raphe to preganglionic sympathetic neurons in the spinal cord (243). Studies involving focal, intranuclear injections of TRH into the DMN will be required to determine whether this region also contributes to the actions of TRH on autonomic function.

Although effects of TRH or pro-TRH-derived peptides on sexual behavior have not been described, projections to the medial preoptic area/medial preoptic nucleus and to the ventral premammillary nucleus raise the possibility that aPVN TRH neurons is involved in the regulation of reproductive functions. The medial preoptic area has a

critical role in sexual behavior (251), whereas the ventral premammillary nucleus has been shown to be activated by pheromonal stimuli (252, 253), and it possesses bidirectional connections with several nuclei related to reproductive control (254). Innervation of these nuclei by TRH neurons in the aPVN may serve to coordinate sexual behavior with the nutritional status of the animal.

Though not a primary objective of this study, the major projection sites of the TRH neurons residing in the rostral part of the perifornical area were also identified. This neuron population co-synthesizes another neuropeptide, urocortin 3 (UCN3). Contrary to the aPVN TRH neurons, perifornical TRH/UCN3 neurons were found to densely innervate the ventromedial nucleus, especially its dorsomedial part. This region of the ventromedial nucleus was shown by Elmquist et al. (255) to express leptin receptors and to be activated by circulating leptin (114, 256). Insofar as selective removal of leptin receptors from these neurons results in increased fat mass and body weight (257), it is possible that perifornical/UCN3 TRH neurons also have important regulatory effects on energy homeostasis.

Table 10. Major projection fields of TRH neurons in the aPVN and perifornical area identified by tract-tracing methods

aPVN TRH neurons	**Perifornical TRH neurons**
Arcuate nucleus	Ventromedial nucleus
Dorsomedial nucleus	Dorsomedial nucleus
Tuber cinereum area	Ventral premammillary nucleus
Ventral premammillary nucleus	Medial preoptic area and nucleus
Medial preoptic area and nucleus	Lateral septal nucleus
Paraventricular nucleus of the thalamus	Bed nucleus of the stria terminalis
Central amygdaloid nucleus	Medial amygdaloid nucleus
Bed nucleus of the stria terminalis	Amygdalohippocampal area
Lateral septal nucleus	

A major difference between the projections of aPVN and perifornical TRH neurons, however, is that perifornical TRH neurons project more extensively to extrahypothalamic limbic areas. Retrograde labeling from the ventral lateral septum suggests that almost an order of magnitude more TRH neurons project to the lateral septum from the perifornical area than from the aPVN. In addition, perifornical TRH neurons densely innervate the medial amygdaloid nucleus and amygdalohippocampal

area. These regions are involved in the regulation of a variety of behaviors, including sexual behavior, feeding behavior, aggression, coping with stressful situations, and emotional responses (258-267). Given that the endogenous TRH system plays a key role in regulating anxiety and depression in rodents (268) and that TRH also has antidepressant effects in humans (269-271), perifornical TRH neurons may be involved in mood regulation. A role of perifornical TRH neurons in sexual behavior and the hypothalamic-pituitary-gonadal axis is also suggested by their projections to the medial preoptic region, ventral premammillary nucleus, and a narrow zone between the dorsomedial and ventromedial nuclei. The latter region has been implicated in regulation of the hypothalamic-pituitary-gonadal axis via RF-amide-related peptide-expressing neurons in this region (272, 273) that inhibit gonadotropin release (274).

7. Conclusions

We conclude that three major cell populations give rise to the NPY innervation of hypophysiotropic CRH neurons: adrenergic and noradrenergic NPY neurons of the brainstem, and NPY/AGRP neurons of the arcuate nucleus. Approximately, two thirds of the NPY innervation originates from the brainstem catecholaeminergic neurons, while the remaining one third arises from the arcuate nucleus.

In spite of the known acute stimulatory effect of NPY on CRH neurons, we have revealed that the chronic administration of NPY decreases CRH mRNA expression in the PVN. Thus, we propose that NPY pathways ascending from the brainstem have an acute activating effect on CRH neurons in response to glucoprivation, infection, and inflammation, whereas neurons located in the arcuate nucleus exert a chronic inhibitory effect on CRH gene expression in association with fasting. The concept that NPY could exert both inhibitory and stimulatory effects on CRH neurons raises the possibility that NPY may exert different effects on the HPA axis depending upon the origin of the NPY input and nature of the specific physiological stimuli.

We have elucidated that the adrenergic and noradrenergic neurons of the brainstem contribute unequally to the catecholaminergic innervation of hypophysiotropic TRH neurons, similarly to the innervation of the hypophysiotropic CRH neurons. We suggest that adrenergic and noradrenergic cell groups may each mediate the effects of different physiological conditions on the hypothalamic-pituitary-thyroid axis through direct effects on hypophysiotropic TRH neurons.

We have described the projection fields of aPVN TRH neurons. Our results raise the possibility that this non-hypophysiotropic TRH cell population might influence energy homeostasis, thermoregulation, prolactin synthesis, and possibly sexual function. In contrast, perifornical TRH neurons may be involved primarily in regulation of limbic functions and, therefore, may be functionally different from aPVN TRH neurons. Partially overlapping projections of the TRH neurons from both regions, and in particular the heavy innervation to the ventromedial nucleus, potentially implicate at least a subpopulation of perifornical TRH neurons in the control of food intake. These studies provide important initial data from which physiological studies can be designed to better understand the potential role of these cell groups.

8. Summary

The hypophysiotropic corticotropin-releasing hormone (CRH)- and thyrotropin-releasing hormone (TRH)-synthesizing neurons in the hypothalamic paraventricular nucleus (PVN) play important roles in the regulation of energy homeostasis, primarily through the regulation of the hypothalamic-pituitary-adrenocortical and hypothalamic-pituitary-thyroid axes, respectively. One of the most important regulators of the hypophysiotropic CRH neurons is neuropeptide Y (NPY). Using multiple labeling immunohistochemistry and selective lesions, we have elucidated that approximately two thirds of the NPY innervation of the hypophysiotropic CRH neurons originate from the brainstem catecholaminergic neurons, while the arcuate nucleus contributes to the remaining part of this innervation. Though acute administration of NPY stimulates the hypophysiotropic CRH neurons, during fasting the elevated levels of NPY in the arcuate nucleus are accompanied with the inhibition of CRH expression. To examine this discrepancy, we infused NPY icv. for three days, then performed quantitative *in situ* hybridization for CRH mRNA in the PVN. We have revealed that in contrast to the acute effect of NPY, chronic administration markedly decreases CRH mRNA levels in the PVN. According to these results, we suggest that during fasting the prolonged increase of NPY in the arcuate nucleus contribute to the inhibition of CRH gene expression.

Since the adrenergic and noradrenergic neurons of the brainstem may respond differently to various physiological stimuli, using multiple labeling immunohistochemistry we have explored the contributions of the two neuronal groups in the innervation of the hypophysiotropic TRH neurons. Both adrenergic and noradrenergic axons innervate the hypophysiotropic TRH neurons, although, there is a predominance of adrenergic fibers. We propose that the different neuropeptides, which are co-expressed in adrenergic and noradrenergic neuron groups, contribute to the specific response of brainstem catecholaminergic neurons to various stimuli.

A non-hypophysiotropic TRH neuron population, which is located in the anterior parvocellular subdivision of the PVN (aPVN) are innervated by the feeding-related neurons of the arcuate nucleus. To determine how these TRH neurons are integrated within the brain, the major projection fields of this cell group were studied by

anterograde and retrograde tract-tracing methods. As this neuronal group innervated brain regions that are involved in the regulation of food intake, prolactin synthesis, locomotor activity and thermogenesis, we hypothesize that the TRH neurons in the aPVN play an important part in the maintaince of energy homeostasis.

9. Összefoglalás

A hipotalamusz paraventrikuláris magjában (PVN) elhelyezkedő hipofizeotróf corticotropin-releasing hormont (CRH) és thyrotropin-releasing hormont (TRH) termelő neuronok fontos szerepet játszanak az energia homeosztázis fenntartásában, elsősorban a hipotalamusz-hipofízis-mellékvesekéreg, illetve a hipotalamusz-hipofízis-pajzsmirigy tengelyek szabályozásán keresztül.

A hipofizeotróf CRH neuronok szabályozásában kiemelkedő szerepet tölt be a neuropeptid Y (NPY). Többes immunfluoreszcens jelölés alkalmazásával és szelektív irtás segítségével kimutattuk, hogy a hipofizeotróf CRH neuronok NPY innervációjának körülbelül kétharmada az agytörzsi katekolaminerg magokból származik, míg a fennmaradó egyharmad az arcuatus idegmagból ered. Habár az akut NPY beadás serkenti a hipofizeotróf CRH neuronokat, éhezés során az arcuatus idegmagban megemelkedő NPY szint mellett a CRH neuronok gátoltak. Ezen ellentmondás hátterének tisztázására, három napon keresztül NPY-t injektáltunk patkányok agykamrájába, majd kvantitatív *in situ* hibridizációval vizsgáltuk a PVN-ben a CRH mRNS mennyiségét. Kimutattuk, hogy az NPY – akut hatásával ellentétben – krónikusan adagolva szignifikánsan csökkenti a CRH mRNS szintjét a PVN-ben. Eredményeink alapján úgy gondoljuk, hogy éhezés során az arcuatus idegmagból eredő axonokból tartósan ürülő NPY hozzájárul a CRH expresszió gátlásához.

Mivel az agytörzsi adrenerg és noradrenerg neuronok eltérő válaszokat adhatnak különböző fiziológiai behatásokra, többes immunfluoreszcens jelölés alkalmazásával megvizsgáltuk a két sejtcsoport szerepét a hipofizeotróf TRH neuronok beidegzésében. Az adrenerg és noradrenerg axonok egyaránt beidegzik a hipofizeotróf TRH neuronokat, habár e beidegzésben az adrenerg rostok túlsúlya érvényesül. Úgy véljük, hogy az adrenerg és noradrenerg neuroncsoportokban expresszálódó különböző neuropeptidek hozzájárulhatnak az agytörzsi katekolaminerg neuronok specifikus válaszának kialakításához.

A PVN anterior parvocelluláris almagjában (aPVN) található nem-hipofizeotróf TRH neuronokat beidegzik az arcuatus idegmag táplálkozás szempontjából fontos idegsejtjei. Hogy feltárjuk ezen TRH sejtek kapcsolatrendszerét, anterográd és retrográd pályajelölési módszerekkel meghatároztuk e sejtek vetületeit. Mivel a sejtcsoport által

beidegzett területek részt vesznek a táplálékfelvétel, a prolaktin szintézis, a motoros aktivitás és a hőháztartás szabályozásában, feltételezzük, hogy az aPVN területén elhelyezkedő TRH neuronok fontos szerepet játszanak az energia homeosztázis szabályozásában.

10. References

1. **Vettor R, Fabris R, Pagano C, Federspil G** 2002 Neuroendocrine regulation of eating behavior. J Endocrinol Invest 25:836-854
2. **Strader AD, Woods SC** 2005 Gastrointestinal hormones and food intake. Gastroenterology 128:175-191
3. **Friedman JM** 1998 Leptin, leptin receptors, and the control of body weight. Nutr Rev 56:s38-46; discussion s54-75
4. **Erickson JC, Hollopeter G, Palmiter RD** 1996 Attenuation of the obesity syndrome of ob/ob mice by the loss of neuropeptide Y. Science 274:1704-1707
5. **Montague CT, Farooqi IS, Whitehead JP, Soos MA, Rau H, Wareham NJ, Sewter CP, Digby JE, Mohammed SN, Hurst JA, Cheetham CH, Earley AR, Barnett AH, Prins JB, O'Rahilly S** 1997 Congenital leptin deficiency is associated with severe early-onset obesity in humans. Nature 387:903-908
6. **Zhang Y, Proenca R, Maffei M, Barone M, Leopold L, Friedman JM** 1994 Positional cloning of the mouse obese gene and its human homologue. Nature 372:425-432
7. **Considine RV, Caro JF** 1997 Leptin and the regulation of body weight. Int J Biochem Cell Biol 29:1255-1272
8. **Schwartz MW, Woods SC, Porte D, Jr., Seeley RJ, Baskin DG** 2000 Central nervous system control of food intake. Nature 404:661-671
9. **Lee MJ, Fried SK** 2009 Integration of hormonal and nutrient signals that regulate leptin synthesis and secretion. Am J Physiol Endocrinol Metab 296:E1230-1238
10. **Moreno-Aliaga MJ, Stanhope KL, Havel PJ** 2001 Transcriptional regulation of the leptin promoter by insulin-stimulated glucose metabolism in 3t3-l1 adipocytes. Biochem Biophys Res Commun 283:544-548
11. **Bradley RL, Cheatham B** 1999 Regulation of ob gene expression and leptin secretion by insulin and dexamethasone in rat adipocytes. Diabetes 48:272-278
12. **Bradley RL, Kokkotou EG, Maratos-Flier E, Cheatham B** 2000 Melanin-concentrating hormone regulates leptin synthesis and secretion in rat adipocytes. Diabetes 49:1073-1077
13. **Wang B, Trayhurn P** 2006 Acute and prolonged effects of TNF-alpha on the expression and secretion of inflammation-related adipokines by human adipocytes differentiated in culture. Pflugers Arch 452:418-427
14. **Kos K, Harte AL, James S, Snead DR, O'Hare JP, McTernan PG, Kumar S** 2007 Secretion of neuropeptide Y in human adipose tissue and its role in maintenance of adipose tissue mass. Am J Physiol Endocrinol Metab 293:E1335-1340
15. **Serradeil-Le Gal C, Lafontan M, Raufaste D, Marchand J, Pouzet B, Casellas P, Pascal M, Maffrand JP, Le Fur G** 2000 Characterization of NPY receptors controlling lipolysis and leptin secretion in human adipocytes. FEBS Lett 475:150-156
16. **Lee MJ, Fried SK** 2006 Multilevel regulation of leptin storage, turnover, and secretion by feeding and insulin in rat adipose tissue. J Lipid Res 47:1984-1993
17. **Ricci MR, Lee MJ, Russell CD, Wang Y, Sullivan S, Schneider SH, Brolin RE, Fried SK** 2005 Isoproterenol decreases leptin release from rat and human

adipose tissue through posttranscriptional mechanisms. Am J Physiol Endocrinol Metab 288:E798-804
18. **Kolaczynski JW, Considine RV, Ohannesian J, Marco C, Opentanova I, Nyce MR, Myint M, Caro JF** 1996 Responses of leptin to short-term fasting and refeeding in humans: a link with ketogenesis but not ketones themselves. Diabetes 45:1511-1515
19. **Becker DJ, Ongemba LN, Brichard V, Henquin JC, Brichard SM** 1995 Diet- and diabetes-induced changes of ob gene expression in rat adipose tissue. FEBS Lett 371:324-328
20. **Fruhbeck G** 2001 A heliocentric view of leptin. Proc Nutr Soc 60:301-318
21. **Korczynska J, Stelmanska E, Swierczynski J** 2003 Differential effect of long-term food restriction on fatty acid synthase and leptin gene expression in rat white adipose tissue. Horm Metab Res 35:593-597
22. **Kojima M, Hosoda H, Date Y, Nakazato M, Matsuo H, Kangawa K** 1999 Ghrelin is a growth-hormone-releasing acylated peptide from stomach. Nature 402:656-660
23. **Wren AM, Small CJ, Ward HL, Murphy KG, Dakin CL, Taheri S, Kennedy AR, Roberts GH, Morgan DG, Ghatei MA, Bloom SR** 2000 The novel hypothalamic peptide ghrelin stimulates food intake and growth hormone secretion. Endocrinology 141:4325-4328
24. **Tschop M, Smiley DL, Heiman ML** 2000 Ghrelin induces adiposity in rodents. Nature 407:908-913
25. **Ariyasu H, Takaya K, Tagami T, Ogawa Y, Hosoda K, Akamizu T, Suda M, Koh T, Natsui K, Toyooka S, Shirakami G, Usui T, Shimatsu A, Doi K, Hosoda H, Kojima M, Kangawa K, Nakao K** 2001 Stomach is a major source of circulating ghrelin, and feeding state determines plasma ghrelin-like immunoreactivity levels in humans. J Clin Endocrinol Metab 86:4753-4758
26. **Tschop M, Wawarta R, Riepl RL, Friedrich S, Bidlingmaier M, Landgraf R, Folwaczny C** 2001 Post-prandial decrease of circulating human ghrelin levels. J Endocrinol Invest 24:RC19-21
27. **Cummings DE, Purnell JQ, Frayo RS, Schmidova K, Wisse BE, Weigle DS** 2001 A preprandial rise in plasma ghrelin levels suggests a role in meal initiation in humans. Diabetes 50:1714-1719
28. **Sanchez J, Oliver P, Pico C, Palou A** 2004 Diurnal rhythms of leptin and ghrelin in the systemic circulation and in the gastric mucosa are related to food intake in rats. Pflugers Arch 448:500-506
29. **Sanchez J, Oliver P, Palou A, Pico C** 2004 The inhibition of gastric ghrelin production by food intake in rats is dependent on the type of macronutrient. Endocrinology 145:5049-5055
30. **Tannous dit El Khoury D, Obeid O, Azar ST, Hwalla N** 2006 Variations in postprandial ghrelin status following ingestion of high-carbohydrate, high-fat, and high-protein meals in males. Ann Nutr Metab 50:260-269
31. **Cummings DE** 2006 Ghrelin and the short- and long-term regulation of appetite and body weight. Physiol Behav 89:71-84
32. **Liddle RA** 1997 Cholecystokinin cells. Annu Rev Physiol 59:221-242
33. **Greenough A, Cole G, Lewis J, Lockton A, Blundell J** 1998 Untangling the effects of hunger, anxiety, and nausea on energy intake during intravenous cholecystokinin octapeptide (CCK-8) infusion. Physiol Behav 65:303-310

34. **Geary N** 2004 Endocrine controls of eating: CCK, leptin, and ghrelin. Physiol Behav 81:719-733
35. **West DB, Fey D, Woods SC** 1984 Cholecystokinin persistently suppresses meal size but not food intake in free-feeding rats. Am J Physiol 246:R776-787
36. **Crawley JN, Beinfeld MC** 1983 Rapid development of tolerance to the behavioural actions of cholecystokinin. Nature 302:703-706
37. **Tsunoda Y, Yao H, Park J, Owyang C** 2003 Cholecystokinin synthesizes and secretes leptin in isolated canine gastric chief cells. Biochem Biophys Res Commun 310:681-684
38. **Douglas BR, Jansen JB, de Jong AJ, Lamers CB** 1990 Effect of various triglycerides on plasma cholecystokinin levels in rats. J Nutr 120:686-690
39. **Lewis LD, Williams JA** 1990 Regulation of cholecystokinin secretion by food, hormones, and neural pathways in the rat. Am J Physiol 258:G512-518
40. **Adrian TE, Ferri GL, Bacarese-Hamilton AJ, Fuessl HS, Polak JM, Bloom SR** 1985 Human distribution and release of a putative new gut hormone, peptide YY. Gastroenterology 89:1070-1077
41. **Batterham RL, Bloom SR** 2003 The gut hormone peptide YY regulates appetite. Ann N Y Acad Sci 994:162-168
42. **Batterham RL, Cowley MA, Small CJ, Herzog H, Cohen MA, Dakin CL, Wren AM, Brynes AE, Low MJ, Ghatei MA, Cone RD, Bloom SR** 2002 Gut hormone PYY(3-36) physiologically inhibits food intake. Nature 418:650-654
43. **Ueno H, Yamaguchi H, Mizuta M, Nakazato M** 2008 The role of PYY in feeding regulation. Regul Pept 145:12-16
44. **Taylor IL** 1985 Distribution and release of peptide YY in dog measured by specific radioimmunoassay. Gastroenterology 88:731-737
45. **Turton MD, O'Shea D, Gunn I, Beak SA, Edwards CM, Meeran K, Choi SJ, Taylor GM, Heath MM, Lambert PD, Wilding JP, Smith DM, Ghatei MA, Herbert J, Bloom SR** 1996 A role for glucagon-like peptide-1 in the central regulation of feeding. Nature 379:69-72
46. **Hwa JJ, Ghibaudi L, Williams P, Witten MB, Tedesco R, Strader CD** 1998 Differential effects of intracerebroventricular glucagon-like peptide-1 on feeding and energy expenditure regulation. Peptides 19:869-875
47. **Holst JJ** 1997 Enteroglucagon. Annu Rev Physiol 59:257-271
48. **Kieffer TJ, McIntosh CH, Pederson RA** 1995 Degradation of glucose-dependent insulinotropic polypeptide and truncated glucagon-like peptide 1 in vitro and in vivo by dipeptidyl peptidase IV. Endocrinology 136:3585-3596
49. **Lavin JH, Wittert GA, Andrews J, Yeap B, Wishart JM, Morris HA, Morley JE, Horowitz M, Read NW** 1998 Interaction of insulin, glucagon-like peptide 1, gastric inhibitory polypeptide, and appetite in response to intraduodenal carbohydrate. Am J Clin Nutr 68:591-598
50. **Ranganath LR, Beety JM, Morgan LM, Wright JW, Howland R, Marks V** 1996 Attenuated GLP-1 secretion in obesity: cause or consequence? Gut 38:916-919
51. **Berthoud HR, Lynn PA, Blackshaw LA** 2001 Vagal and spinal mechanosensors in the rat stomach and colon have multiple receptive fields. Am J Physiol Regul Integr Comp Physiol 280:R1371-1381

52. **Phillips RJ, Powley TL** 2000 Tension and stretch receptors in gastrointestinal smooth muscle: re-evaluating vagal mechanoreceptor electrophysiology. Brain Res Brain Res Rev 34:1-26
53. **Wang YH, Tache Y, Sheibel AB, Go VL, Wei JY** 1997 Two types of leptin-responsive gastric vagal afferent terminals: an in vitro single-unit study in rats. Am J Physiol 273:R833-837
54. **Buyse M, Ovesjo ML, Goiot H, Guilmeau S, Peranzi G, Moizo L, Walker F, Lewin MJ, Meister B, Bado A** 2001 Expression and regulation of leptin receptor proteins in afferent and efferent neurons of the vagus nerve. Eur J Neurosci 14:64-72
55. **Burdyga G, Spiller D, Morris R, Lal S, Thompson DG, Saeed S, Dimaline R, Varro A, Dockray GJ** 2002 Expression of the leptin receptor in rat and human nodose ganglion neurones. Neuroscience 109:339-347
56. **Date Y, Murakami N, Toshinai K, Matsukura S, Niijima A, Matsuo H, Kangawa K, Nakazato M** 2002 The role of the gastric afferent vagal nerve in ghrelin-induced feeding and growth hormone secretion in rats. Gastroenterology 123:1120-1128
57. **le Roux CW, Neary NM, Halsey TJ, Small CJ, Martinez-Isla AM, Ghatei MA, Theodorou NA, Bloom SR** 2005 Ghrelin does not stimulate food intake in patients with surgical procedures involving vagotomy. J Clin Endocrinol Metab 90:4521-4524
58. **Schwartz MW, Seeley RJ, Campfield LA, Burn P, Baskin DG** 1996 Identification of targets of leptin action in rat hypothalamus. J Clin Invest 98:1101-1106
59. **Chen HY, Trumbauer ME, Chen AS, Weingarth DT, Adams JR, Frazier EG, Shen Z, Marsh DJ, Feighner SD, Guan XM, Ye Z, Nargund RP, Smith RG, Van der Ploeg LH, Howard AD, MacNeil DJ, Qian S** 2004 Orexigenic action of peripheral ghrelin is mediated by neuropeptide Y and agouti-related protein. Endocrinology 145:2607-2612
60. **Bado A, Levasseur S, Attoub S, Kermorgant S, Laigneau JP, Bortoluzzi MN, Moizo L, Lehy T, Guerre-Millo M, Le Marchand-Brustel Y, Lewin MJ** 1998 The stomach is a source of leptin. Nature 394:790-793
61. **Berthoud HR** 2008 The vagus nerve, food intake and obesity. Regul Pept 149:15-25
62. **Raybould HE, Glatzle J, Freeman SL, Whited K, Darcel N, Liou A, Bohan D** 2006 Detection of macronutrients in the intestinal wall. Auton Neurosci 125:28-33
63. **Kopin AS, Mathes WF, McBride EW, Nguyen M, Al-Haider W, Schmitz F, Bonner-Weir S, Kanarek R, Beinborn M** 1999 The cholecystokinin-A receptor mediates inhibition of food intake yet is not essential for the maintenance of body weight. J Clin Invest 103:383-391
64. **Moran TH, Baldessarini AR, Salorio CF, Lowery T, Schwartz GJ** 1997 Vagal afferent and efferent contributions to the inhibition of food intake by cholecystokinin. Am J Physiol 272:R1245-1251
65. **Koda S, Date Y, Murakami N, Shimbara T, Hanada T, Toshinai K, Niijima A, Furuya M, Inomata N, Osuye K, Nakazato M** 2005 The role of the vagal nerve in peripheral PYY3-36-induced feeding reduction in rats. Endocrinology 146:2369-2375

66. **Williams DL** 2009 Minireview: finding the sweet spot: peripheral versus central glucagon-like peptide 1 action in feeding and glucose homeostasis. Endocrinology 150:2997-3001
67. **Meister B, Ceccatelli S, Hokfelt T, Anden NE, Anden M, Theodorsson E** 1989 Neurotransmitters, neuropeptides and binding sites in the rat mediobasal hypothalamus: effects of monosodium glutamate (MSG) lesions. Exp Brain Res 76:343-368
68. **Kerkerian L, Pelletier G** 1986 Effects of monosodium L-glutamate administration on neuropeptide Y-containing neurons in the rat hypothalamus. Brain Res 369:388-390
69. **Norsted E, Gomuc B, Meister B** 2008 Protein components of the blood-brain barrier (BBB) in the mediobasal hypothalamus. J Chem Neuroanat 36:107-121
70. **Burguera B, Couce ME** 2001 Leptin access into the brain: a saturated transport mechanism in obesity. Physiol Behav 74:717-720
71. **Tang-Christensen M, Holst JJ, Hartmann B, Vrang N** 1999 The arcuate nucleus is pivotal in mediating the anorectic effects of centrally administered leptin. Neuroreport 10:1183-1187
72. **Dawson R, Pelleymounter MA, Millard WJ, Liu S, Eppler B** 1997 Attenuation of leptin-mediated effects by monosodium glutamate-induced arcuate nucleus damage. Am J Physiol 273:E202-206
73. **Legradi G, Emerson CH, Ahima RS, Rand WM, Flier JS, Lechan RM** 1998 Arcuate nucleus ablation prevents fasting-induced suppression of ProTRH mRNA in the hypothalamic paraventricular nucleus. Neuroendocrinology 68:89-97
74. **Elias CF, Lee C, Kelly J, Aschkenasi C, Ahima RS, Couceyro PR, Kuhar MJ, Saper CB, Elmquist JK** 1998 Leptin activates hypothalamic CART neurons projecting to the spinal cord. Neuron 21:1375-1385
75. **Vrang N, Larsen PJ, Clausen JT, Kristensen P** 1999 Neurochemical characterization of hypothalamic cocaine- amphetamine-regulated transcript neurons. J Neurosci 19:RC5
76. **Yaswen L, Diehl N, Brennan MB, Hochgeschwender U** 1999 Obesity in the mouse model of pro-opiomelanocortin deficiency responds to peripheral melanocortin. Nat Med 5:1066-1070
77. **Gropp E, Shanabrough M, Borok E, Xu AW, Janoschek R, Buch T, Plum L, Balthasar N, Hampel B, Waisman A, Barsh GS, Horvath TL, Bruning JC** 2005 Agouti-related peptide-expressing neurons are mandatory for feeding. Nat Neurosci 8:1289-1291
78. **Krude H, Biebermann H, Luck W, Horn R, Brabant G, Gruters A** 1998 Severe early-onset obesity, adrenal insufficiency and red hair pigmentation caused by POMC mutations in humans. Nat Genet 19:155-157
79. **Coll AP, Loraine Tung YC** 2009 Pro-opiomelanocortin (POMC)-derived peptides and the regulation of energy homeostasis. Mol Cell Endocrinol 300:147-151
80. **Farooqi IS, O'Rahilly S** 2008 Mutations in ligands and receptors of the leptin-melanocortin pathway that lead to obesity. Nat Clin Pract Endocrinol Metab 4:569-577
81. **Huszar D, Lynch CA, Fairchild-Huntress V, Dunmore JH, Fang Q, Berkemeier LR, Gu W, Kesterson RA, Boston BA, Cone RD, Smith FJ,**

Campfield LA, Burn P, Lee F 1997 Targeted disruption of the melanocortin-4 receptor results in obesity in mice. Cell 88:131-141

82. **Chen AS, Metzger JM, Trumbauer ME, Guan XM, Yu H, Frazier EG, Marsh DJ, Forrest MJ, Gopal-Truter S, Fisher J, Camacho RE, Strack AM, Mellin TN, MacIntyre DE, Chen HY, Van der Ploeg LH** 2000 Role of the melanocortin-4 receptor in metabolic rate and food intake in mice. Transgenic Res 9:145-154
83. **Farooqi IS, Keogh JM, Yeo GS, Lank EJ, Cheetham T, O'Rahilly S** 2003 Clinical spectrum of obesity and mutations in the melanocortin 4 receptor gene. N Engl J Med 348:1085-1095
84. **Butler AA, Kesterson RA, Khong K, Cullen MJ, Pelleymounter MA, Dekoning J, Baetscher M, Cone RD** 2000 A unique metabolic syndrome causes obesity in the melanocortin-3 receptor-deficient mouse. Endocrinology 141:3518-3521
85. **Chen AS, Marsh DJ, Trumbauer ME, Frazier EG, Guan XM, Yu H, Rosenblum CI, Vongs A, Feng Y, Cao L, Metzger JM, Strack AM, Camacho RE, Mellin TN, Nunes CN, Min W, Fisher J, Gopal-Truter S, MacIntyre DE, Chen HY, Van der Ploeg LH** 2000 Inactivation of the mouse melanocortin-3 receptor results in increased fat mass and reduced lean body mass. Nat Genet 26:97-102
86. **Wierup N, Richards WG, Bannon AW, Kuhar MJ, Ahren B, Sundler F** 2005 CART knock out mice have impaired insulin secretion and glucose intolerance, altered beta cell morphology and increased body weight. Regul Pept 129:203-211
87. **Broberger C, Johansen J, Johansson C, Schalling M, Hokfelt T** 1998 The neuropeptide Y/agouti gene-related protein (AGRP) brain circuitry in normal, anorectic, and monosodium glutamate-treated mice. Proc Natl Acad Sci U S A 95:15043-15048
88. **Hahn TM, Breininger JF, Baskin DG, Schwartz MW** 1998 Coexpression of Agrp and NPY in fasting-activated hypothalamic neurons. Nat Neurosci 1:271-272
89. **Graham M, Shutter JR, Sarmiento U, Sarosi I, Stark KL** 1997 Overexpression of Agrt leads to obesity in transgenic mice. Nat Genet 17:273-274
90. **Levine AS, Morley JE** 1984 Neuropeptide Y: a potent inducer of consummatory behavior in rats. Peptides 5:1025-1029
91. **Stanley BG, Leibowitz SF** 1985 Neuropeptide Y injected in the paraventricular hypothalamus: a powerful stimulant of feeding behavior. Proc Natl Acad Sci U S A 82:3940-3943
92. **Luquet S, Perez FA, Hnasko TS, Palmiter RD** 2005 NPY/AgRP neurons are essential for feeding in adult mice but can be ablated in neonates. Science 310:683-685
93. **Erickson JC, Clegg KE, Palmiter RD** 1996 Sensitivity to leptin and susceptibility to seizures of mice lacking neuropeptide Y. Nature 381:415-421
94. **Qian S, Chen H, Weingarth D, Trumbauer ME, Novi DE, Guan X, Yu H, Shen Z, Feng Y, Frazier E, Chen A, Camacho RE, Shearman LP, Gopal-Truter S, MacNeil DJ, Van der Ploeg LH, Marsh DJ** 2002 Neither agouti-

related protein nor neuropeptide Y is critically required for the regulation of energy homeostasis in mice. Mol Cell Biol 22:5027-5035

95. **Michel MC, Beck-Sickinger A, Cox H, Doods HN, Herzog H, Larhammar D, Quirion R, Schwartz T, Westfall T** 1998 XVI. International Union of Pharmacology recommendations for the nomenclature of neuropeptide Y, peptide YY, and pancreatic polypeptide receptors. Pharmacol Rev 50:143-150
96. **Schaffhauser AO, Whitebread S, Haener R, Hofbauer KG, Stricker-Krongrad A** 1998 Neuropeptide Y Y1 receptor antisense oligodeoxynucleotides enhance food intake in energy-deprived rats. Regul Pept 75-76:417-423
97. **Duhault J, Boulanger M, Chamorro S, Boutin JA, Della Zuana O, Douillet E, Fauchere JL, Feletou M, Germain M, Husson B, Vega AM, Renard P, Tisserand F** 2000 Food intake regulation in rodents: Y5 or Y1 NPY receptors or both? Can J Physiol Pharmacol 78:173-185
98. **Higuchi H, Niki T, Shiiya T** 2008 Feeding behavior and gene expression of appetite-related neuropeptides in mice lacking for neuropeptide Y Y5 receptor subclass. World J Gastroenterol 14:6312-6317
99. **Pritchard LE, Armstrong D, Davies N, Oliver RL, Schmitz CA, Brennand JC, Wilkinson GF, White A** 2004 Agouti-related protein (83-132) is a competitive antagonist at the human melanocortin-4 receptor: no evidence for differential interactions with pro-opiomelanocortin-derived ligands. J Endocrinol 180:183-191
100. **Yang YK, Thompson DA, Dickinson CJ, Wilken J, Barsh GS, Kent SB, Gantz I** 1999 Characterization of Agouti-related protein binding to melanocortin receptors. Mol Endocrinol 13:148-155
101. **Schwartz MW, Sipols AJ, Marks JL, Sanacora G, White JD, Scheurink A, Kahn SE, Baskin DG, Woods SC, Figlewicz DP, et al.** 1992 Inhibition of hypothalamic neuropeptide Y gene expression by insulin. Endocrinology 130:3608-3616
102. **Mizuno TM, Mobbs CV** 1999 Hypothalamic agouti-related protein messenger ribonucleic acid is inhibited by leptin and stimulated by fasting. Endocrinology 140:814-817
103. **Stephens TW, Basinski M, Bristow PK, Bue-Valleskey JM, Burgett SG, Craft L, Hale J, Hoffmann J, Hsiung HM, Kriauciunas A, et al.** 1995 The role of neuropeptide Y in the antiobesity action of the obese gene product. Nature 377:530-532
104. **Takahashi KA, Cone RD** 2005 Fasting induces a large, leptin-dependent increase in the intrinsic action potential frequency of orexigenic arcuate nucleus neuropeptide Y/Agouti-related protein neurons. Endocrinology 146:1043-1047
105. **Kristensen P, Judge ME, Thim L, Ribel U, Christjansen KN, Wulff BS, Clausen JT, Jensen PB, Madsen OD, Vrang N, Larsen PJ, Hastrup S** 1998 Hypothalamic CART is a new anorectic peptide regulated by leptin. Nature 393:72-76
106. **Mizuno TM, Kleopoulos SP, Bergen HT, Roberts JL, Priest CA, Mobbs CV** 1998 Hypothalamic pro-opiomelanocortin mRNA is reduced by fasting and [corrected] in ob/ob and db/db mice, but is stimulated by leptin. Diabetes 47:294-297

107. **Cowley MA, Smart JL, Rubinstein M, Cerdan MG, Diano S, Horvath TL, Cone RD, Low MJ** 2001 Leptin activates anorexigenic POMC neurons through a neural network in the arcuate nucleus. Nature 411:480-484
108. **Fekete C, Singru PS, Sanchez E, Sarkar S, Christoffolete MA, Riberio RS, Rand WM, Emerson CH, Bianco AC, Lechan RM** 2006 Differential effects of central leptin, insulin, or glucose administration during fasting on the hypothalamic-pituitary-thyroid axis and feeding-related neurons in the arcuate nucleus. Endocrinology 147:520-529
109. **Xu AW, Kaelin CB, Takeda K, Akira S, Schwartz MW, Barsh GS** 2005 PI3K integrates the action of insulin and leptin on hypothalamic neurons. J Clin Invest 115:951-958
110. **Bagnol D, Lu XY, Kaelin CB, Day HE, Ollmann M, Gantz I, Akil H, Barsh GS, Watson SJ** 1999 Anatomy of an endogenous antagonist: relationship between Agouti-related protein and proopiomelanocortin in brain. J Neurosci 19:RC26
111. **Fekete C, Legradi G, Mihaly E, Huang QH, Tatro JB, Rand WM, Emerson CH, Lechan RM** 2000 alpha-Melanocyte-stimulating hormone is contained in nerve terminals innervating thyrotropin-releasing hormone-synthesizing neurons in the hypothalamic paraventricular nucleus and prevents fasting-induced suppression of prothyrotropin-releasing hormone gene expression. J Neurosci 20:1550-1558
112. **Loewy S** 1990 Central regulations of anatomic functions. New York: Oxford University Press
113. **Sawchenko PE, Swanson LW, Grzanna R, Howe PR, Bloom SR, Polak JM** 1985 Colocalization of neuropeptide Y immunoreactivity in brainstem catecholaminergic neurons that project to the paraventricular nucleus of the hypothalamus. J Comp Neurol 241:138-153
114. **Elias CF, Kelly JF, Lee CE, Ahima RS, Drucker DJ, Saper CB, Elmquist JK** 2000 Chemical characterization of leptin-activated neurons in the rat brain. J Comp Neurol 423:261-281
115. **Fekete C, Wittmann G, Liposits Z, Lechan RM** 2004 Origin of cocaine- and amphetamine-regulated transcript (CART)-immunoreactive innervation of the hypothalamic paraventricular nucleus. J Comp Neurol 469:340-350
116. **Das M, Vihlen CS, Legradi G** 2007 Hypothalamic and brainstem sources of pituitary adenylate cyclase-activating polypeptide nerve fibers innervating the hypothalamic paraventricular nucleus in the rat. J Comp Neurol 500:761-776
117. **Ishizaki K, Honma S, Katsuno Y, Abe H, Masubuchi S, Namihira M, Honma K** 2003 Gene expression of neuropeptide Y in the nucleus of the solitary tract is activated in rats under restricted daily feeding but not under 48-h food deprivation. Eur J Neurosci 17:2097-2105
118. **Babic T, Townsend RL, Patterson LM, Sutton GM, Zheng H, Berthoud HR** 2009 Phenotype of neurons in the nucleus of the solitary tract that express CCK-induced activation of the ERK signaling pathway. Am J Physiol Regul Integr Comp Physiol 296:R845-854
119. **Perello M, Stuart RC, Nillni EA** 2007 Differential effects of fasting and leptin on proopiomelanocortin peptides in the arcuate nucleus and in the nucleus of the solitary tract. Am J Physiol Endocrinol Metab 292:E1348-1357

120. **Fekete C, Mihaly E, Luo LG, Kelly J, Clausen JT, Mao Q, Rand WM, Moss LG, Kuhar M, Emerson CH, Jackson IM, Lechan RM** 2000 Association of cocaine- and amphetamine-regulated transcript-immunoreactive elements with thyrotropin-releasing hormone-synthesizing neurons in the hypothalamic paraventricular nucleus and its role in the regulation of the hypothalamic-pituitary-thyroid axis during fasting. J Neurosci 20:9224-9234
121. **Shioda S, Funahashi H, Nakajo S, Yada T, Maruta O, Nakai Y** 1998 Immunohistochemical localization of leptin receptor in the rat brain. Neurosci Lett 243:41-44
122. **Wang L, Barachina MD, Martinez V, Wei JY, Tache Y** 2000 Synergistic interaction between CCK and leptin to regulate food intake. Regul Pept 92:79-85
123. **Lutz TA** The role of amylin in the control of energy homeostasis. Am J Physiol Regul Integr Comp Physiol
124. **Lennard DE, Eckert WA, Merchenthaler I** 1993 Corticotropin-releasing hormone neurons in the paraventricular nucleus project to the external zone of the median eminence: a study combining retrograde labeling with immunocytochemistry. J Neuroendocrinol 5:175-181
125. **Niimi M, Takahara J, Hashimoto K, Kawanishi K** 1988 Immunohistochemical identification of corticotropin releasing factor-containing neurons projecting to the stalk-median eminence of the rat. Peptides 9:589-593
126. **Kawano H, Tsuruo Y, Bando H, Daikoku S** 1991 Hypophysiotrophic TRH-producing neurons identified by combining immunohistochemistry for pro-TRH and retrograde tracing. J Comp Neurol 307:531-538
127. **Sawchenko PE, Imaki T, Potter E, Kovacs K, Imaki J, Vale W** 1993 The functional neuroanatomy of corticotropin-releasing factor. Ciba Found Symp 172:5-21; discussion 21-29
128. **Valassi E, Scacchi M, Cavagnini F** 2008 Neuroendocrine control of food intake. Nutr Metab Cardiovasc Dis 18:158-168
129. **Menzaghi F, Heinrichs SC, Pich EM, Tilders FJ, Koob GF** 1993 Functional impairment of hypothalamic corticotropin-releasing factor neurons with immunotargeted toxins enhances food intake induced by neuropeptide Y. Brain Res 618:76-82
130. **Sasaki K, Cripe TP, Koch SR, Andreone TL, Petersen DD, Beale EG, Granner DK** 1984 Multihormonal regulation of phosphoenolpyruvate carboxykinase gene transcription. The dominant role of insulin. J Biol Chem 259:15242-15251
131. **Christ-Crain M, Kola B, Lolli F, Fekete C, Seboek D, Wittmann G, Feltrin D, Igreja SC, Ajodha S, Harvey-White J, Kunos G, Muller B, Pralong F, Aubert G, Arnaldi G, Giacchetti G, Boscaro M, Grossman AB, Korbonits M** 2008 AMP-activated protein kinase mediates glucocorticoid-induced metabolic changes: a novel mechanism in Cushing's syndrome. FASEB J 22:1672-1683
132. **Masuzaki H, Paterson J, Shinyama H, Morton NM, Mullins JJ, Seckl JR, Flier JS** 2001 A transgenic model of visceral obesity and the metabolic syndrome. Science 294:2166-2170
133. **Nieuwenhuizen AG, Rutters F** 2008 The hypothalamic-pituitary-adrenal-axis in the regulation of energy balance. Physiol Behav 94:169-177

134. **Slieker LJ, Sloop KW, Surface PL, Kriauciunas A, LaQuier F, Manetta J, Bue-Valleskey J, Stephens TW** 1996 Regulation of expression of ob mRNA and protein by glucocorticoids and cAMP. J Biol Chem 271:5301-5304
135. **Ahima RS, Prabakaran D, Mantzoros C, Qu D, Lowell B, Maratos-Flier E, Flier JS** 1996 Role of leptin in the neuroendocrine response to fasting. Nature 382:250-252
136. **Dallman MF, Akana SF, Bhatnagar S, Bell ME, Choi S, Chu A, Horsley C, Levin N, Meijer O, Soriano LR, Strack AM, Viau V** 1999 Starvation: early signals, sensors, and sequelae. Endocrinology 140:4015-4023
137. **Hanson ES, Levin N, Dallman MF** 1997 Elevated corticosterone is not required for the rapid induction of neuropeptide Y gene expression by an overnight fast. Endocrinology 138:1041-1047
138. **Brady LS, Smith MA, Gold PW, Herkenham M** 1990 Altered expression of hypothalamic neuropeptide mRNAs in food-restricted and food-deprived rats. Neuroendocrinology 52:441-447
139. **Isse T, Ueta Y, Serino R, Noguchi J, Yamamoto Y, Nomura M, Shibuya I, Lightman SL, Yamashita H** 1999 Effects of leptin on fasting-induced inhibition of neuronal nitric oxide synthase mRNA in the paraventricular and supraoptic nuclei of rats. Brain Res 846:229-235
140. **Li C, Chen P, Smith MS** 2000 Corticotropin releasing hormone neurons in the paraventricular nucleus are direct targets for neuropeptide Y neurons in the arcuate nucleus: an anterograde tracing study. Brain Res 854:122-129
141. **Liposits Z, Sievers L, Paull WK** 1988 Neuropeptide-Y and ACTH-immunoreactive innervation of corticotropin releasing factor (CRF)-synthesizing neurons in the hypothalamus of the rat. An immunocytochemical analysis at the light and electron microscopic levels. Histochemistry 88:227-234
142. **Fekete C, Legradi G, Mihaly E, Tatro JB, Rand WM, Lechan RM** 2000 alpha-Melanocyte stimulating hormone prevents fasting-induced suppression of corticotropin-releasing hormone gene expression in the rat hypothalamic paraventricular nucleus. Neurosci Lett 289:152-156
143. **Smith SM, Vaughan JM, Donaldson CJ, Rivier J, Li C, Chen A, Vale WW** 2004 Cocaine- and amphetamine-regulated transcript activates the hypothalamic-pituitary-adrenal axis through a corticotropin-releasing factor receptor-dependent mechanism. Endocrinology 145:5202-5209
144. **Lu XY, Barsh GS, Akil H, Watson SJ** 2003 Interaction between alpha-melanocyte-stimulating hormone and corticotropin-releasing hormone in the regulation of feeding and hypothalamo-pituitary-adrenal responses. J Neurosci 23:7863-7872
145. **Wittmann G, Liposits Z, Lechan RM, Fekete C** 2005 Origin of cocaine- and amphetamine-regulated transcript-containing axons innervating hypophysiotropic corticotropin-releasing hormone-synthesizing neurons in the rat. Endocrinology 146:2985-2991
146. **Suda T, Tozawa F, Iwai I, Sato Y, Sumitomo T, Nakano Y, Yamada M, Demura H** 1993 Neuropeptide Y increases the corticotropin-releasing factor messenger ribonucleic acid level in the rat hypothalamus. Brain Res Mol Brain Res 18:311-315

147. **Brunton PJ, Bales J, Russell JA** 2006 Neuroendocrine stress but not feeding responses to centrally administered neuropeptide Y are suppressed in pregnant rats. Endocrinology 147:3737-3745
148. **Merchenthaler I, Liposits Z** 1994 Mapping of thyrotropin-releasing hormone (TRH) neuronal systems of rat forebrain projecting to the median eminence and the OVLT. Immunocytochemistry combined with retrograde labeling at the light and electron microscopic levels. Acta Biol Hung 45:361-374
149. **Nussey SS WS** 2001 Endocrinology: An integrated approach. Oxford: BIOS scientific Publishers Ltd
150. **Silva JE** 2003 The thermogenic effect of thyroid hormone and its clinical implications. Ann Intern Med 139:205-213
151. **Ribeiro MO, Carvalho SD, Schultz JJ, Chiellini G, Scanlan TS, Bianco AC, Brent GA** 2001 Thyroid hormone--sympathetic interaction and adaptive thermogenesis are thyroid hormone receptor isoform--specific. J Clin Invest 108:97-105
152. **Cannon B, Nedergaard J** 2004 Brown adipose tissue: function and physiological significance. Physiol Rev 84:277-359
153. **Oppenheimer JH, Schwartz HL, Lane JT, Thompson MP** 1991 Functional relationship of thyroid hormone-induced lipogenesis, lipolysis, and thermogenesis in the rat. J Clin Invest 87:125-132
154. **Kong WM, Martin NM, Smith KL, Gardiner JV, Connoley IP, Stephens DA, Dhillo WS, Ghatei MA, Small CJ, Bloom SR** 2004 Triiodothyronine stimulates food intake via the hypothalamic ventromedial nucleus independent of changes in energy expenditure. Endocrinology 145:5252-5258
155. **Lechan RM, Fekete C** 2006 The TRH neuron: a hypothalamic integrator of energy metabolism. Prog Brain Res 153:209-235
156. **Nishiyama T, Kawano H, Tsuruo Y, Maegawa M, Hisano S, Adachi T, Daikoku S, Suzuki M** 1985 Hypothalamic thyrotropin-releasing hormone (TRH)-containing neurons involved in the hypothalamic-hypophysial-thyroid axis. Light microscopic immunohistochemistry. Brain Res 345:205-218
157. **Segerson TP, Kauer J, Wolfe HC, Mobtaker H, Wu P, Jackson IM, Lechan RM** 1987 Thyroid hormone regulates TRH biosynthesis in the paraventricular nucleus of the rat hypothalamus. Science 238:78-80
158. **Perello M, Nillni EA** 2007 The biosynthesis and processing of neuropeptides: lessons from prothyrotropin releasing hormone (proTRH). Front Biosci 12:3554-3565
159. **Wittmann G, Liposits Z, Lechan RM, Fekete C** 2004 Medullary adrenergic neurons contribute to the cocaine- and amphetamine-regulated transcript-immunoreactive innervation of thyrotropin-releasing hormone synthesizing neurons in the hypothalamic paraventricular nucleus. Brain Res 1006:1-7
160. **Wittmann G, Liposits Z, Lechan RM, Fekete C** 2002 Medullary adrenergic neurons contribute to the neuropeptide Y-ergic innervation of hypophysiotropic thyrotropin-releasing hormone-synthesizing neurons in the rat. Neurosci Lett 324:69-73
161. **Kim MS, Small CJ, Stanley SA, Morgan DG, Seal LJ, Kong WM, Edwards CM, Abusnana S, Sunter D, Ghatei MA, Bloom SR** 2000 The central melanocortin system affects the hypothalamo-pituitary thyroid axis and may mediate the effect of leptin. J Clin Invest 105:1005-1011

162. **Stanley SA, Small CJ, Murphy KG, Rayes E, Abbott CR, Seal LJ, Morgan DG, Sunter D, Dakin CL, Kim MS, Hunter R, Kuhar M, Ghatei MA, Bloom SR** 2001 Actions of cocaine- and amphetamine-regulated transcript (CART) peptide on regulation of appetite and hypothalamo-pituitary axes in vitro and in vivo in male rats. Brain Res 893:186-194
163. **Mountjoy KG, Robbins LS, Mortrud MT, Cone RD** 1992 The cloning of a family of genes that encode the melanocortin receptors. Science 257:1248-1251
164. **Sarkar S, Legradi G, Lechan RM** 2002 Intracerebroventricular administration of alpha-melanocyte stimulating hormone increases phosphorylation of CREB in TRH- and CRH-producing neurons of the hypothalamic paraventricular nucleus. Brain Res 945:50-59
165. **Satoh T, Yamada M, Iwasaki T, Mori M** 1996 Negative regulation of the gene for the preprothyrotropin-releasing hormone from the mouse by thyroid hormone requires additional factors in conjunction with thyroid hormone receptors. J Biol Chem 271:27919-27926
166. **Harris M, Aschkenasi C, Elias CF, Chandrankunnel A, Nillni EA, Bjoorbaek C, Elmquist JK, Flier JS, Hollenberg AN** 2001 Transcriptional regulation of the thyrotropin-releasing hormone gene by leptin and melanocortin signaling. J Clin Invest 107:111-120
167. **Fekete C, Kelly J, Mihaly E, Sarkar S, Rand WM, Legradi G, Emerson CH, Lechan RM** 2001 Neuropeptide Y has a central inhibitory action on the hypothalamic-pituitary-thyroid axis. Endocrinology 142:2606-2613
168. **Fekete C, Sarkar S, Rand WM, Harney JW, Emerson CH, Bianco AC, Beck-Sickinger A, Lechan RM** 2002 Neuropeptide Y1 and Y5 receptors mediate the effects of neuropeptide Y on the hypothalamic-pituitary-thyroid axis. Endocrinology 143:4513-4519
169. **Broberger C, Visser TJ, Kuhar MJ, Hokfelt T** 1999 Neuropeptide Y innervation and neuropeptide-Y-Y1-receptor-expressing neurons in the paraventricular hypothalamic nucleus of the mouse. Neuroendocrinology 70:295-305
170. **Kishi T, Aschkenasi CJ, Choi BJ, Lopez ME, Lee CE, Liu H, Hollenberg AN, Friedman JM, Elmquist JK** 2005 Neuropeptide Y Y1 receptor mRNA in rodent brain: distribution and colocalization with melanocortin-4 receptor. J Comp Neurol 482:217-243
171. **Fekete C, Sarkar S, Rand WM, Harney JW, Emerson CH, Bianco AC, Lechan RM** 2002 Agouti-related protein (AGRP) has a central inhibitory action on the hypothalamic-pituitary-thyroid (HPT) axis; comparisons between the effect of AGRP and neuropeptide Y on energy homeostasis and the HPT axis. Endocrinology 143:3846-3853
172. **Haskell-Luevano C, Monck EK** 2001 Agouti-related protein functions as an inverse agonist at a constitutively active brain melanocortin-4 receptor. Regul Pept 99:1-7
173. **Fekete C, Marks DL, Sarkar S, Emerson CH, Rand WM, Cone RD, Lechan RM** 2004 Effect of Agouti-related protein in regulation of the hypothalamic-pituitary-thyroid axis in the melanocortin 4 receptor knockout mouse. Endocrinology 145:4816-4821
174. **Sarkar S, Lechan RM** 2003 Central administration of neuropeptide Y reduces alpha-melanocyte-stimulating hormone-induced cyclic adenosine 5'-

monophosphate response element binding protein (CREB) phosphorylation in pro-thyrotropin-releasing hormone neurons and increases CREB phosphorylation in corticotropin-releasing hormone neurons in the hypothalamic paraventricular nucleus. Endocrinology 144:281-291

175. **Bellinger LL, Bernardis LL** 2002 The dorsomedial hypothalamic nucleus and its role in ingestive behavior and body weight regulation: lessons learned from lesioning studies. Physiol Behav 76:431-442
176. **Jacobowitz DM, O'Donohue TL** 1978 alpha-Melanocyte stimulating hormone: immunohistochemical identification and mapping in neurons of rat brain. Proc Natl Acad Sci U S A 75:6300-6304
177. **Legradi G, Lechan RM** 1999 Agouti-related protein containing nerve terminals innervate thyrotropin-releasing hormone neurons in the hypothalamic paraventricular nucleus. Endocrinology 140:3643-3652
178. **Mihaly E, Fekete C, Legradi G, Lechan RM** 2001 Hypothalamic dorsomedial nucleus neurons innervate thyrotropin-releasing hormone-synthesizing neurons in the paraventricular nucleus. Brain Res 891:20-31
179. **Shioda S, Nakai Y, Sato A, Sunayama S, Shimoda Y** 1986 Electron-microscopic cytochemistry of the catecholaminergic innervation of TRH neurons in the rat hypothalamus. Cell Tissue Res 245:247-252
180. **Liposits Z** 1993 Ultrastructure of hypothalamic paraventricular neurons. Crit Rev Neurobiol 7:89-162
181. **Lechan RM, Segerson TP** 1989 Pro-TRH gene expression and precursor peptides in rat brain. Observations by hybridization analysis and immunocytochemistry. Ann N Y Acad Sci 553:29-59
182. **Lewis K, Li C, Perrin MH, Blount A, Kunitake K, Donaldson C, Vaughan J, Reyes TM, Gulyas J, Fischer W, Bilezikjian L, Rivier J, Sawchenko PE, Vale WW** 2001 Identification of urocortin III, an additional member of the corticotropin-releasing factor (CRF) family with high affinity for the CRF2 receptor. Proc Natl Acad Sci U S A 98:7570-7575
183. **Li C, Vaughan J, Sawchenko PE, Vale WW** 2002 Urocortin III-immunoreactive projections in rat brain: partial overlap with sites of type 2 corticotrophin-releasing factor receptor expression. J Neurosci 22:991-1001
184. **Fekete EM, Inoue K, Zhao Y, Rivier JE, Vale WW, Szucs A, Koob GF, Zorrilla EP** 2007 Delayed satiety-like actions and altered feeding microstructure by a selective type 2 corticotropin-releasing factor agonist in rats: intra-hypothalamic urocortin 3 administration reduces food intake by prolonging the post-meal interval. Neuropsychopharmacology 32:1052-1068
185. **Chen P, Vaughan J, Donaldson C, Vale WW, Li C** 2009 Injection of Urocortin 3 into the ventromedial hypothalamus modulates feeding, blood glucose levels and hypothalamic POMC gene expression but not the HPA axis. Am J Physiol Endocrinol Metab
186. **Legradi G, Lechan RM** 1998 The arcuate nucleus is the major source for neuropeptide Y-innervation of thyrotropin-releasing hormone neurons in the hypothalamic paraventricular nucleus. Endocrinology 139:3262-3270
187. **Paxinos G WC** 1998 The Rat Brain in Stereotaxic Coordinates. San Diego, CA: Academic Press

188. **Thompson RC, Seasholtz AF, Herbert E** 1987 Rat corticotropin-releasing hormone gene: sequence and tissue-specific expression. Mol Endocrinol 1:363-370
189. **Kakucska I, Qi Y, Clark BD, Lechan RM** 1993 Endotoxin-induced corticotropin-releasing hormone gene expression in the hypothalamic paraventricular nucleus is mediated centrally by interleukin-1. Endocrinology 133:815-821
190. **Wittmann G, Fuzesi T, Liposits Z, Lechan RM, Fekete C** 2009 Distribution and axonal projections of neurons coexpressing thyrotropin-releasing hormone and urocortin 3 in the rat brain. J Comp Neurol 517:825-840
191. **Schiltz JC, Sawchenko PE** 2007 Specificity and generality of the involvement of catecholaminergic afferents in hypothalamic responses to immune insults. J Comp Neurol 502:455-467
192. **Bohn MC, Dreyfus CF, Friedman WJ, Markey KA** 1987 Glucocorticoid effects on phenylethanolamine N-methyltransferase (PNMT) in explants of embryonic rat medulla oblongata. Brain Res 465:257-266
193. **Mihaly E, Fekete C, Lechan RM, Liposits Z** 2002 Corticotropin-releasing hormone-synthesizing neurons of the human hypothalamus receive neuropeptide Y-immunoreactive innervation from neurons residing primarily outside the infundibular nucleus. J Comp Neurol 446:235-243
194. **Suzuki S, Solberg LC, Redei EE, Handa RJ** 2001 Prepro-thyrotropin releasing hormone 178-199 immunoreactivity is altered in the hypothalamus of the Wistar-Kyoto strain of rat. Brain Res 913:224-233
195. **Cunningham ET, Jr., Bohn MC, Sawchenko PE** 1990 Organization of adrenergic inputs to the paraventricular and supraoptic nuclei of the hypothalamus in the rat. J Comp Neurol 292:651-667
196. **Cunningham ET, Jr., Sawchenko PE** 1988 Anatomical specificity of noradrenergic inputs to the paraventricular and supraoptic nuclei of the rat hypothalamus. J Comp Neurol 274:60-76
197. **Ritter S, Llewellyn-Smith I, Dinh TT** 1998 Subgroups of hindbrain catecholamine neurons are selectively activated by 2-deoxy-D-glucose induced metabolic challenge. Brain Res 805:41-54
198. **Li AJ, Ritter S** 2004 Glucoprivation increases expression of neuropeptide Y mRNA in hindbrain neurons that innervate the hypothalamus. Eur J Neurosci 19:2147-2154
199. **Li AJ, Wang Q, Ritter S** 2006 Differential responsiveness of dopamine-beta-hydroxylase gene expression to glucoprivation in different catecholamine cell groups. Endocrinology 147:3428-3434
200. **Ritter S, Watts AG, Dinh TT, Sanchez-Watts G, Pedrow C** 2003 Immunotoxin lesion of hypothalamically projecting norepinephrine and epinephrine neurons differentially affects circadian and stressor-stimulated corticosterone secretion. Endocrinology 144:1357-1367
201. **Ritter S, Bugarith K, Dinh TT** 2001 Immunotoxic destruction of distinct catecholamine subgroups produces selective impairment of glucoregulatory responses and neuronal activation. J Comp Neurol 432:197-216
202. **Ste Marie L, Palmiter RD** 2003 Norepinephrine and epinephrine-deficient mice are hyperinsulinemic and have lower blood glucose. Endocrinology 144:4427-4432

203. **Bugarith K, Dinh TT, Li AJ, Speth RC, Ritter S** 2005 Basomedial hypothalamic injections of neuropeptide Y conjugated to saporin selectively disrupt hypothalamic controls of food intake. Endocrinology 146:1179-1191
204. **Sindelar DK, Ste Marie L, Miura GI, Palmiter RD, McMinn JE, Morton GJ, Schwartz MW** 2004 Neuropeptide Y is required for hyperphagic feeding in response to neuroglucopenia. Endocrinology 145:3363-3368
205. **Ericsson A, Kovacs KJ, Sawchenko PE** 1994 A functional anatomical analysis of central pathways subserving the effects of interleukin-1 on stress-related neuroendocrine neurons. J Neurosci 14:897-913
206. **Buller K, Xu Y, Dayas C, Day T** 2001 Dorsal and ventral medullary catecholamine cell groups contribute differentially to systemic interleukin-1beta-induced hypothalamic pituitary adrenal axis responses. Neuroendocrinology 73:129-138
207. **Fekete C, Singru PS, Sarkar S, Rand WM, Lechan RM** 2005 Ascending brainstem pathways are not involved in lipopolysaccharide-induced suppression of thyrotropin-releasing hormone gene expression in the hypothalamic paraventricular nucleus. Endocrinology 146:1357-1363
208. **Dimitrov EL, DeJoseph MR, Brownfield MS, Urban JH** 2007 Involvement of neuropeptide Y Y1 receptors in the regulation of neuroendocrine corticotropin-releasing hormone neuronal activity. Endocrinology 148:3666-3673
209. **Pronchuk N, Beck-Sickinger AG, Colmers WF** 2002 Multiple NPY receptors Inhibit GABA(A) synaptic responses of rat medial parvocellular effector neurons in the hypothalamic paraventricular nucleus. Endocrinology 143:535-543
210. **Wahlestedt C, Skagerberg G, Ekman R, Heilig M, Sundler F, Hakanson R** 1987 Neuropeptide Y (NPY) in the area of the hypothalamic paraventricular nucleus activates the pituitary-adrenocortical axis in the rat. Brain Res 417:33-38
211. **Mefford IN** 1988 Epinephrine in mammalian brain. Prog Neuropsychopharmacol Biol Psychiatry 12:365-388
212. **Lynch GS, Ryall JG** 2008 Role of beta-adrenoceptor signaling in skeletal muscle: implications for muscle wasting and disease. Physiol Rev 88:729-767
213. **Agnati LF, Fuxe K, Benfenati F, Battistini N, Harfstrand A, Tatemoto K, Hokfelt T, Mutt V** 1983 Neuropeptide Y in vitro selectivity increases the number of alpha 2-adrenergic binding sites in membranes of the medulla oblongata of the rat. Acta Physiol Scand 118:293-295
214. **Khanna S, Sibbald JR, Day TA** 1993 Neuropeptide Y modulation of A1 noradrenergic neuron input to supraoptic vasopressin cells. Neurosci Lett 161:60-64
215. **Agarwal A, Halvorson LM, Legradi G** 2005 Pituitary adenylate cyclase-activating polypeptide (PACAP) mimics neuroendocrine and behavioral manifestations of stress: Evidence for PKA-mediated expression of the corticotropin-releasing hormone (CRH) gene. Brain Res Mol Brain Res 138:45-57
216. **Lee SL, Stewart K, Goodman RH** 1988 Structure of the gene encoding rat thyrotropin releasing hormone. J Biol Chem 263:16604-16609

217. **Dun SL, Ng YK, Brailoiu GC, Ling EA, Dun NJ** 2002 Cocaine- and amphetamine-regulated transcript peptide-immunoreactivity in adrenergic C1 neurons projecting to the intermediolateral cell column of the rat. J Chem Neuroanat 23:123-132
218. **Levin MC, Sawchenko PE, Howe PR, Bloom SR, Polak JM** 1987 Organization of galanin-immunoreactive inputs to the paraventricular nucleus with special reference to their relationship to catecholaminergic afferents. J Comp Neurol 261:562-582
219. **Krulich L** 1982 Neurotransmitter control of thyrotropin secretion. Neuroendocrinology 35:139-147
220. **Perello M, Stuart RC, Vaslet CA, Nillni EA** 2007 Cold exposure increases the biosynthesis and proteolytic processing of prothyrotropin-releasing hormone in the hypothalamic paraventricular nucleus via beta-adrenoreceptors. Endocrinology 148:4952-4964
221. **Sanchez E, Uribe RM, Corkidi G, Zoeller RT, Cisneros M, Zacarias M, Morales-Chapa C, Charli JL, Joseph-Bravo P** 2001 Differential responses of thyrotropin-releasing hormone (TRH) neurons to cold exposure or suckling indicate functional heterogeneity of the TRH system in the paraventricular nucleus of the rat hypothalamus. Neuroendocrinology 74:407-422
222. **Uribe RM, Redondo JL, Charli JL, Joseph-Bravo P** 1993 Suckling and cold stress rapidly and transiently increase TRH mRNA in the paraventricular nucleus. Neuroendocrinology 58:140-145
223. **Zoeller RT, Kabeer N, Albers HE** 1990 Cold exposure elevates cellular levels of messenger ribonucleic acid encoding thyrotropin-releasing hormone in paraventricular nucleus despite elevated levels of thyroid hormones. Endocrinology 127:2955-2962
224. **Tapia-Arancibia L, Arancibia S, Astier H** 1985 Evidence for alpha 1-adrenergic stimulatory control of in vitro release of immunoreactive thyrotropin-releasing hormone from rat median eminence: in vivo corroboration. Endocrinology 116:2314-2319
225. **Baffi JS, Palkovits M** 2000 Fine topography of brain areas activated by cold stress. A fos immunohistochemical study in rats. Neuroendocrinology 72:102-113
226. **Ishikawa K, Taniguchi Y, Kurosumi K, Suzuki M** 1986 Origin of septal thyrotropin-releasing hormone in the rat. Neuroendocrinology 44:54-58
227. **Merchenthaler I** 1991 Co-localization of enkephalin and TRH in perifornical neurons of the rat hypothalamus that project to the lateral septum. Brain Res 544:177-180
228. **Vijayan E, McCann SM** 1977 Suppression of feeding and drinking activity in rats following intraventricular injection of thyrotropin releasing hormone (TRH). Endocrinology 100:1727-1730
229. **Vogel RA, Cooper BR, Barlow TS, Prange AJ, Jr., Mueller RA, Breese GR** 1979 Effects of thyrotropin-releasing hormone on locomotor activity, operant performance and ingestive behavior. J Pharmacol Exp Ther 208:161-168
230. **Morley JE** 1980 The neuroendocrine control of appetite: the role of the endogenous opiates, cholecystokinin, TRH, gamma-amino-butyric-acid and the diazepam receptor. Life Sci 27:355-368

231. **Suzuki T, Kohno H, Sakurada T, Tadano T, Kisara K** 1982 Intracranial injection of thyrotropin releasing hormone (TRH) suppresses starvation-induced feeding and drinking in rats. Pharmacol Biochem Behav 17:249-253
232. **Horita A** 1998 An update on the CNS actions of TRH and its analogs. Life Sci 62:1443-1448
233. **Steward CA, Horan TL, Schuhler S, Bennett GW, Ebling FJ** 2003 Central administration of thyrotropin releasing hormone (TRH) and related peptides inhibits feeding behavior in the Siberian hamster. Neuroreport 14:687-691
234. **Morton GJ, Cummings DE, Baskin DG, Barsh GS, Schwartz MW** 2006 Central nervous system control of food intake and body weight. Nature 443:289-295
235. **Van der Werf YD, Witter MP, Groenewegen HJ** 2002 The intralaminar and midline nuclei of the thalamus. Anatomical and functional evidence for participation in processes of arousal and awareness. Brain Res Brain Res Rev 39:107-140
236. **Castaneda TR, Jurgens H, Wiedmer P, Pfluger P, Diano S, Horvath TL, Tang-Christensen M, Tschop MH** 2005 Obesity and the neuroendocrine control of energy homeostasis: the role of spontaneous locomotor activity. J Nutr 135:1314-1319
237. **Ju G, Swanson LW** 1989 Studies on the cellular architecture of the bed nuclei of the stria terminalis in the rat: I. Cytoarchitecture. J Comp Neurol 280:587-602
238. **Dong HW, Petrovich GD, Swanson LW** 2001 Topography of projections from amygdala to bed nuclei of the stria terminalis. Brain Res Brain Res Rev 38:192-246
239. **Kelley AE** 2004 Ventral striatal control of appetitive motivation: role in ingestive behavior and reward-related learning. Neurosci Biobehav Rev 27:765-776
240. **Morrow NS, Hodgson DM, Garrick T** 1996 Microinjection of thyrotropin-releasing hormone analogue into the central nucleus of the amygdala stimulates gastric contractility in rats. Brain Res 735:141-148
241. **Freeman ME, Kanyicska B, Lerant A, Nagy G** 2000 Prolactin: structure, function, and regulation of secretion. Physiol Rev 80:1523-1631
242. **Dannies PS, Tashjian AH, Jr.** 1974 Pyroglutamyl-histidyl-prolineamide (TRH). A neurohormone which affects the release and synthesis of prolactin and thyrotropin. Isr J Med Sci 10:1294-1304
243. **Nillni EA, Sevarino KA** 1999 The biology of pro-thyrotropin-releasing hormone-derived peptides. Endocr Rev 20:599-648
244. **Goldstein J, Perello M, Nillni EA** 2007 PreproThyrotropin-releasing hormone 178-199 affects tyrosine hydroxylase biosynthesis in hypothalamic neurons: a possible role for pituitary prolactin regulation. J Mol Neurosci 31:69-82
245. **Hori T, Yamasaki M, Asami T, Koga H, Kiyohara T** 1988 Responses of anterior hypothalamic-preoptic thermosensitive neurons to thyrotropin releasing hormone and cyclo(His-Pro). Neuropharmacology 27:895-901
246. **Chi ML, Lin MT** 1983 Involvement of adrenergic receptor mechanisms within hypothalamus in the fever induced by amphetamine and thyrotropin-releasing hormone in the rat. J Neural Transm 58:213-222

247. **Bianco AC, Salvatore D, Gereben B, Berry MJ, Larsen PR** 2002 Biochemistry, cellular and molecular biology, and physiological roles of the iodothyronine selenodeiodinases. Endocr Rev 23:38-89
248. **Morrison SF, Nakamura K, Madden CJ** 2008 Central control of thermogenesis in mammals. Exp Physiol 93:773-797
249. **Horiuchi J, McDowall LM, Dampney RA** 2006 Differential control of cardiac and sympathetic vasomotor activity from the dorsomedial hypothalamus. Clin Exp Pharmacol Physiol 33:1265-1268
250. **McDowall LM, Horiuchi J, Dampney RA** 2007 Effects of disinhibition of neurons in the dorsomedial hypothalamus on central respiratory drive. Am J Physiol Regul Integr Comp Physiol 293:R1728-1735
251. **Balthazart J, Ball GF** 2007 Topography in the preoptic region: differential regulation of appetitive and consummatory male sexual behaviors. Front Neuroendocrinol 28:161-178
252. **Yokosuka M, Matsuoka M, Ohtani-Kaneko R, Iigo M, Hara M, Hirata K, Ichikawa M** 1999 Female-soiled bedding induced fos immunoreactivity in the ventral part of the premammillary nucleus (PMv) of the male mouse. Physiol Behav 68:257-261
253. **Cavalcante JC, Bittencourt JC, Elias CF** 2006 Female odors stimulate CART neurons in the ventral premammillary nucleus of male rats. Physiol Behav 88:160-166
254. **Canteras NS, Simerly RB, Swanson LW** 1992 Projections of the ventral premammillary nucleus. J Comp Neurol 324:195-212
255. **Elmquist JK, Bjorbaek C, Ahima RS, Flier JS, Saper CB** 1998 Distributions of leptin receptor mRNA isoforms in the rat brain. J Comp Neurol 395:535-547
256. **Elmquist JK, Ahima RS, Maratos-Flier E, Flier JS, Saper CB** 1997 Leptin activates neurons in ventrobasal hypothalamus and brainstem. Endocrinology 138:839-842
257. **Dhillon H, Zigman JM, Ye C, Lee CE, McGovern RA, Tang V, Kenny CD, Christiansen LM, White RD, Edelstein EA, Coppari R, Balthasar N, Cowley MA, Chua S, Jr., Elmquist JK, Lowell BB** 2006 Leptin directly activates SF1 neurons in the VMH, and this action by leptin is required for normal body-weight homeostasis. Neuron 49:191-203
258. **Simerly RB, Chang C, Muramatsu M, Swanson LW** 1990 Distribution of androgen and estrogen receptor mRNA-containing cells in the rat brain: an in situ hybridization study. J Comp Neurol 294:76-95
259. **Heeb MM, Yahr P** 1996 c-Fos immunoreactivity in the sexually dimorphic area of the hypothalamus and related brain regions of male gerbils after exposure to sex-related stimuli or performance of specific sexual behaviors. Neuroscience 72:1049-1071
260. **Kollack-Walker S, Watson SJ, Akil H** 1997 Social stress in hamsters: defeat activates specific neurocircuits within the brain. J Neurosci 17:8842-8855
261. **Koolhaas JM, Everts H, de Ruiter AJ, de Boer SF, Bohus B** 1998 Coping with stress in rats and mice: differential peptidergic modulation of the amygdala-lateral septum complex. Prog Brain Res 119:437-448
262. **Ciccocioppo R, Fedeli A, Economidou D, Policani F, Weiss F, Massi M** 2003 The bed nucleus is a neuroanatomical substrate for the anorectic effect of

corticotropin-releasing factor and for its reversal by nociceptin/orphanin FQ. J Neurosci 23:9445-9451
263. **Fujisaki M, Hashimoto K, Iyo M, Chiba T** 2004 Role of the amygdalo-hippocampal transition area in the fear expression: evaluation by behavior and immediate early gene expression. Neuroscience 124:247-260
264. **Herman JP, Ostrander MM, Mueller NK, Figueiredo H** 2005 Limbic system mechanisms of stress regulation: hypothalamo-pituitary-adrenocortical axis. Prog Neuropsychopharmacol Biol Psychiatry 29:1201-1213
265. **Hahn JD, Coen CW** 2006 Comparative study of the sources of neuronal projections to the site of gonadotrophin-releasing hormone perikarya and to the anteroventral periventricular nucleus in female rats. J Comp Neurol 494:190-214
266. **King BM** 2006 Amygdaloid lesion-induced obesity: relation to sexual behavior, olfaction, and the ventromedial hypothalamus. Am J Physiol Regul Integr Comp Physiol 291:R1201-1214
267. **Bakshi VP, Newman SM, Smith-Roe S, Jochman KA, Kalin NH** 2007 Stimulation of lateral septum CRF2 receptors promotes anorexia and stress-like behaviors: functional homology to CRF1 receptors in basolateral amygdala. J Neurosci 27:10568-10577
268. **Zeng H, Schimpf BA, Rohde AD, Pavlova MN, Gragerov A, Bergmann JE** 2007 Thyrotropin-releasing hormone receptor 1-deficient mice display increased depression and anxiety-like behavior. Mol Endocrinol 21:2795-2804
269. **Kastin AJ, Ehrensing RH, Schalch DS, Anderson MS** 1972 Improvement in mental depression with decreased thyrotropin response after administration of thyrotropin-releasing hormone. Lancet 2:740-742
270. **Prange AJ, Jr., Lara PP, Wilson IC, Alltop LB, Breese GR** 1972 Effects of thyrotropin-releasing hormone in depression. Lancet 2:999-1002
271. **Callahan AM, Frye MA, Marangell LB, George MS, Ketter TA, L'Herrou T, Post RM** 1997 Comparative antidepressant effects of intravenous and intrathecal thyrotropin-releasing hormone: confounding effects of tolerance and implications for therapeutics. Biol Psychiatry 41:264-272
272. **Hinuma S, Shintani Y, Fukusumi S, Iijima N, Matsumoto Y, Hosoya M, Fujii R, Watanabe T, Kikuchi K, Terao Y, Yano T, Yamamoto T, Kawamata Y, Habata Y, Asada M, Kitada C, Kurokawa T, Onda H, Nishimura O, Tanaka M, Ibata Y, Fujino M** 2000 New neuropeptides containing carboxy-terminal RFamide and their receptor in mammals. Nat Cell Biol 2:703-708
273. **Liu Q, Guan XM, Martin WJ, McDonald TP, Clements MK, Jiang Q, Zeng Z, Jacobson M, Williams DL, Jr., Yu H, Bomford D, Figueroa D, Mallee J, Wang R, Evans J, Gould R, Austin CP** 2001 Identification and characterization of novel mammalian neuropeptide FF-like peptides that attenuate morphine-induced antinociception. J Biol Chem 276:36961-36969
274. **Kriegsfeld LJ, Mei DF, Bentley GE, Ubuka T, Mason AO, Inoue K, Ukena K, Tsutsui K, Silver R** 2006 Identification and characterization of a gonadotropin-inhibitory system in the brains of mammals. Proc Natl Acad Sci U S A 103:2410-2415

11. List of publications underlying the thesis

1. T. Füzesi, G. Wittmann, Z. Liposits, R.M. Lechan, C. Fekete
   Contribution of noradrenergic and adrenergic cell groups of the brainstem and agouti-related protein-synthesizing neurons of the arcuate nucleus to neuropeptide-y innervation of corticotropin-releasing hormone neurons in hypothalamic paraventricular nucleus of the rat.
   Endocrinology. 2007 Nov;148(11):5442-50.

2. G. Wittmann, T. Füzesi., P.S. Singru, Z. Liposits., R.M. Lechan, C. Fekete
   Efferent projections of thyrotropin-releasing hormone-synthesizing neurons residing in the anterior parvocellular subdivision of the hypothalamic paraventricular nucleus
   Journal of Comparative Neurology 2009 Jul 20;515(3):313-30

3. T. Füzesi; G. Wittmann, R.M. Lechan, Z. Liposits, C. Fekete
   Noradrenergic Innervation of Hypophysiotropic Thyrotropin-Releasing Hormone-Synthesizing Neurons in Rats
   Brain Research, 2009 Oct 19;1294:38-44. Epub 2009 Aug 6.

12. List of publications related to the subject of the thesis

4. T. Füzesi, E. Sánchez, G. Wittmann, P.S. Singru, C. Fekete, R.M. Lechan
Regulation of cocaine-and amphetamine-regulated transcript-(CART) synthesizing neurons of the hypothalamic paraventricular nucleus by endotoxin; Implications for LPS-induced regulation of energy homeostasis
Journal of Neuroendocrinology, 2008 Sep;20(9):1058-66.

5. G. Wittmann, T. Füzesi, Z. Liposits, R.M. Lechan, C. Fekete
Distribution and axonal projections of neurons co-expressing thyrotropin-releasing hormone and urocortin 3 in the rat brain
Journal of Comparative Neurology, 2009 Dec 20;517(6):825-40.

6. Kádár A., Sánchez E., Wittmann G., Singru P. S., Füzesi T., Marsili A., Larsen P. R., Liposits Zs., Lechan R. M., Fekete Cs.
Distribution of Hypophysiotropic Thyrotropin-Releasing Hormone (TRH)-Synthesizing Neurons in the Hypothalamic Paraventricular Nucleus of the Mouse
Journal of Comparative Neurology, manuscript accepted (2010).

13. Acknowledgements

I express my deep gratitude to Dr. Csaba Fekete, my tutor. He devoted so much time and attention to teach me scientific research since the years I was a graduate student at university. I thank him that he has fully promoted my professional development.

I am very grateful to Professor Zsolt Liposits, Head of the Laboratory of Endocrine Neurobiology, who has provided me absolute support to progress in scientific research.

My sincere thanks to Professor Ronald M. Lechan at Tufts University in Boston, for his collaborative efforts.

Special thanks to Gábor Wittmann, who was a friend and tireless help, from both the professional and the human point of view.

I wish to express my thanks to our assistants whom I worked together with: Éva Laki, Ágnes Simon, Veronika Maruzs. I appreciate their careful and precise work that was a great help of me.

I am very thankful to my closest colleagues Andrea Kádár and Barbara Vida for successful cooperation and the joyful hours spent together.

I would like to thank all of my colleagues in the Laboratory of Endocrine Neurobiology for advices and technical supports, and for their great companionship: Zsuzsanna Bardóczi, Bekó Norbertné, Levente Deli, Dr. Márton Doleschall, Péter Egri, Dr. Imre Farkas, Dr. Balázs Gereben, Vivien Hársfalvi, Dr. Erik Hrabovszky, Andrea Juhász, Dr. Imre Kalló, Barna László, Petra Mohácsik, Csilla Molnár, Kata Nagyunyomi-Sényi, Viktória Novák, Anna Sárvári, Dr. Miklós Sárvári, Edit Szabó, Márta Turek, Dr. Gergely Túri, Dr. Anikó Zeöld.

I would also like to express my thanks to the members of the Medical Gene Technological Unit, especially to Dr. Ferenc Erdélyi, Head of the Unit, and to Mária Szűcs and Rozália Szafner for having always been helpful when I worked in the animal facility.